New Jersey Institute of Technology

Digital Commons @ NJIT

Theses   Electronic Theses and Dissertations

Fall 1-31-1998

Removal of VOCs from superfactant-flushed wastewater by membrane based modified pervaporation process

Anirban Das
New Jersey Institute of Technology

Recommended Citation

ABSTRACT

REMOVAL OF VOCs FROM SURFACTANT-FLUSHED WASTEWATER BY MEMBRANE BASED MODIFIED PERVAPORATION PROCESS

by
Anirban Das

An aqueous solution of a volatile organic compound (VOC) e.g. trichloroethylene (TCE) is passed through the bores of hydrophobic microporous polypropylene hollow fibers having a plasma polymerized silicone coating on the fiber outside diameter; a vacuum is maintained on the shell side of the fiber to remove the VOC and recover it by condensation. Process performance has been obtained over a range of feed flow rates, concentrations of VOC and the surfactant (sodium dodecyl sulfate (SDS)). In solutions without surfactant or low surfactant concentrations, the pores are not wetted and remain gas-filled. The VOC is stripped from the solution into the gas-filled pores, diffuse through the gas-filled pore and then permeate through the silicone coating to the shell side where vacuum removes it. This process is termed "stripmeation". The observed VOC permeation and removal behavior in stripmeation has been modeled using resistances-in-series approach; the model-estimated values compare well with the experimental values for surfactant-free feed solutions. For surfactant-containing feed solutions, with an increase in surfactant concentration the VOC flux decreases. Experiments conducted to identify and estimate the resistances show that as the surfactant solution wets the pores, the water-filled pores offer additional resistance. Other resistances may be due to unavailability of VOC in the aqueous phase and an adsorbed surfactant layer on the polypropylene substrate. Comparison between tube-side feed and shell-side feed was made for aqueous and surfactant feed. The tube-side feed-based operation performs much better.

REMOVAL OF VOCs FROM SURFACTANT-FLUSHED WASTEWATER BY MEMBRANE BASED MODIFIED PERVAPORATION PROCESS

by
Anirban Das

A Thesis
Submitted to the Faculty of
New Jersey Institute of Technology
in Partial Fulfillment of the Requirements for the Degree of
Master of Science in Chemical Engineering

Department of Chemical Engineering,
Chemistry, and Environmental Science

January 1998

Blank Page

To Appa and Ma

APPROVAL PAGE

REMOVAL OF VOCs FROM SURFACTANT-FLUSHED WASTEWATER BY MEMBRANE BASED MODIFIED PERVAPORATION PROCESS

Anirban Das

1/6/98
Date

Dr. Kamalesh K. Sirkar, Thesis Advisor
Professor of Chemical Engineering
New Jersey Institute of Technology

1/6/98
Date

Dr. Marinos Xanthos, Committee Member
Associate Professor of Chemical Engineering
New Jersey Institute of Technology

1/6/98
Date

Dr. Robert Luo, Committee Member
Assistant Professor of Chemical Engineering
New Jersey Institute of Technology

BIOGRAPHICAL SKETCH

Author: Anirban Das

Degree: Master of Science

Date: January 1998

Undergraduate and Graduate Education:

Master of Science in Chemical Engineering,
New Jersey Institute of Technology, Newark, NJ, 1998

Bachelor of Chemical Engineering (B.ChE),
Jadavpur University, Calcutta, India, 1995

Major: Chemical Engineering

ACKNOWLEDGMENT

TABLE OF CONTENTS

TABLE OF CONTENTS
(Continued)

TABLE OF CONTENTS
(Continued)

LIST OF TABLES

LIST OF FIGURES

LIST OF FIGURES
(Continued)

xi

Figure   **Page**

NOMENCLATURE

a = parameter in $(Q_i/\delta_s) = a \times \exp(b\,Px)$, $(\dfrac{gmol - cm}{cm^2 - cmHg - s})$

b = parameter in $(Q_i/\delta_s) = a \times \exp(b\,Px)$, (atm^{-1})

A_m = membrane area based on fiber outside diameter, (cm^2)

B_j = coefficient in the jth term of an infinite series (Skelland, 1974)

$\bar{c_i}$ = mean speed of molecules, (cm/s)

C_{il}' = bulk phase feed concentration of species i, $(gmol/cc)$

C_{ili}' = concentration of species i in the aqueous feed phase at the aqueous-pore gas interface, $(gmol/cc)$

C_{igi}' = concentration of species i in the vapor phase at the aqueous-pore gas interface, $(gmol/cc)$

C_{igmi}' = concentration of species i in the vapor phase at the pore gas-silicone membrane interface, $(gmol/cc)$

C_{imi}' = concentration of species i in the membrane at the pore gas-silicone membrane interface, $(gmol/cc)$

C_{imi}'' = concentration of species i in the membrane at the silicone membrane-vacuum side interface, $(gmol/cc)$

C_{imp}'' = concentration of species i in the vacuum side at the silicone membrane-vacuum side interface, $(gmol/cc)$

C_{ip}'' = bulk concentration of species i in the vacuum side, $(gmol/cc)$

C_{ipl}'' = hypothetical equilibrium liquid phase concentration in equilibrium with the vacuum side gas phase, $(gmol/cc)$

C_{inlet} =   feed aqueous inlet concentration of TCE, (gmol/cc)

C_{outlet} =   feed aqueous outlet concentration of TCE, (gmol/cc)

C^p_{inlet} =   hypothetical permeate aqueous concentration of TCE at feed inlet location in equilibrium with the vacuum phase, (gmol/cc)

C^p_{outlet} =   hypothetical permeate aqueous concentration of TCE at feed outlet location in equilibrium with the vacuum phase, (gmol/cc)

ΔC_{lm} =   logarithmic mean aqueous concentration of TCE as defined by Eq. (19), (gmol/cc)

C'_{inlet} =   feed gas inlet concentration of TCE, (gmol/cc)

C'_{outlet} =   feed gas outlet concentration of TCE, (gmol/cc)

C''_{inlet} =   permeate vapor concentration of TCE at feed inlet, (gmol/cc)

C''_{outlet} =   permeate vapor concentration of TCE at feed outlet location, (gmol/cc)

ΔC^v_{lm} =   logarithmic mean vapor concentration of TCE as defined by Eq (23), (gmol/cc)

d_i =   inner diameter of Celgard hollow fiber, (cm)

d_o =   outer diameter of Celgard hollow fiber, (cm)

d_{lm} =   logarithmic mean diameter of Celgard hollow fiber, $\dfrac{(d_o - d_i)}{\ln(d_o / d_i)}$,(cm)

D_{igp} =   diffusion coefficient of TCE in the gaseous pore, (cm^2/s)

D_{il} =   diffusion coefficient of TCE in water, (cm^2/s)

H_i =   Henry's law constant for species i defined by Eq.(1), (mg/L)$_{liq}$ /(mg/L)$_{vap}$

J_i = permeation flux of species i, (gmol/cm^2 min)

J^v_i = permeation flux of species i in vapor permeation experiments, (gmol/cm^2 min)

J_w = permeation flux of water, (gmol/cm^2 min)

K_o = overall mass transfer coefficient defined by Eq. (4), (cm/s)

K_{owet} = overall mass transfer coefficient when pores are wetted, (cm/s)

k^p_g = vacuum side mass transfer coefficient , (cm/s)

k^f_{gp} = mass transfer coefficient for mass transfer across the gas-filled pore, (cm/s)

k^f_{wp} = mass transfer coefficient for mass transfer across the water-filled pore, (cm/s)

k^f_l = aqueous phase mass transfer coefficient for mass transfer across the feed side boundary layer, (cm/s)

k_m = mass transfer coefficient for transport across the membrane, (cm/s)

l = active length of the module, (cm)

m_{vp} = distribution coefficient of TCE between the vacuum side and the membrane

m_{vf} = distribution coefficient of TCE between the membrane and the gaseous phase

M_i = molecular weight of species i

N = number of hollow fibers

P = pressure, (atm)

Q = volumetric flow rate, (cc/min)

Q_i = permeablity of VOC, ($\dfrac{\text{gmol} - \text{cm}}{\text{cm}^2 - \text{cmHg} - \text{s}}$)

r_i = radius of a tube, (cm)

R_i = permeation rate of species i per unit permeator length, (gmol/cm s)

Re = Reynolds number as defined by Eq.(16)

Sc = Schmidt number defined as $\dfrac{\mu_i}{\rho_i D_v}$

Sh = Sherwood number as defined by Eq.(20)

t = time, (s)

v = linear velocity of the feed, (cm/s)

V_{TCE} = volume of TCE collected, (cc)

V_{H_2O} = volume of water collected , (cc)

x = mole fraction of VOC in the feed gas at any location

Greek symbols

δ_s = fiber substrate thickness, (cm)

ε = porosity of the Celgard fibers

τ = tortuosity of pores in the Celgard fibers

π = 3.1416

ρ_{H_2O} = density of water, (g/cc)

ρ_{TCE} = density of TCE, (g/cc)

μ_{H_2O} = viscosity of water, (g/cm s)

CHAPTER 1

INTRODUCTION

1.1 The Problem

The presence of volatile organic compounds (VOCs) such as trichloroethylene (TCE), trichloroethane (TCA), benzene, toluene, carbon tetrachloride etc. in the subsoil has become a potential source of ground water contamination. These contaminants find their way into the subsoil from various sources of civilian and military activity. A few examples are the widespread use of chlorinated hydrocarbons as degreasers, cleaners and solvents; leak from underground storage tanks, municipal and industrial landfill sites; release of VOCs into the atmosphere via effluent industrial streams.

The contamination of ground water by such organic compounds poses a serious health hazard that needs urgent attention. TCE, one of the commonly found contaminants, is known to be a carcinogen for humans (Havinga and Cotruvo, 1990). The presence of VOCs in ground water has led the US Environmental Protection Agency (EPA) to regulate the use of VOCs. About half of the 129 US EPA priority pollutants are VOCs. The US EPA has established drinking water standards (EPA/ 540/ SR-94/512) wherein, TCE and benzene have been limited to 3 and 5 μg/L contaminant level respectively.

In groundwater such VOCs often exist as non-aqueous phase liquid pools (NAPLs). NAPLs are of two types: light NAPLs(LNAPLs) that have low viscosity and density and float in water and dense NAPLs (DNAPLs) which sink under water. The NAPLs have a very low solubility in water making their removal difficult. The capillary

forces acting on these migrating organic contaminants act to retain a portion of the organic liquid within the pores (Abriola et al., 1995). DNAPLs that have low viscosities and high densities tend to migrate under gravitational forces deep into the aquifer formations (Abriola et al., 1995), thus making the clean up more difficult.

VOCs are also emitted in large quantities (150,000 tons/year) from wastewater treatment and storage disposal facilities (Shen and Sewell, 1988). It is evident that conventional waste treatment technologies are inadequate to remove or contain VOCs and there is an immediate need to have an effective technology to solve the growing problem.

1.2 Traditional Remediation Technologies

Over the past few years, a number of technologies have been developed and used to remove VOCs from the soil matrix. Subsurface remediation was initially the method of choice for removing the organic contaminants. The methodology used was simple: water was pumped through the subsoil to dissolve the NAPLs/ DNAPLs to bring them above the ground for subsequent treatment. This technique, commonly called 'pump and treat', has been widely used but has soon proved to be inefficient as the NAPLs/ DNAPLs have low aqueous solubility (solubilities of TCE and toluene in water at 25° C are 1000 – 1250 mg/L and 500 mg/L respectively). Water, due to its relatively high surface tension, is unable to wet the pores in the soil matrix and mobilize the organic compounds.

Soil Vapor Extraction (SVE) is another technique (Ball and Wolf, 1990) that has been used to remove VOCs from contaminated soils. This technique involves using vacuum to volatilize the VOCs from the soil. The extracted air is subsequently treated to

remove the contaminants and then discharged to the atmosphere. The process maybe applied in situ to subsurface soils or above ground to excavated soil piles. The process has not been very successful and its use has been limited as many of the parameters involved are yet to be fully characterized or understood.

In the last couple of years, it has become evident that a more effective strategy to counter the problem would be to modify the 'pump and treat' method such that one might be able to solubilize more of the NAPLs/ DNAPLs present in the subsoil. The focus was on pumping a solution through the subsoil that had the ability to mobilize and solubilize much larger amounts of NAPLs/ DNAPLs than water.

1.3 Surfactant Enhanced Aquifer Remediation (SEAR)

The use of a surfactant solution to extract the contaminants from the soil has proved to be a very effective technique. Fountain et al.(1995) have carried out successful field studies using surfactant enhanced remediation and their results show high removal of DNAPLs, the performance being limited by site hydrology. Prior to such studies, Ellis et al. (1985) and Nash (1987) have reported lab scale and field test results respectively, that had demonstrated the potential of this technology. More recently, Pennel et al. (1993) have been successful in removing sorbed or deposited polychlorinated biphenyls (PCBs) and polycyclic hydrocarbons (PCH) using surfactant washing. Food grade surfactants have also been successful in removing TCE, trans-1, 2 dichloroethylene (DCE) tetrachloroethylene (TCE) from aqueous solutions (Shiau et al., 1995).

SEAR process which is simply a modification of the conventional 'pump and treat' method involves pumping a suitable surfactant solution through the subsoil. The

presence of surfactants increases the apparent solubility of the contaminant in the water via encapsulation in the hydrophobic micellar core and also reduces the interfacial tension between water and the NAPLs/ DNAPLs. Therefore, the surfactant solution is able to penetrate the porous structure of the soil to extract the contaminant and ultimately solubilize it. Hence the SEAR process can enhance contaminated site remediation by increasing contaminant solubility, decreasing contaminant mobility and their migration, and increasing the rate of biodegradation of contaminants in the porous soil structure.

1.4 Removal of VOCs from Surfactant-flushed Wastewater

The success of SEAR processes implies that now one has large volumes of over-ground surfactant-flushed wastewater rich in VOCs, surfactants, alcohols, polymers and dissolved salts. This wastewater needs to be treated to remove VOCs and other contaminants so that they can be discharged or recirculated back into the subsoil. In this section a few important techniques that are being used for VOC removal from surfactant-flushed wastewater are discussed.

Air stripping has been one of the methods to remove VOCs from an aqueous phase. But this process has significant limitations in terms of cost effectiveness and operational ease. Groundwater often promotes fouling due to iron oxidation and carbon precipitation reducing process efficiency and increasing maintenance costs. The presence of surfactants causes foaming in the columns, therefore requiring the addition of anti-foaming agents. If such agents are added, recirculation of the treated solution to the subsoil is no longer possible, thus defeating the purpose. Further, the VOC-laden air stream needs to be treated before it may be discharged to the atmosphere.

Solvent extraction has also been one of the techniques used to extract VOCs from micellar solutions (Clark et al., 1993a; Oma et al., 1993a). Gannon et al. (1989) have successfully used solvent extraction to remove dichlorobenzene (DCB) and naphthalene from sodium dodecyl sulphate (SDS) solutions without emulsion formation. Underwood et al. (1993) have effectively used hexane to extract phenanthrene and naphthalene from SDS solutions. They reported removals as high as 90% at low flow rates. But the process suffers from some significant disadvantages like limited surface area for mass transfer, difficulty in regenerating the solvent for reuse and low rate of extraction kinetics.

Activated carbon beds have been efficiently used to remove VOCs from contaminated surfactant solutions but they are only practical at low VOC concentrations (Lipski and Cote, 1990). Regeneration of spent carbon at high VOC concentrations is expensive and needs to conform to stringent EPA regulations. The process also proves ineffective when the aqueous solution is surfactant rich as the organic compounds compete for adsorption sites with the surfactants resulting in site saturation and lower removal rates.

1.5 Proposed Technology for VOC Removal from Surfactant Solutions

The processes discussed in section 1.4 have not been effective in removing VOCs in aqueous solutions. There is therefore need for an alternate method that performs successfully and is cost effective. The alternate method proposed in this study is a hollow fiber membrane based modified pervaporation process (PV). This novel technique, a single step continuous process, has been studied in this research to remove VOCs from the waste generated from SEAR processes. In the modified pervaporation process, the

surfactant rich contaminated water flows through the lumen of a set of hydrophobic hollow fiber membranes with vacuum being pulled from the shell side. The microporous hollow fiber is coated on the shell side with a nonporous membrane that is highly selective to the VOC over water. There are two types of situation: either the pore is gas-filled (non-wetted) or the pore is wetted. When the pore is nonwetted, the VOC is stripped into the gas-filled pores of the hydrophobic substrate, permeates through the nonporous silicone skin and is recovered by condensation of the shell-side permeate stream. A schematic representation of the process is illustrated in Fig. 1.1. The coating is a thin nonporous hydrophobic membrane of polydimethylsiloxane(PDMS), a rubbery polymer, more commonly known as silicone. The membrane is plasma polymerized on the hydrophobic microporous polypropylene substrate. The permeate side vapor, highly enriched in VOCs is condensed and the condensate separates into two layers of organic and aqueous phases. An extraordinary level of waste volume reduction is achieved by the membrane PV process. In case the pore is wetted, the surfactant as well as micelles are going to be present in the pores. Any free VOC in the pore will be removed by conventional pervaporation mechanism through the silicone membrane, namely dissolution in the membrane, diffusion through the membrane and desorption into the vacuum stream. This is illustrated in Figure 1.2. This novel method can reduce VOC concentration in the treated surfactant solutions to ppm level. The treated surfactant solution may now be reused for subsurface remediation thus making the SEAR process more cost effective.
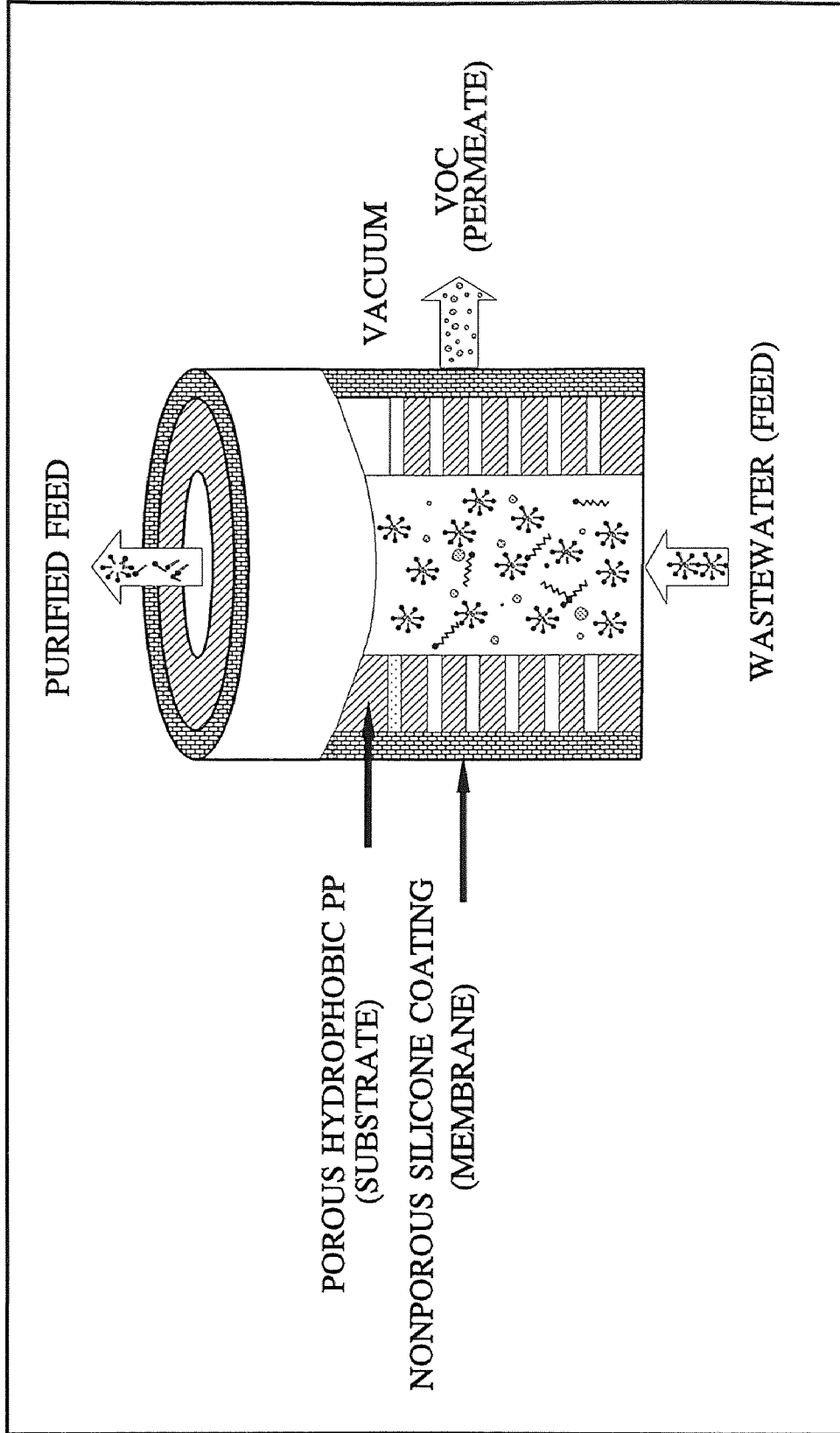
Figure 1.1. Removal of VOCs from surfactant-flushed wastewater by pervaporation through a hollow fiber membrane with non-wetted pores
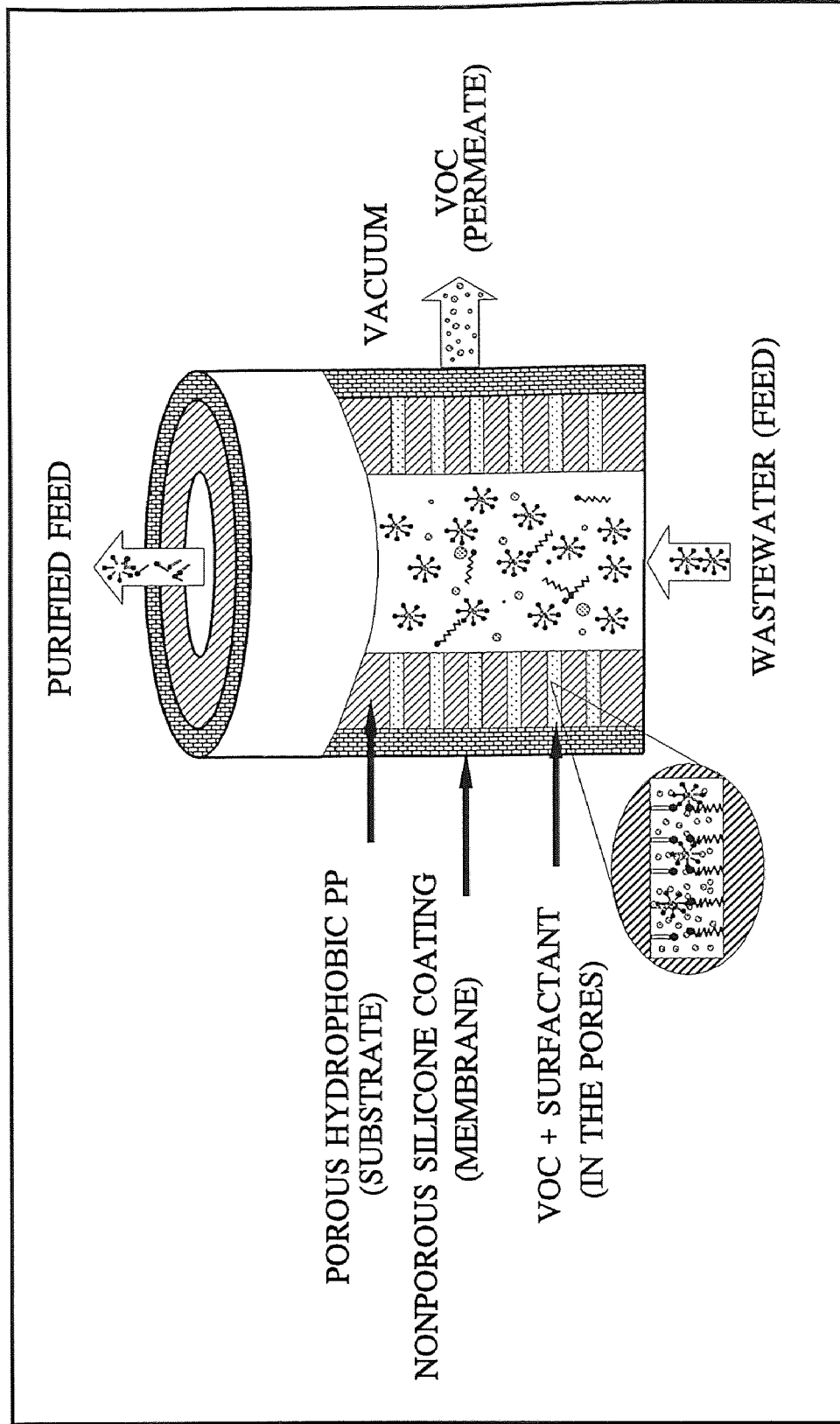
Figure 1.2. Removal of VOCs from surfactant-flushed wastewater by pervaporation through a hollow fiber membrane with wetted pores

1.6 Research Objectives

Chandra (1996) and Saraf (1997) have already established that the membrane-based PV process is an efficient and effective technique to remove VOCs and oils from surfactant flushed wastewater. This research therefore focuses on characterizing the process at a more detailed level and aims at developing an understanding of the behavior of the transport parameters under different process conditions. The general objectives of this research can be divided into four categories:

a. Develop a hollow fiber membrane-based pervaporation process on a bench scale to remove and recover VOCs from surfactant flushed ground water contaminated with NAPLs and DNAPLs.

b. Identify the resistances to mass transport in the above system, determine the controlling resistances and, obtain an estimate of the membrane resistance.

c. Characterize the performance of the PV process under various process conditions.

d. Demonstrate the efficiency and utility of such a process using prototype hollow fiber membrane modules.

1.7 Research Methodology

For the purposes of this research, TCE has been chosen as the model VOC. TCE is one of the priority pollutants declared by the EPA and has been declared a chronic waste ("U" waste; NO.U228) in EPA 40 CFR 261.33. SDS, an anionic surfactant, has been used to simulate a model surfactant feed.

The research was carried out in four phases:

Phase 1:   *TCE-water system*

a.   Conduct bench scale experiments to study the effect of TCE concentration on TCE removal, TCE flux, TCE mass transfer coefficient and water flux.

b.   Conduct bench scale experiments to study the effect of hydrodynamics on TCE removal, TCE flux, TCE mass transfer coefficient and water flux.

Phase 2:   *Resistances-in-series model*

a.   Conduct vapor permeation runs using TCE in nitrogen as feed to estimate the permeance of the membrane coating.

b.   Using theoretical solutions and experimental data determine the applicability of the resistances-in-series model to the TCE-water system.

Phase 3:   *TCE-water-SDS system*

a.   Conduct bench scale experiments to study the effects of surfactant concentration on TCE removal, TCE flux, TCE mass transfer coefficient and water flux.

b.   Conduct bench scale experiments to study the effects of hydrodynamics on TCE removal, TCE flux, TCE mass transfer coefficient and water flux.

Phase 4:   *Wetted-pore Experiments*

a.   Conduct bench-scale experiments with wetted (water-filled) pores using aqueous TCE solution as feed.

b.   Conduct bench-scale experiments with wetted pores using surfactant solution, containing TCE, as feed.

CHAPTER 2

THEORY

2.1 Pervaporation

Pervaporation is a rate-controlled membrane separation process. In pervaporation, the liquid mixture (feed) to be separated is placed in contact with one side of the membrane and the permeated product (permeate) is removed as a low-pressure vapor on the other side. This is illustrated in Figure 2.1. The driving force for mass transport is the chemical potential gradient across the membrane. The driving force can be created by applying either a vacuum or an inert purge on the permeate side to maintain permeate partial pressure of each species to be transferred lower than the partial pressure of each species in the vapor phase in equilibrium with the feed liquid.

2.2 Stripmeation

In the pervaporation process, the feed liquid is in direct contact with the membrane. But there can be systems where the feed solution is not in direct contact with the membrane. An example of such a system would be an aqueous solution of TCE passing on the tube side of a hollow fiber membrane comprising of a hydrophobic microporous support coated with a nonporous hydrophobic silicone skin on the outside surface. The feed solution does not wet the polypropylene substrate pores. If the pores are not wetted then the pores will be gas-filled. The membrane in this case is in contact with the vapor of the feed instead of the liquid feed. Any VOC in the water will be stripped into the gas-filled pore and then will be permeated through the silicone skin subjected to vacuum on the shell side via vapor permeation. This is not conventional pervaporation since the liquid
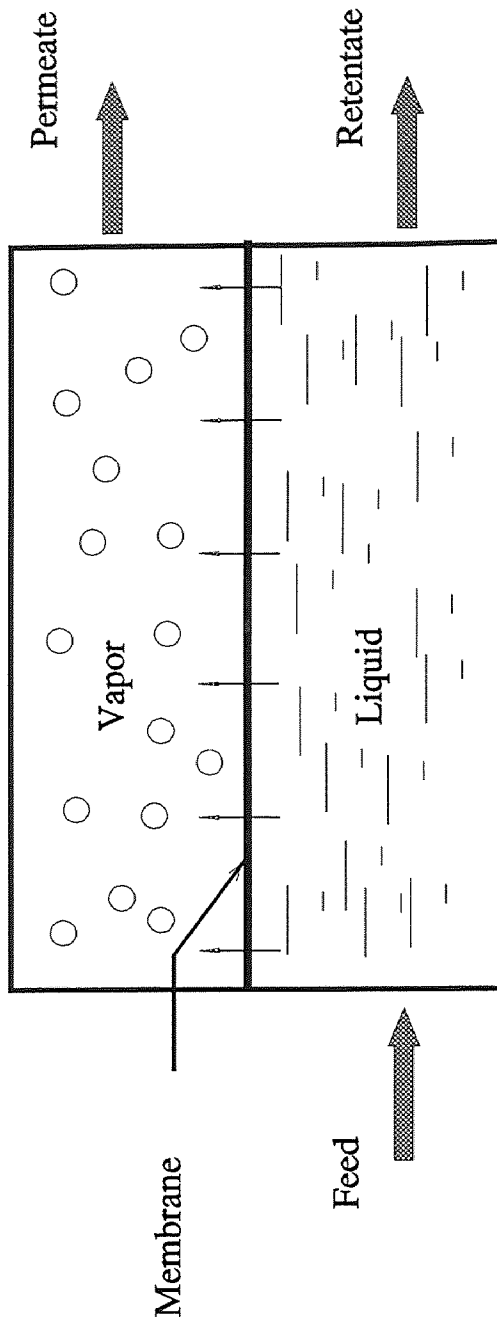
Figure 2.1. Schematic diagram of the pervaporation process

feed is not in direct contact with the VOC-selective plasma polymerized silicone membrane layer. It is akin to the process of evapomeation (Uragami and Saito, 1990; Uragami and Shinomiya, 1992) and may be termed more correctly as 'stripmeation'. In fact, it combines locally air stripping and vapor permeation.

Figure 2.2 shows a schematic of the stripmeation process. In this system, when a vacuum is applied on the permeate side, the feed solution is vaporized. The vapor in the pore is in equilibrium with the feed liquid and Henry's Law may be used to estimate the equilibrium partitioning at the liquid-vapor interface. The vapor in the pore gets absorbed into the membrane, diffuses through it, and then is stripped out of the membrane to the vacuum phase. At high solute concentrations, membrane shrinking and swelling may affect properties such as permeability and selectivity.

T. Uragami and M. Saito (1989) compared pervaporation and evapomeation processes for methanol/water, ethanol/water systems using alginic acid membranes. They reported higher flux and higher separation factor for evapomeation compared to conventional pervaporation. Uragami and Morikiwa(1992), compared pervaporation and evapomeation processes for system, such as methanol/water, ethanol/water, 1-propanol/water while using PDMS membranes. They reported higher selectivity for evapomeation but pervaporation performed better in terms of solute flux. If a temperature difference was maintained in the system, i.e. if the membrane was kept at constant temperature and the feed temperature was increased, the flux and selectivity for the case of evapomeation increased significantly.

14
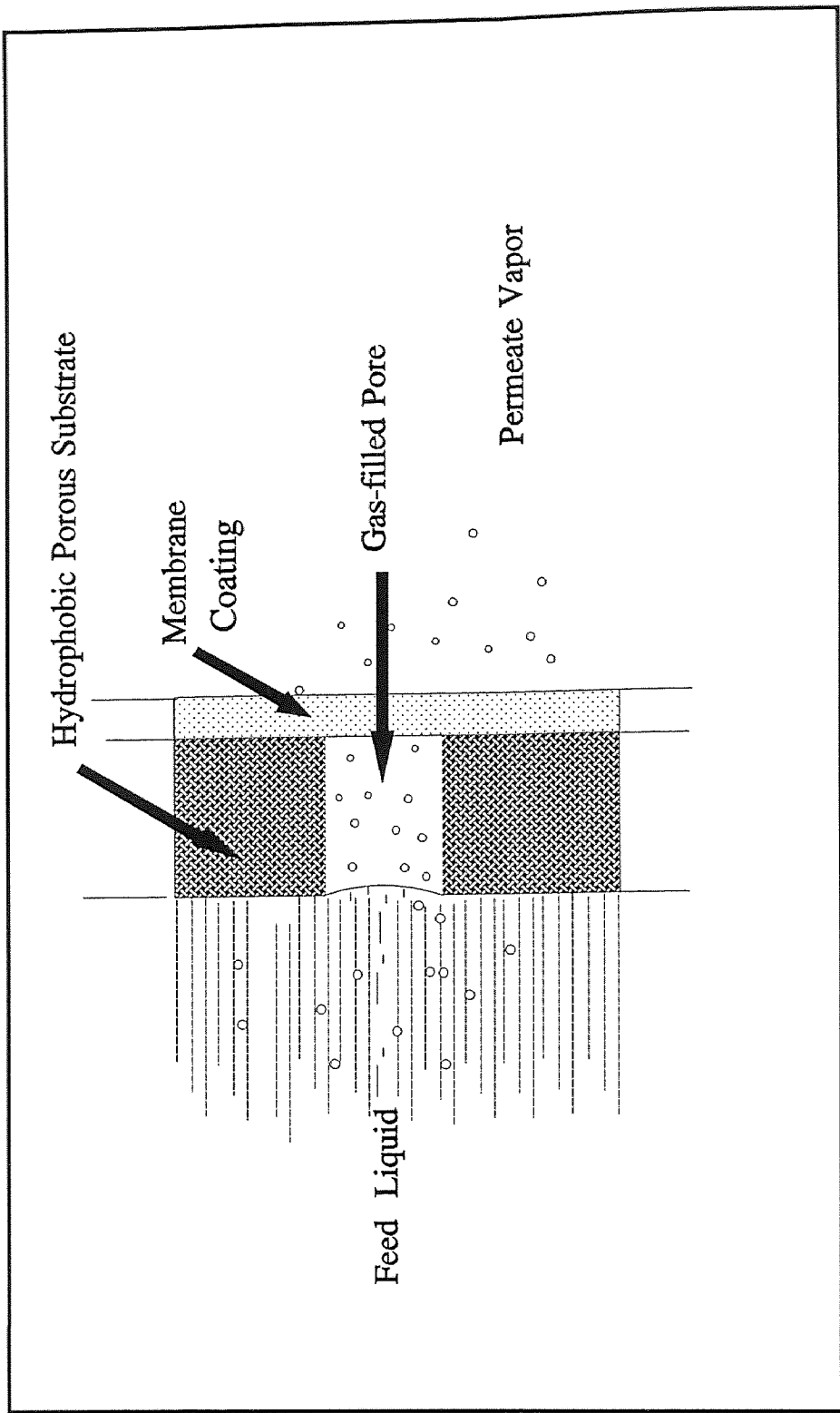
Figure 2.2. Schematic of a hollow fiber membrane based stripmeation process

2.3 Resistances-in-Series Model for the Overall Mass Transfer Coefficient

Consider Figure 2.3 which illustrates the solute concentration profiles in the aqueous solution, the gas-filled pore in the hydrophobic microporous substrate, the ultrathin silicone membrane on the fiber outside diameter and the vacuum region present on the shell side. There are three phase interfaces (aqueous-pore gas; pore gas-silicone membrane; silicone membrane-vacuum side) and four resistances (tube-side aqueous boundary layer; gas-filled pore; silicone membrane; vacuum-side boundary layer). Define three partition coefficients for the three phase interfaces:

$$C_{ili}{}' = H_i C_{igi}{}' \tag{1}$$

$$C_{imi}{}' = m_{vf} C_{igmi}{}' \tag{2}$$

$$C_{imp}{}'' = m_{vp} C_{imi}{}'' \tag{3}$$

where $C_{ipl}{}''$ is a hypothetical liquid phase concentration in equilibrium with the vacuum side gas phase concentration of C_{ip}''. The individual transfer coefficients The molar rate of transfer of species i per unit length of the hollow fiber, R_i, may be expressed in terms of an overall mass-transfer coefficient K_o as well as four individual mass-transfer coefficients as follows:

$$R_i = K_o \pi d_o (C_{il}{}' - C_{ipl}{}'') \tag{4}$$

may be defined by:

aqueous boundary layer : $R_i = k_i^f \pi d_i (C_{il}{}' - C_{ili}{}')$ \hfill (5)
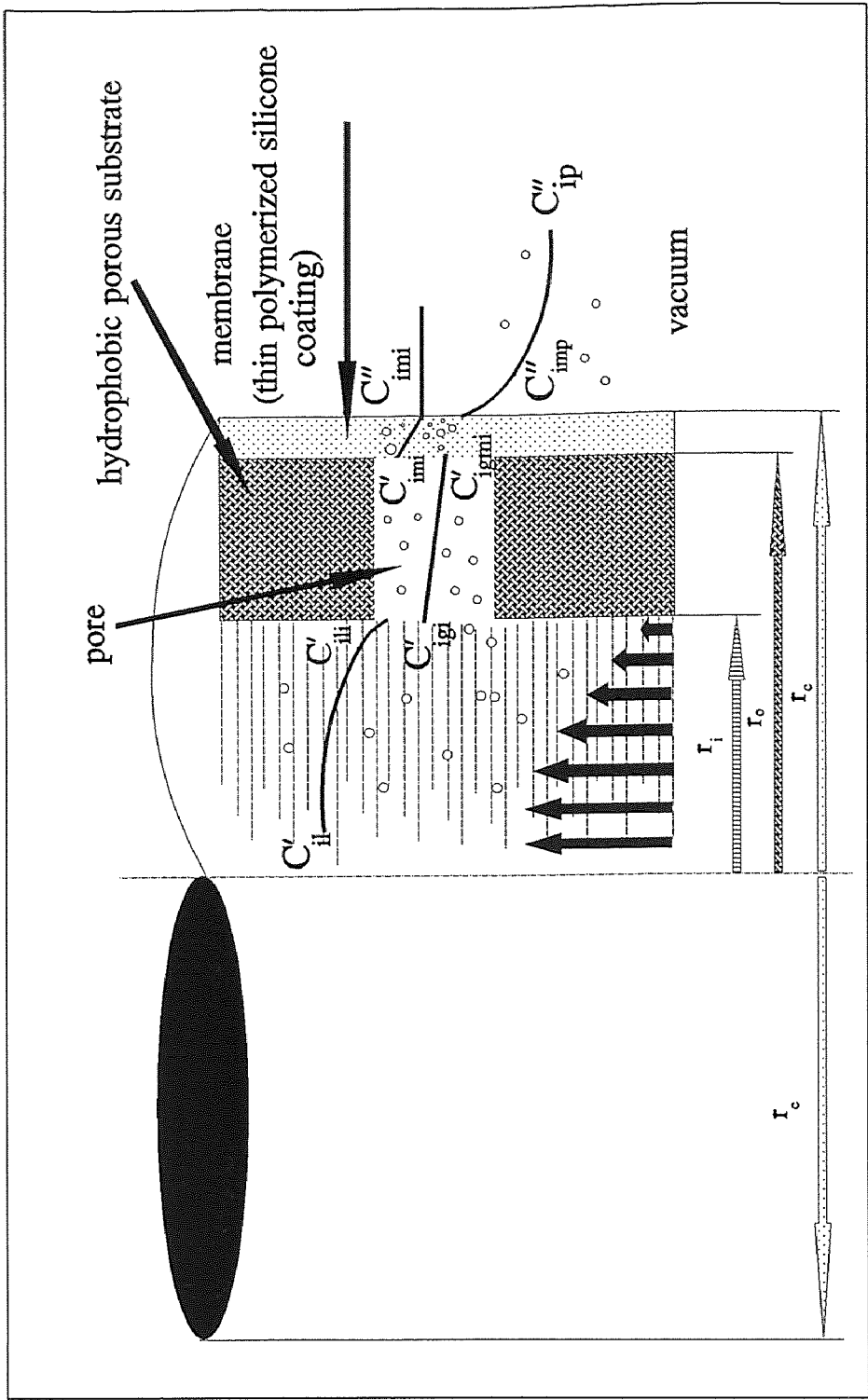
Figure 2.3. Concentration profile of a VOC in a hollow fiber membrane based stripmeation process

$$\text{gas filled pore}: R_i = k_{gp}^f \pi d_{lm}(C_{igi}{}' - C_{igmi}{}') \tag{6}$$

$$\text{silicone membrane}: R_i = k_m \pi d_o (C_{imi}{}' - C_{imi}{}'') \tag{7}$$

$$\text{vacuum boundary layer}: R_i = k_g^p \pi d_o (C_{imp}{}'' - C_{ip}{}'') \tag{8}$$

There will be an additional interfacial resistance at the aqueous solution-pore gas interface if surfactants are present in the system. No such resistance due to a monomolecular surfactant layer has been considered here since surfactants are absent in the stripmeation system under consideration.

At steady state, the R_i s through all of the resistances-in-series are equal to one another and to that in Eq. (4). One can therefore obtain

$$\frac{1}{K_o d_o} = \frac{1}{k_l^f d_i} + \frac{H_i}{k_{gp}^f d_{lm}} + \frac{H_i}{m_{vf} k_m d_o} + \frac{H_i}{k_g^p m_{vf} m_{vp} d_o} \tag{9}$$

The resistance of the vacuum side boundary layer is assumed to be negligible compared to others (Yang et al., 1995). One obtains

$$\frac{1}{K_o} = \frac{d_o}{d_i}\frac{1}{k_l^f} + \frac{d_o}{d_{lm}}\frac{H_i}{k_{gp}^f} + \frac{H_i}{m_{vf} k_m} \tag{10}$$

Of these, it may be easily demonstrated that the mass-transfer coefficient for the gas-filled pore is very large and the corresponding resistance may be neglected in comparison to the other terms:

$$\frac{H_i}{k_{gp}^f} = \frac{H_i}{\dfrac{D_{igp}\varepsilon}{\delta_s \tau}} \cong \frac{2.75}{\dfrac{0.0106994 \times 0.4}{2.5 \times 10^{-3} \times 2.49}}\frac{cm}{sec} = 3.99\frac{\sec}{cm} \tag{11}$$

Here D_{igp}, the diffusion coefficient of the solute in the pore gas phase, is obtained from (Rangarajan et al., 1984)

$$D_{igp} = 1.0133 \times 10^6 r_p \frac{RT}{M_i \overline{c_i}} \qquad (12a)$$

where $\overline{c_i}$, the mean speed of the molecule, is given by

$$\overline{c_i} = (8.1064 \times 10^6 \frac{RT}{\pi M_i})^{\frac{1}{2}} \qquad (12b)$$

The value of H_i, Henry's law constant per Eq. (1), is obtained as 2.75 (mg/L)$_{liq}$ / (mg/L)$_{vap}$ from Turner et al. (1996). δ_S is the fiber substrate thickness given by [(290 − 240)/2] μm=2.5 $\times 10^{-3}$ cm. Since the observed values of the overall mass-transfer coefficient K_o is in the range of 10^{-4} cm/sec, the gas-filled pore resistance in Eq. (10) may be neglected leading to

$$\frac{1}{K_O} = \frac{d_o}{d_i} \frac{1}{k_i^f} + \frac{H_i}{m_{vf} k_m} \qquad (13)$$

Since the mass transfer behavior in laminar flow through the fiber bore is relatively well defined, experimental measurement of the solute vapor permeation transfer coefficient through the nonporous silicone coating ought to allow one to calculate the value of K_o which may then be compared with the experimentally - obtained K_o. The experimental strategy adopted in this thesis therefore includes separate determination of the vapor permeation-based removal of TCE from N$_2$ through the silicone membrane when both sides have gaseous phases and no liquid phase. It must be noted here that the value of k_i^f here corresponds to a somewhat variable boundary condition, namely, the TCE concentration at the silicone membrane coating changes along the fiber length. The

solutions that are available for tube-side laminar flow mass transfer with developing concentration boundary layer correspond to constant wall flux or constant wall concentration (Skelland, 1974); the corresponding limiting values of the Sherwood number at very low Graetz numbers are 4.36 and 3.56 respectively. This will introduce some uncertainty in the estimates of k_i^f to be used in Eq. (13) to calculate K_o.

The expression for Sherwood number for laminar fully developed velocity profile in a tube of length 1 with constant wall concentration is given by the expression (Skelland, 1974)

$$Sh\Big|_{lm} = \frac{k_i^f d_i}{D_{il}} = \frac{1}{4}(\frac{d_i}{l})ReSc \ln\left[\sum_{j=1}^{j=0}\frac{-4B_j}{\beta_j^2}(\frac{d\phi_j}{dr_+})_{r_+=1}\exp(\frac{-\beta_j^2(x/r_i)}{ReSc})\right]^{-1} \tag{14}$$

Note that this is based on the logarithmic-mean concentration difference over the whole tube. The value of k_i^f is calculated from Eq. (14) for substitution in Eq. (13).

CHAPTER 3

MATERIALS AND METHODS

3.1 Chemicals and Gases Used

Trichloroethylene (purity 99.9%, FW 131.39, density 1.456 g/cc), methanol (purity 99.9%, FW 32.04), from Fischer Scientific (Springfield, NJ); ultrapure nitrogen, helium, air, trichloroethylene and liquid carbon dioxide from Matheson (E. Rutherford, NJ).

3.2 Hollow Fiber Membrane Modules

The hollow fiber membrane modules contained hydrophobic microporous hollow fiber substrate (240 μm/290 μm ID/OD; polypropylene Celgard X-10, Hoechst Celanese, Charlotte, NC) having a plasma polymerized thin nonporous silicone (PDMS) skin on the outer surface. The geometrical characteristics of the module are given in Table 3.1. Detailed fabrication procedure is provided in Chandra (1996).

3.3 Experimental Setup

3.3.1 Modified Pervaporation Experiments

The experimental setup for pervaporation is shown schematically in Figure 3.1. The feed solution was pumped into the hollow fiber module from a collapsible Teflon feed bag(Cole Parmer, Vernon Hills, IL) which prevented formation of headspace during the experimental run. A peristaltic Masterflex pump with a digital console drive (Model 7523-20, Cole Parmer, Vernon Hills, IL) was used for pumping the feed solution. Teflon bags of different capacities, 1.2, 2.1, 4.7 and 18.8 liters were used depending on the flow

Table 3.1. Module Characteristics

Module No.	Fiber Substrate	Membrane Coating	No. of Fibers	I.D (μm)	O.D (μm)	Active Length (cm)	Mass Transfer Area Based on O.D. (cm^2)	Remarks
1.	Celgard* (X-10)	Silicone**	75	240	290	20.5	140.1	Fabricated in lab

* Porosity (ε_m) is 0.3 and tortuosity (τ_m) is 3.5 (Prasad and Sirkar ,1988)

** Plasma polymerized by AMT Inc., Minnetonka, MN.
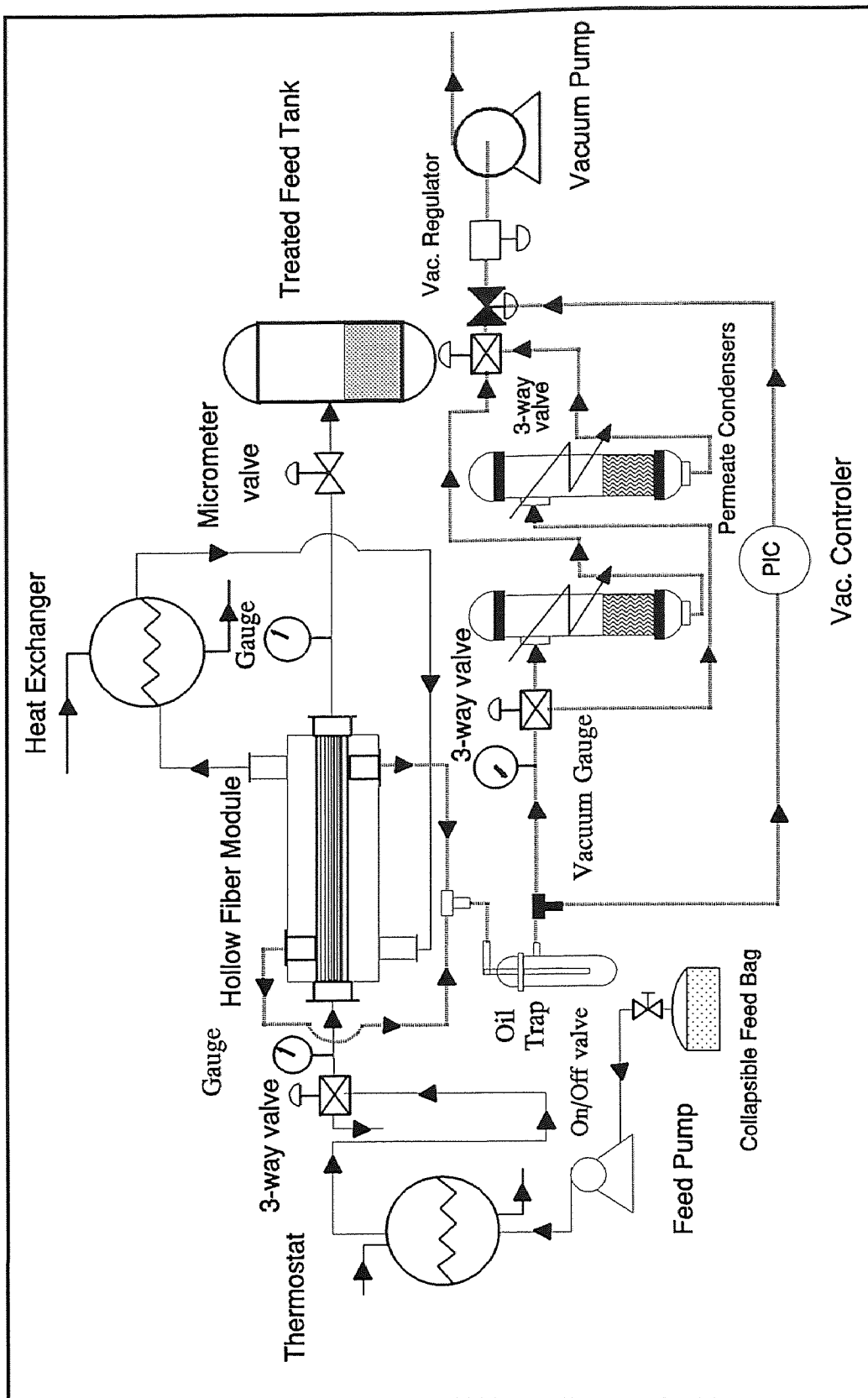
Figure 3.1. Schematic of experimental setup for VOC removal from feed solutions with or without surfactants

rate and duration of the experiment. Transparent ¼ inch ID Teflon tubing (Cole Parmer, Vernon Hills, IL), and stainless steel fittings (Swagelok, R.S. Crum, New Bruswick, NJ) were used for the feed reservoir and all connecting lines to and from the membrane module. The feed line was connected to a three-way valve (Swagelok, R.S Crum, New Brunswick, NJ) for collection of feed samples. Feed pressure was monitored by using two dial pressure gauges (Cole Parmer, Vernon Hills, IL) at the inlet and outlet respectively. A micrometering valve (Swagelok, R.S Crum, New Brunswick, NJ) was connected to the feed line to regulate the feed pressure. An oilless vacuum pump (KNF, Neuberger, Trenton, NJ, Model UN 726.112 FTP) was used to maintain a vacuum of 20-25 torr. The permeate pressure was controlled by a Digital Vacuum Regulator Model 2000 (J-Kem Scientific St. Louis, MO). Convoluted Teflon tubes (Cole Parmer, Vernon Hills, IL) were used for the vacuum line connection to the condensers. The module was immersed in a polyethylene water bath interfaced to a thermostat (Fischer Scientific, Springfield, NJ) to maintain the desired temperature. Two condensers (Labglass, Vineland, NJ) with a graduated tip were connected in parallel to the vacuum line before the vacuum pump. Dry ice and methanol were used as the cooling medium in Dewar flask (Labglass, Vineland, NJ) inside which the condenser was kept to trap the permeate vapor from the module outlet. The purpose behind using two condensers was to control the permeate collection in two stages, the non-steady and steady-state process operation. The condenser and the feed lines were insulated with glasswool and aluminum foil.

3.3.2 Vapor Permeation Experiments

The experimental setup used for vapor permeation experiments is shown schematically in Fig 3.2. Two streams of gases were used: TCE in nitrogen and pure nitrogen. The flow rates of the two streams were monitored using a Matheson digital readout and control module. Three way valves (Swagelok, R.S Crum, New Brunswick, NJ) V1,V2 and V3 were used at the inlet and the outlet of the module to measure different gas flow rates. All valves had one end connected to an electronic bubble flowmeter (Matheson, E. Rutherford, NJ) marked as BFM in the figure. Stainless steel fittings (Swagelok, R.S. Crum, New Brunswick, NJ) were used for all connecting lines to and from the membrane module. The condenser and the feed lines were insulated with glasswool and aluminum foil. Feed pressure was monitored by a dial pressure gauge (Cole Parmer, Vernon Hills, IL) at the inlet. An oilless vacuum pump (KNF, Neuberger, Trenton, NJ, Model UN 726.112 FTP) was used to maintain a vacuum of 20-25 torr. The permeate pressure was controlled by a Digital Vacuum Regulator Model 2000 (J-Kem Scientific St. Louis, MO). Convoluted Teflon tubes (Cole Parmer, Vernon Hills, IL), were used for the vacuum line connection to the condenser. Experiments were performed at 25°C. One condenser (Labglass, Vineland, NJ) with a graduated tip was connected in parallel to the vacuum line before the vacuum pump. Dry ice and methanol were used as the cooling medium in a Dewar flask (Labglass, Vineland, NJ).
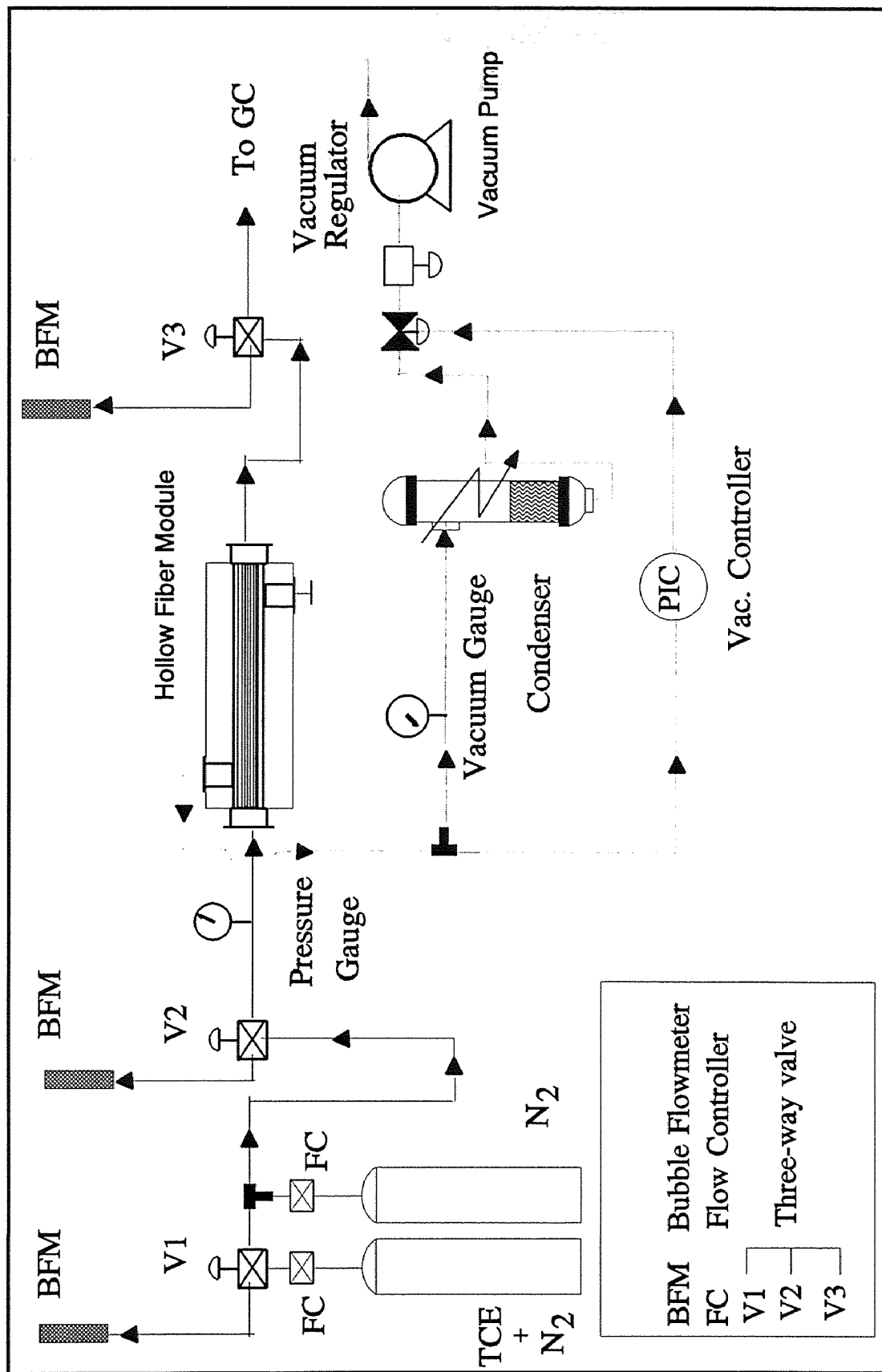
Figure 3.2 Experimental setup for vapor permeation

3.4 Experimental Procedure

3.4.1 Modified Pervaporation Experiments

3.4.1.1 Preparation of Feed: Fresh feed for modified pervaporation experiments was prepared before each experiment to avoid volatilization of TCE. A stock solution of desired surfactant concentration was prepared at least 48 hours before the experiment for proper micelle formation. To prepare a desired concentration of surfactant (w/v), deionized water was heated just above the Kraft Point of SDS (18°-20°C) before adding the surfactant. This enhanced instant solubilization of the surfactant and micelle formation instead of dissociation into ions. This surfactant solution was kept in slow stirring condition for a minimum of 48 hours before adding the TCE. The feed was prepared in a glass vessel with a minimum headspace to avoid volatilization of TCE.

3.4.1.2 Sampling: Sampling of feed and retentate in modified pervaporation experiments was done very carefully to avoid any kind of loss during sample collection and dilution. The feed line was connected to a three-way valve for collection of feed sample. Feed and retentate samples were tested every half hour in the gas chromatograph (GC)/Headspace. At the time of feed sample collection, the three-way valve was opened and the feed was allowed to flow for a minute to avoid any error arising from any stagnant feed in the collection line. Samples were collected in a small 2 ml glass vial and capped immediately with a Teflon-lined cap to avoid TCE loss. For analysis in the GC/Headspace, 13 μl of the sample was taken in a high precision Hamilton microsyringe and was directly injected to a headspace vial of volume 22.5 ml. Same procedure was followed for the retentate sample for the GC.

3.4.1.3 Experiment: The feed solution was pumped from the Erlenmeyer flask into the collapsible Teflon bag before the start of an experimental run. As the collapsible bag prevented headspace formation, TCE volatilization was minimal which kept the feed concentration nearly constant. Feed was kept at a pressure range of 5-7 psig by using a back-pressure micrometer control valve (Swagelok, R. S. Crum, New Brunswick, NJ) in the retentate line. Feed pressure was monitored by using a dial pressure gauge. Vacuum was tested at 20 torr before starting the system. The temperatures of the water bath and the thermostat were fixed at the desired set point before start-up. Almost all experiments were performed at a constant temperature of 25° C. Dry ice was prepared in a dry ice machine using liquid carbon dioxide. Dewar flasks were filled with dry ice and methanol after putting in the condenser to achieve a low cooling temperature (approx. -50°C). Samples were taken every half hour and analyzed. The system generally achieved steady state after 3 hours, after which two 3-way valves were switched to the second condenser for steady state permeate collection. Normal runs were carried out for 6-8 hours. The experiment was stopped once consistent results were obtained from 6 consecutive samples. The volume of the permeate was observed and noted from the collection in the condenser. The volume of water and the VOC could be easily noted as the permeate separated into two distinct organic and aqueous phases. For accurate measurement of water flux, the steady state condenser was weighed before and after each day's experiment using a high precision electronic balance (Mettler, Toledo, OH). After every experiment the module was washed for a few hours with deionized water and filtered nitrogen was passed overnight to dry it before another experiment. For experiments using

surfactant solution as feed, the module was washed with warm water to ensure that the module was free of any residual surfactant molecules.

The TCE pervaporation experiments were planned in three phases. In the first phase experiments were done using aqueous solutions of TCE as feed. The second phase used surfactant solutions containing TCE as feed. In the third phase, experiments were carried out with wetted pores so that one gains a better understanding of the surfactant system. Almost all experiments in the study were repeated at least twice to avoid any experimental error. An experiment was reported if both results were consistent. For reporting purpose, data from one of the experiment from each set and not the average value were taken.

3.4.2 Vapor Permeation Experiments

For vapor permeation experiments the following procedure was followed. At the very outset, vacuum was tested at 20 torr and the condenser was filled with dry ice and methanol to achieve a low cooling temperature (approximately -50°C). The temperature of the water bath was set at 25 °C. The feed gas, which was passed through the tube side, was prepared from two gas streams, TCE in nitrogen and pure nitrogen. Nitrogen was used to dilute the TCE concentration in the feed gas. The flow rates of the TCE-nitrogen and pure nitrogen gas streams were set according to the desired TCE concentration. In the course of the experiment, two TCE-containing N_2 cylinders having TCE concentrations of 220 ppm and 935 ppm were used. The flow rates of TCE and nitrogen were measured by opening V1(Figure 3.2) to the bubble flow meter. During this period, only pure nitrogen gas stream was entering the hollow fiber membrane module and V2 was

switched to the bubble flow meter (BFM) to measure the flow rate of pure nitrogen. When V1 was switched back, both gas streams, TCE-containing nitrogen and nitrogen were entering the module. V2 was then switched to the BFM to measure the total feed gas flow rate. From such measurements, the individual flow rates of the two gas streams were obtained; this allowed the calculation of the concentration of TCE in the feed gas; the value of the total feed flow rate was also obtained. The outlet gas flow rate was measured by switching V3 to the BFM connected to it. Flow rates were measured every 30 minutes. The TCE concentration in the outlet stream was measured by the GC two hours after starting the experiment so that the data collected corresponded to steady state results. After five consistent readings, the experiment was stopped. The flow rates of TCE and nitrogen were reset to some other appropriate values such that one now had a feed gas with a different TCE concentration and the whole procedure was repeated.

3.4.3 Wetted-Pore Experiments

The experimental procedure followed for wetted pore experiments was similar to that for pervaporation experiments, except that the pores of the hollow fiber membrane were wetted prior to starting the experiment. The technique used to wet the pores was similar to that employed by Bhave and Sirkar (1986). The following were the steps performed to wet the pores:

a) Pass an aqueous solution of ethyl alcohol (40%v/v) on the tube side of the hollow fiber membrane module at a flow rate of 0.6 mL/min for a period of three hours.

b) Pass pure water on the tube side of module at a flow rate of 0.6 mL/min for a period of three hours.

c) Repeat steps (b) and (c).

It is assumed that by following the above procedure, water will be immobilized within the pores for the entire thickness of the support (Bhave and Sirkar, 1986). Such a film is considered fully exchanged and is referred to as Immobilized Water Membrane (IWM). In this thesis the term "wetted pores" would always refer to an IWM. After the pores are wetted, the experimental procedure described in Section 3.4.1 is followed.

3.5 Analytical Procedure

3.5.1 Modified Pervaporation Experiments

3.5.1.1 Headspace Gas Chromatography: Aqueous TCE concentration was measured in a HP 6890 series gas chromatograph (GC) using a HP 7694 Headspace Sampler and HP 6890 series integrator (Hewlett Packard, Wilmington, DE). TCE was analyzed by a flame ionization detector (FID) using a HP-5 capillary column (crosslinked 5% PH ME Siloxane) of 30 m length, 320 μm diameter and 1 μm film thickness (Hewlett Packard, Wilmington, DE). Ultrapure nitrogen was used as the carrier gas. Analysis of TCE in aqueous solutions of varying surfactant concentrations posed difficulties in reproducing results using the direct liquid injection headspace techniques because of their sensitivity to matrix variation. It also required proper calibration curves for each sample matrix. This was extremely difficult as the compositions of the samples varied widely or were unknown. The methodology of Full Evaporation Technique (FET) was used to overcome the matrix effect (Markelov and Guzowski, 1993).

This technique was based on a near-complete transfer of analytes from a condensed matrix into a vapor phase. This transfer eliminated the possibility of

contamination from any nonvolatile component in the sample such as SDS, and also the calibration was not affected by the sample matrix. The concept behind the full evaporation technique was to reduce the sample size and increase the temperature to eliminate the matrix effect. Reproducible results were obtained by using 13 μl of sample in a 22.5 ml headspace vial. The optimum headspace oven temperature (100°C), sample volume (13 μl) and sample equilibration time (5 min) were determined after an extensive study by varying each of these parameters one at a time. Sample vials were thermostated in the headspace analyzer for 5 minutes at 100°C.

Headspace vapors were analyzed by pressurizing the vials for 0.15 minute followed by a timed injection of the vapors for 1 minute into the gas chromatographic column. A temperature program was fixed for the GC in order to get clear separation of TCE. The initial oven temperature of the GC was set at 40°C for 1.5 min. In the next step, temperature was ramped at 25°C per min until it reached 75°C, where it was kept for 1 min. In the final step, the temperature was ramped at 40°C per min., until it reached the final temperature of 160°C, which was maintained for 3 min. The carrier gas flow rate was set at 5.0 mL/min. The GC was calibrated every two months to ensure that the correct value for the response factor was being used for the purposes of calculation. Figure 3.3 illustrates the GC calibration plot. The response factor for TCE was calculated to be 0.001868 and did not show significant variation.

3.5.2 Vapor Permeation Experiments

3.5.2.1 Gas Chromatography: In the vapor permeation experiments, the TCE concentration in N_2 at the outlet of the hollow fiber membrane module was measured using
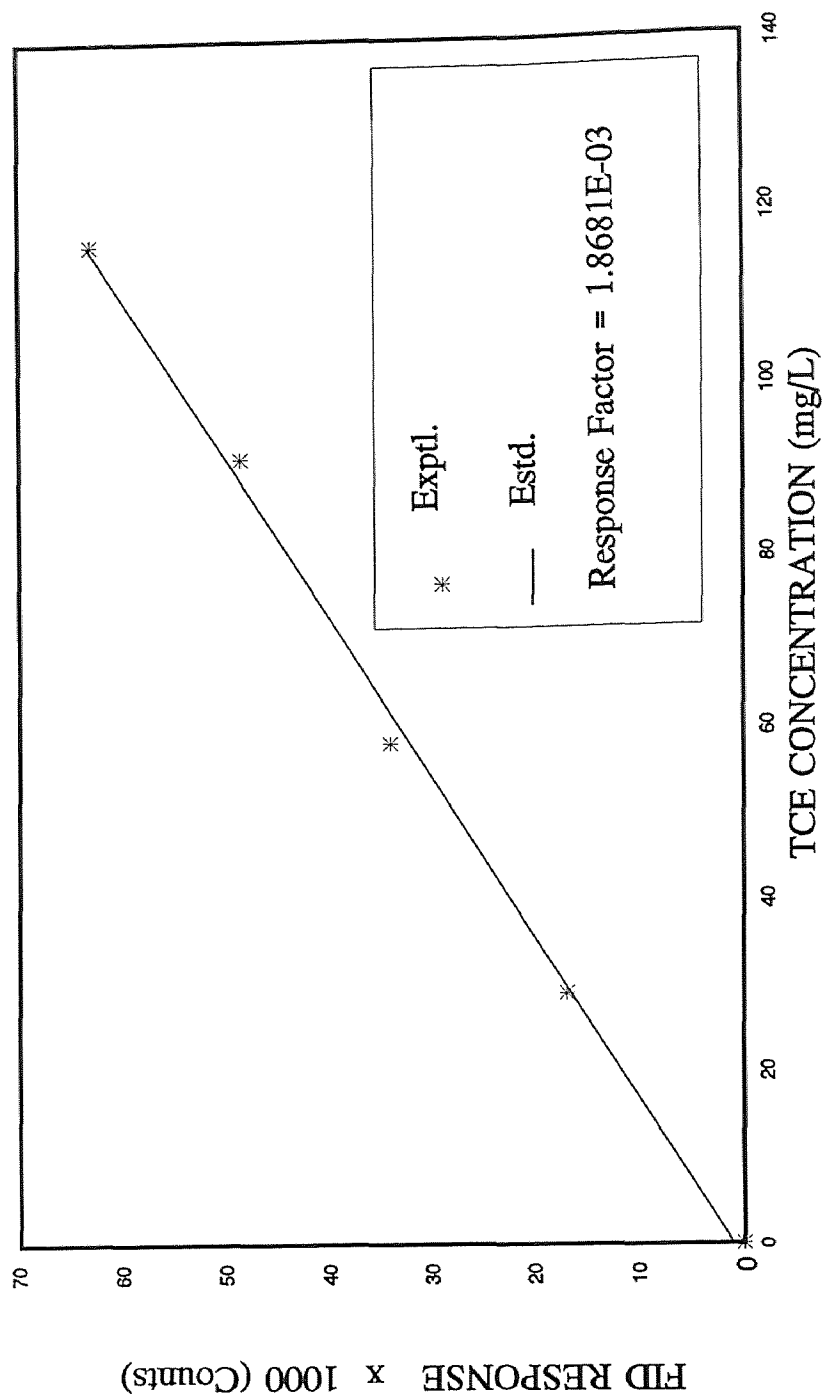
Figure 3.3. Callibration of the FID response for TCE

(HP 6890 GC; Carrier gas Nitrogen=5mL/min; Total flow =2.5 mL/min; Headspace oven =100 C; FID Temp. = 250 C)

a Varian 3400 gas chromatograph (Varian Associates, Sugarland, TX) having a flame ionization detector ; the column employed was a 0.3% Carbowax 20M, Carbopack C, Mesh 80/100, 0.85″ ID, 0.1625″ OD. The carrier gas was helium and the flow rate was maintained at 10 mL/min. The oven, FID and injector were maintained at temperatures of 150 °C, 220 °C and 250 °C respectively. The GC was calibrated for TCE before measurements were made. The calibration plot is shown in Figure 3.4.

3.6 Calculated Quantities

The fluxes of TCE and water were obtained respectively from the volumes of the TCE phase and water phase collected over time t from the membrane of area A_m:

$$J_i = \frac{V_{TCE}\rho_{TCE}}{A_m t} \tag{15a}$$

$$J_W = \frac{V_{H_2O}\rho_{H_2O}}{A_m t} \tag{15b}$$

where J_i and J_w are TCE flux and water flux respectively.

Here A_m is defined as $A_m = \pi d_o N l$ (15c)

where N is the number of hollow fibers of outside diameter d_o and length l. The Reynolds number for flow inside the fiber is defined by

$$Re = \frac{d_i \rho_{H_2O} v}{\mu_{H_2O}} \tag{16}$$

where the velocity of the solution v is obtained from

$$v = \frac{4Q}{60 N \pi d_i^2} \tag{17}$$
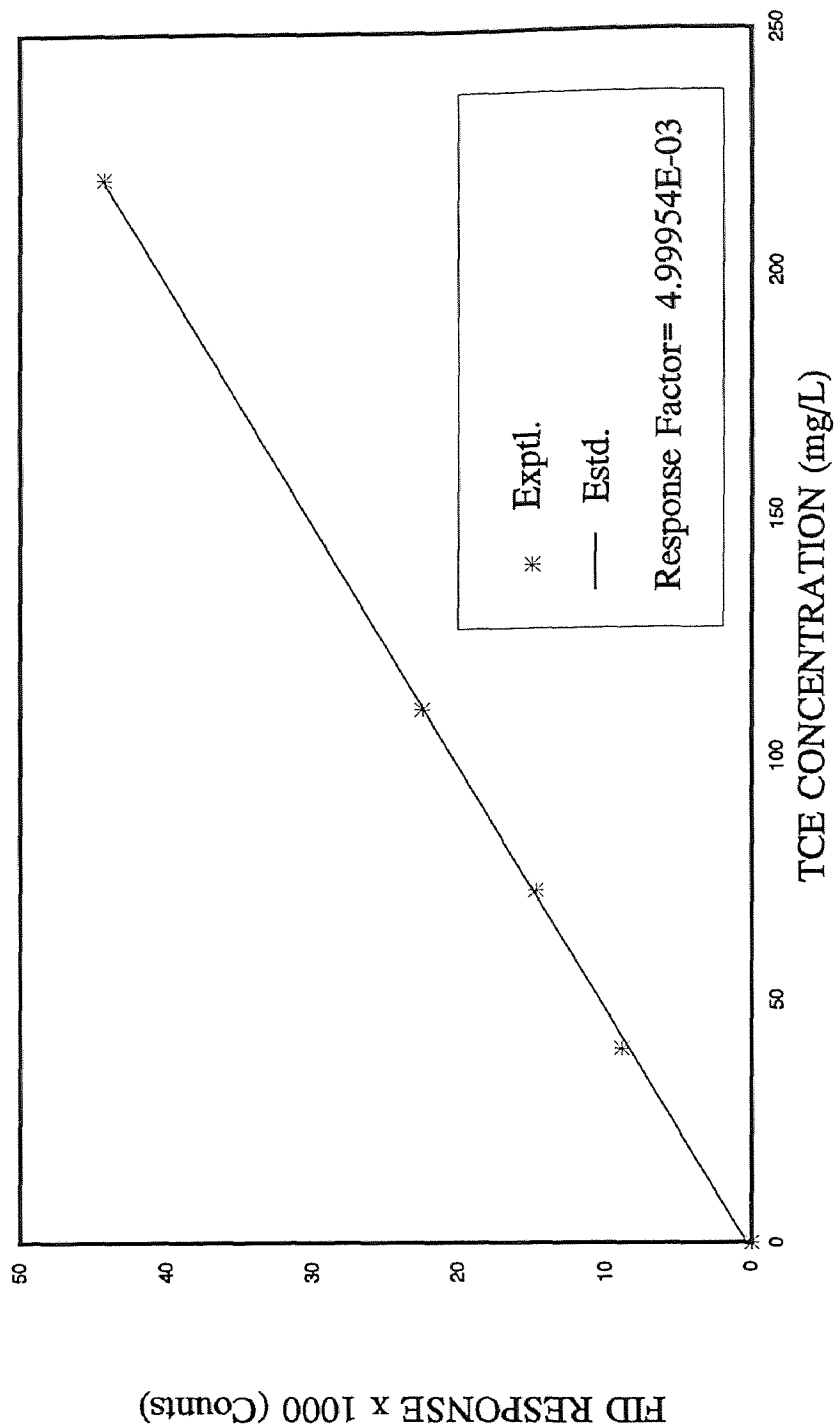
Figure 3.4. Calibration of the FID response to TCE for vapor permeation experiments

(Varian 3400 GC; Carrier Helium =10mL/min; Oven=150 C; FID Temp=220 C; Injector=250 C)

for a volumetric flow rate of Q cc/min. The overall mass transfer coefficient K_o for TCE is obtained from

$$J_i = K_o \, \Delta C_{lm} \tag{18}$$

where ΔC_{lm} is obtained from

$$\Delta C_{lm} = \frac{(C_{inlet} - C_{inlet}^p) - (C_{outlet} - C_{outlet}^P)}{\ln\left[\dfrac{(C_{inlet} - C_{inlet}^p)}{(C_{outlet} - C_{outlet}^P)}\right]} \tag{19}$$

We have assumed that C_{inlet}^p as well as C_{outlet}^p may be neglected in comparison to C_{inlet} and C_{outlet} respectively. The Sherwood number is defined as

$$Sh = \frac{K_o d_o}{D_{il}} \tag{20}$$

where D_{il} is the diffusivity of TCE in water. Percent removal of TCE is defined as

$$\% \, removal = \frac{C_{inlet} - C_{outlet}}{C_{inlet}} \times 100 \tag{21}$$

The permeance , $m_{vf} k_m$, is calculated using

$$J_i^v = m_{vf} k_m \Delta C_{lm}^v \tag{22}$$

where J_i^v is the permeate flux and ΔC_{lm}^v is defined by

$$\Delta C_{lm}^v = \frac{(C_{inlet}^{'} - C_{inlet}^{''}) - (C_{outlet}^{'} - C_{outlet}^{''})}{\ln\dfrac{(C_{inlet}^{'} - C_{inlet}^{''})}{(C_{outlet}^{'} - C_{outlet}^{''})}} \tag{23}$$

CHAPTER 4

RESULTS AND DISCUSSION

This section discusses the experimental results obtained in the course of the study. Initially, the results of the first phase i.e., TCE-water system without any surfactants will be presented and analyzed. Thereafter, the vapor-permeation experimental results are discussed and the value of the membrane resistance is estimated using experimental data and theoretical solutions. The third section of this chapter will report and analyze data from experiments carried out with the TCE-water-SDS system. The last section discusses results from experiments performed with wetted pores.

4.1 TCE-Water System

The effect of various parameters on the removal of TCE from an aqueous solution is considered. All experiments have been conducted at a constant temperature, namely 25°C. Aqueous solution containing a specified concentration of TCE was passed through a hollow fiber module at a particular flow rate. TCE flux, water flux and mass transfer coefficient were calculated according to Eq.(15a), Eq.(15b) and Eq.(18) respectively. The experiments were usually carried out for six hours and sampling was done three hours after the start to ensure that steady state had been achieved.

4.1.1 Tube Side Experiments

Experiments were conducted with the aqueous feed flowing through the lumen of the hollow fiber membrane module. Vacuum was pulled on the shell side. As the feed had no

surfactants, the pores of the hollow fiber were non-wetted i.e. the pores were filled with vapor in air and the silicone membrane was not in contact with the liquid feed. Hence the mode of operation was not pervaporation but stripmeation.

4.1.1.1 Effect of Feed Concentration: The first set of experiments were carried out by varying the TCE concentration. Six experimental runs were performed with the TCE concentration ranging between 180 ppm to 960 ppm. The feed flow rate was maintained at 2.5mL/min for all runs. The observed pressure drop over the module was 2 psig. Figure 4.1 shows the % TCE removal and TCE flux as a function of TCE concentration. TCE removal appears to be reasonably constant varying between 92% and 96%. The TCE flux shows a linear increase with concentration from 5.6 x 10^{-6} g/cm^{2}min to 1.24 x 10^{-5} g/cm^{2}min. The data for water flux are plotted in Figure 4.2. Water flux appears to be unaffected by the change in TCE concentration. As the TCE concentration changes from 180 ppm to 960 ppm, the value of water flux varies from 4.07 x 10^{-5} g/cm^{2}min to 4.81 x 10^{-5} g/cm^{2}min. This variation is within experimental error. Figure 4.3 plots the TCE mass transfer coefficient as a function of TCE concentration. The TCE mass transfer coefficient appears reasonably constant and has an average value of 8.6 x 10^{-4} cm/s. This is expected because theoretically, the mass transfer coefficient is independent of feed concentration and depends on the hydrodynamics and other resistances in the transport path.

4.1.1.2 Effect of Feed Flow Rate: These experiments were carried out at feed flow rates varying from 2.5 mL/min (*Re*=3) to 180mL/min (*Re*=200). TCE concentration was kept in the range of 800 to 900 ppm. Pressure drop over the module showed a
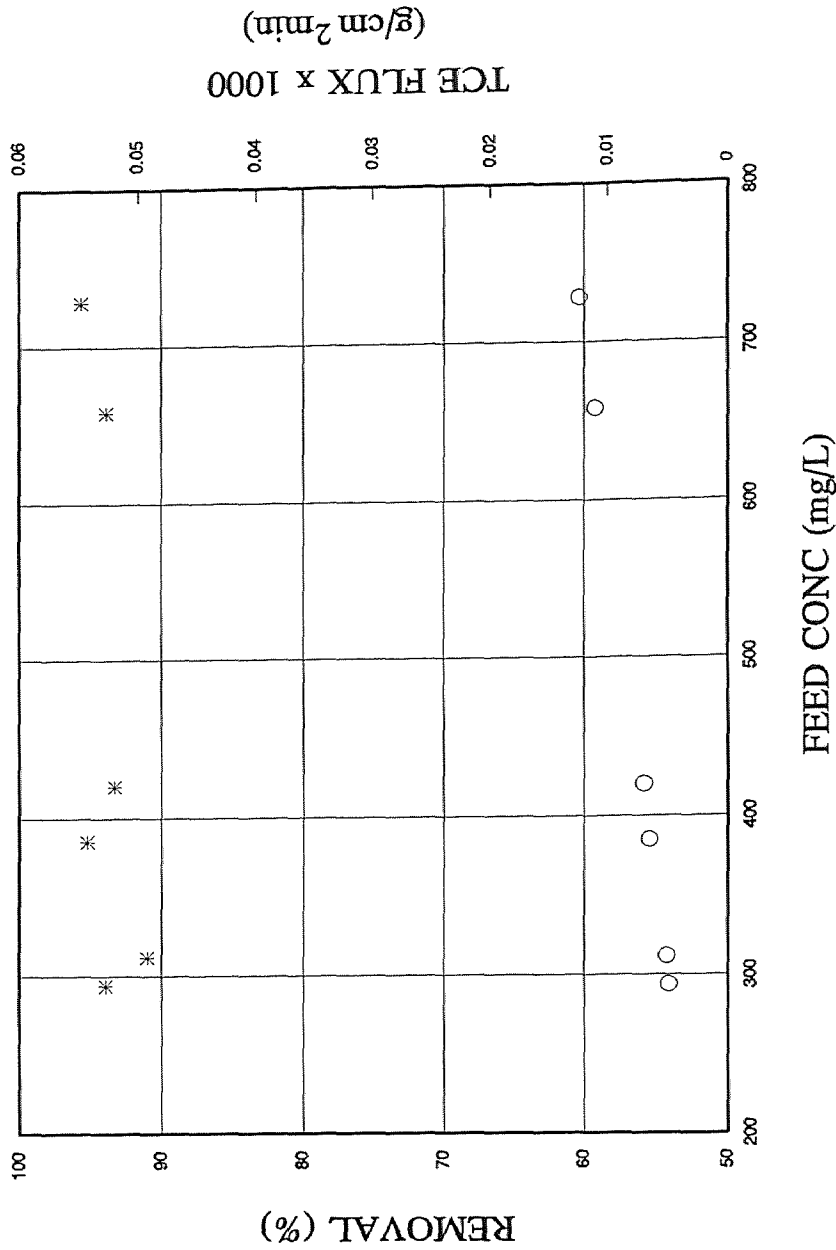
Figure 4.1. TCE removal and TCE flux in stripmeation process.

(Flow Rate = 2.5 mL/min; Vac. = 20 torr; TCE= 200-800 ppm)

✳ Removal   ○ TCE Flux
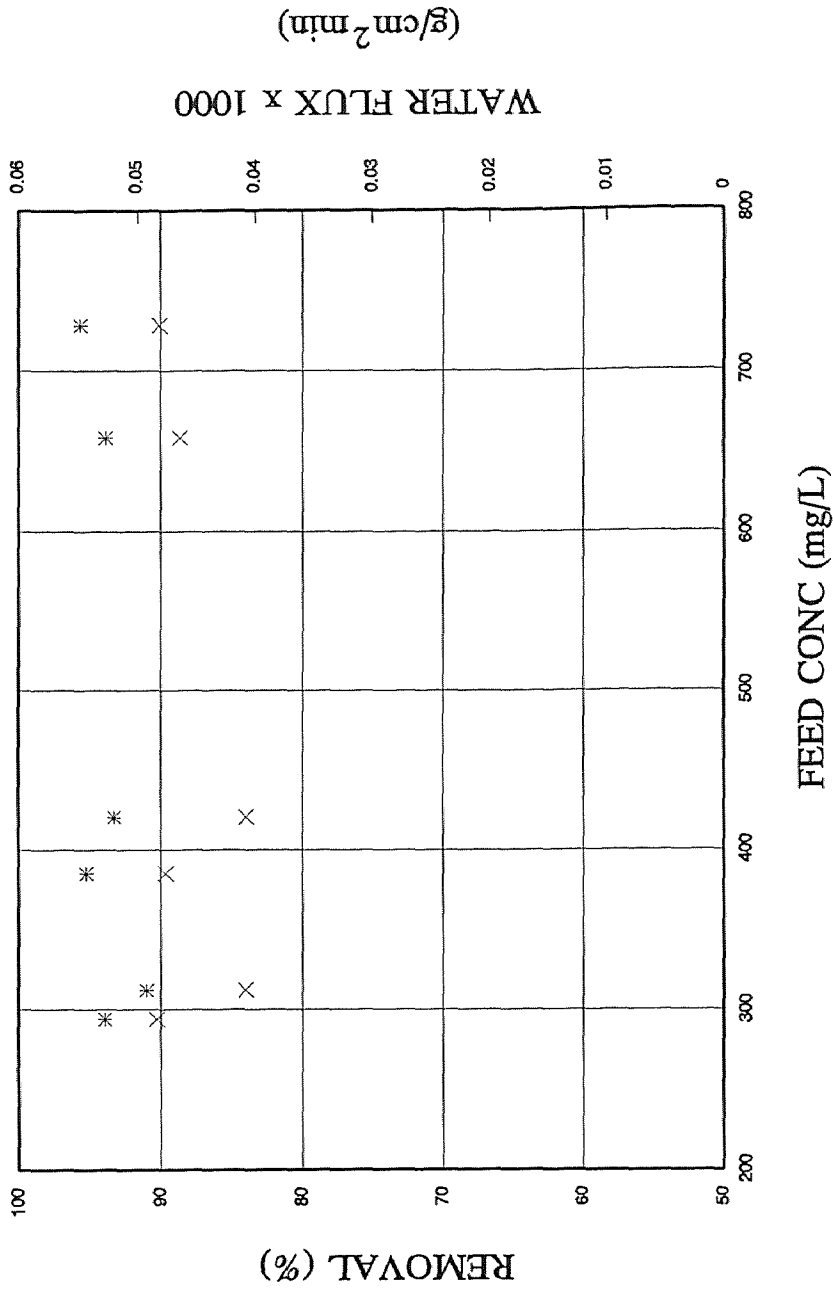
Figure 4.2. TCE removal and water flux in stripmeation process

(Flow Rate = 2.5 mL/min; Vac. = 20 torr; T=25 C; TCE= 200-800 ppm)

✳ Removal   ✕ Water Flux
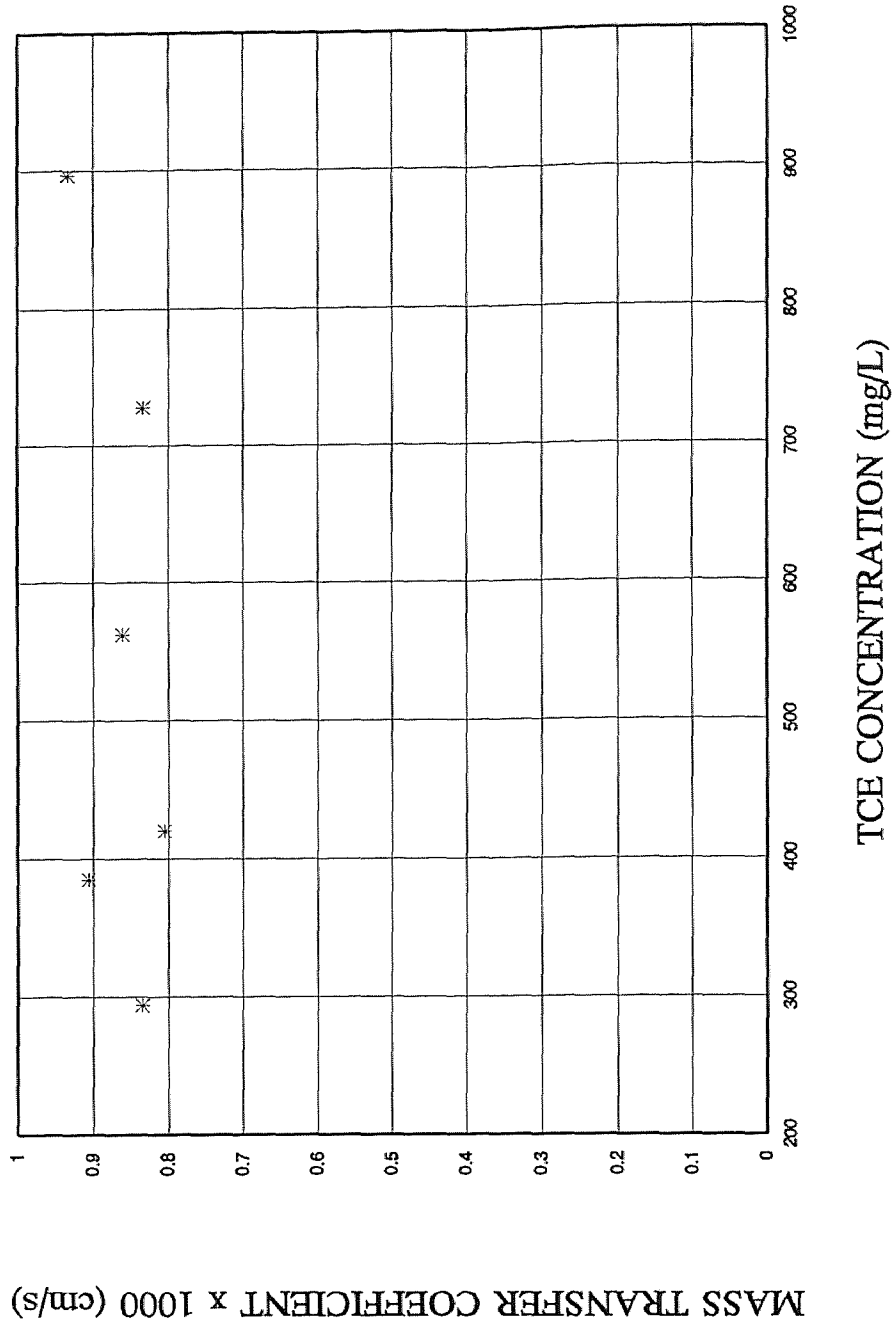
Figure 4.3. TCE mass transfer coefficient in stripmeation process

(Flow Rate =2.5 mL/min; Temp= 25C; Vac. = 20 Torr; TCE =200-800ppm)

significant increase with increase in flow rate as shown in Figure 4.4. Pressure drop increased from 2 psi at a feed flow rate of 2.5 mL/min to 26 psi at a feed flow rate of 180 mL/min. Figure 4.5 shows the TCE removal and TCE flux as a function of the feed flow rate. Removal of TCE drops from 96% at 2.5 mL/min to 9% at 180 mL/min. This is expected because with an increase in flow rate, the residence time gets reduced. Since the membrane mass transfer area is fixed, the extent of TCE removal drops drastically. TCE flux shows a steady increase with increase in feed flow rate. This is an expected result because as the flow rate was increased much more TCE was pumped into the system. Figure 4.6 reports data on water flux. Water flux seems to be unaffected by the changing flow rate and has an average value of 0.04 $g/cm^2 min$. The mass transfer coefficient based on definition in Eq.(18) and the logarithmic concentration difference in Eq.(19) has been plotted in Figure 4.7 as a function of the fiber bore Reynolds number. In the same figure, the mass transfer coefficients according to the Leveque solution and the Graetz solution (Skelland, 1974) are plotted. The mass transfer coefficient obtained from the experimental data represents the overall mass transfer coefficient while the Leveque solution and the Graetz solution yield the theoretical value of the feed side boundary layer mass transfer coefficient. The plot clearly shows that the observed total mass transfer resistance is significantly larger than that due to the feed side boundary layer resistance in the fiber bore. Eq.(13) would suggest this difference to be due to the silicone membrane resistance. This aspect is studied in section 4.2.

42
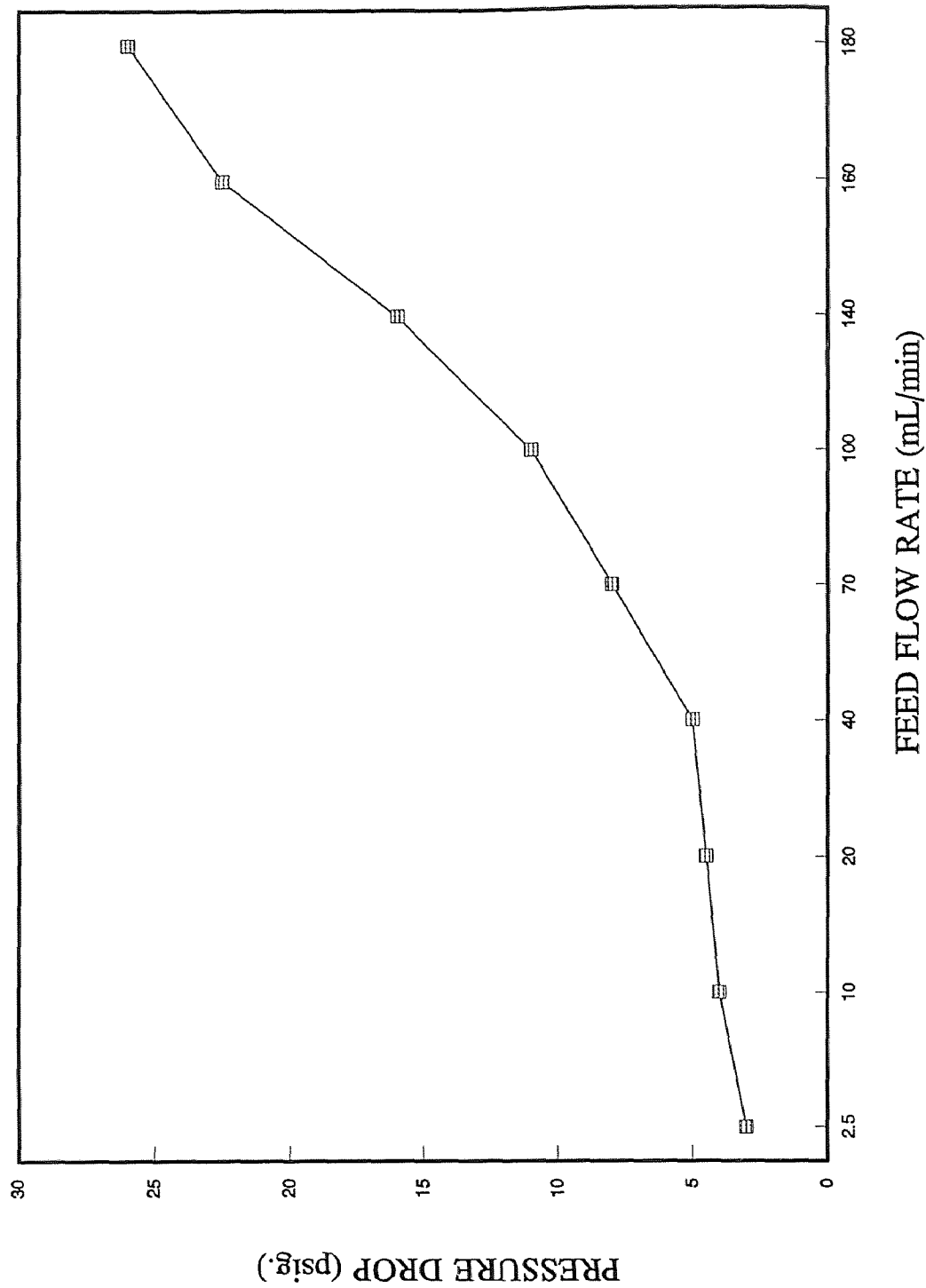
Figure 4.4. Effect of hydrodynamics on pressure drop over the module.

(Temp.= 25 C; TCE Conc. = 700-900 ppm; Vacuum = 20 Torr; Feed-Bleed mode)
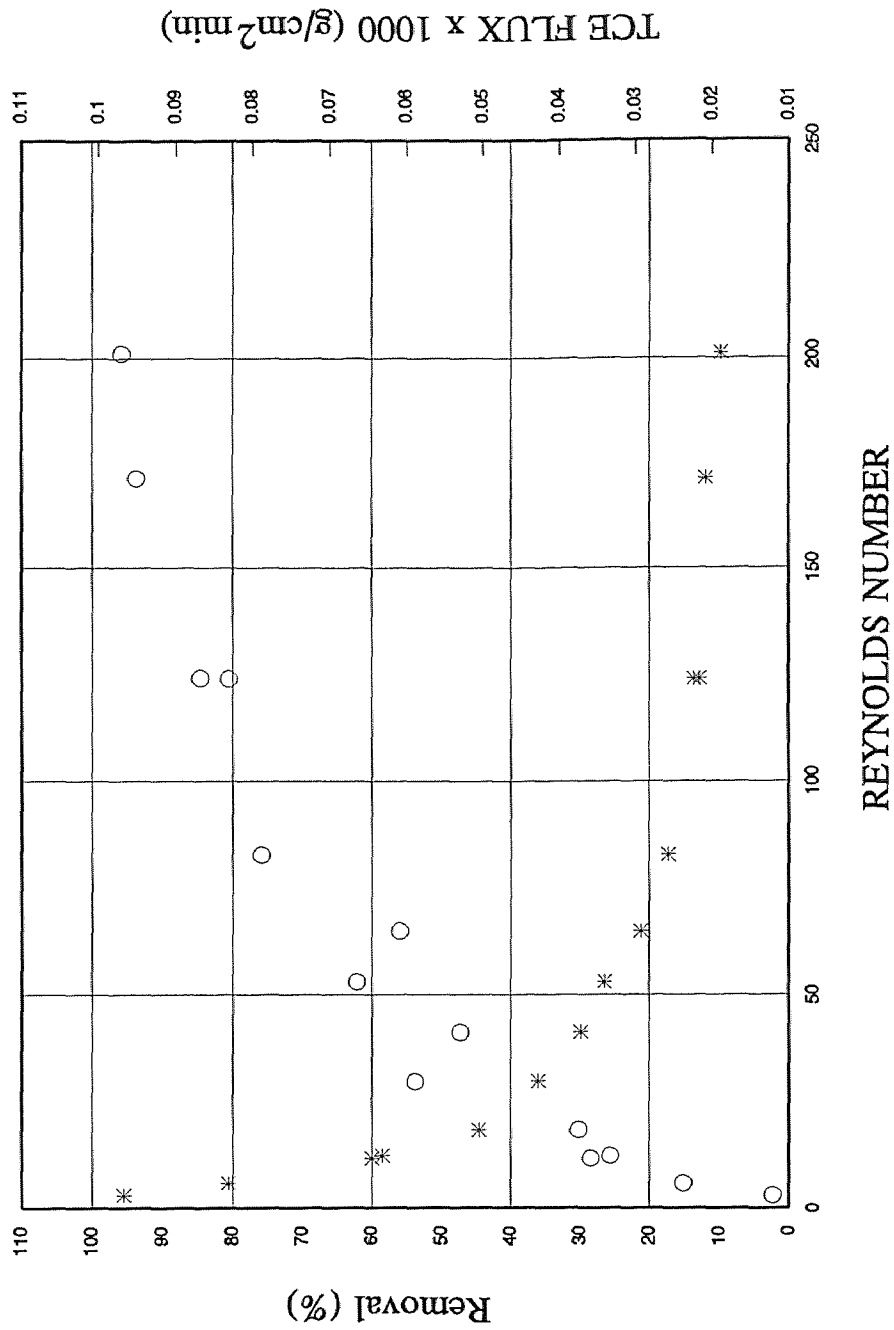
Figure 4.5. Effect of hydrodynamics on TCE removal and TCE flux in stripmeation

(Temp. = 25C; TCE Conc= 700-900 ppm; Single module feed-bleed mode)

＊ TCE Removal   ○ TCE flux
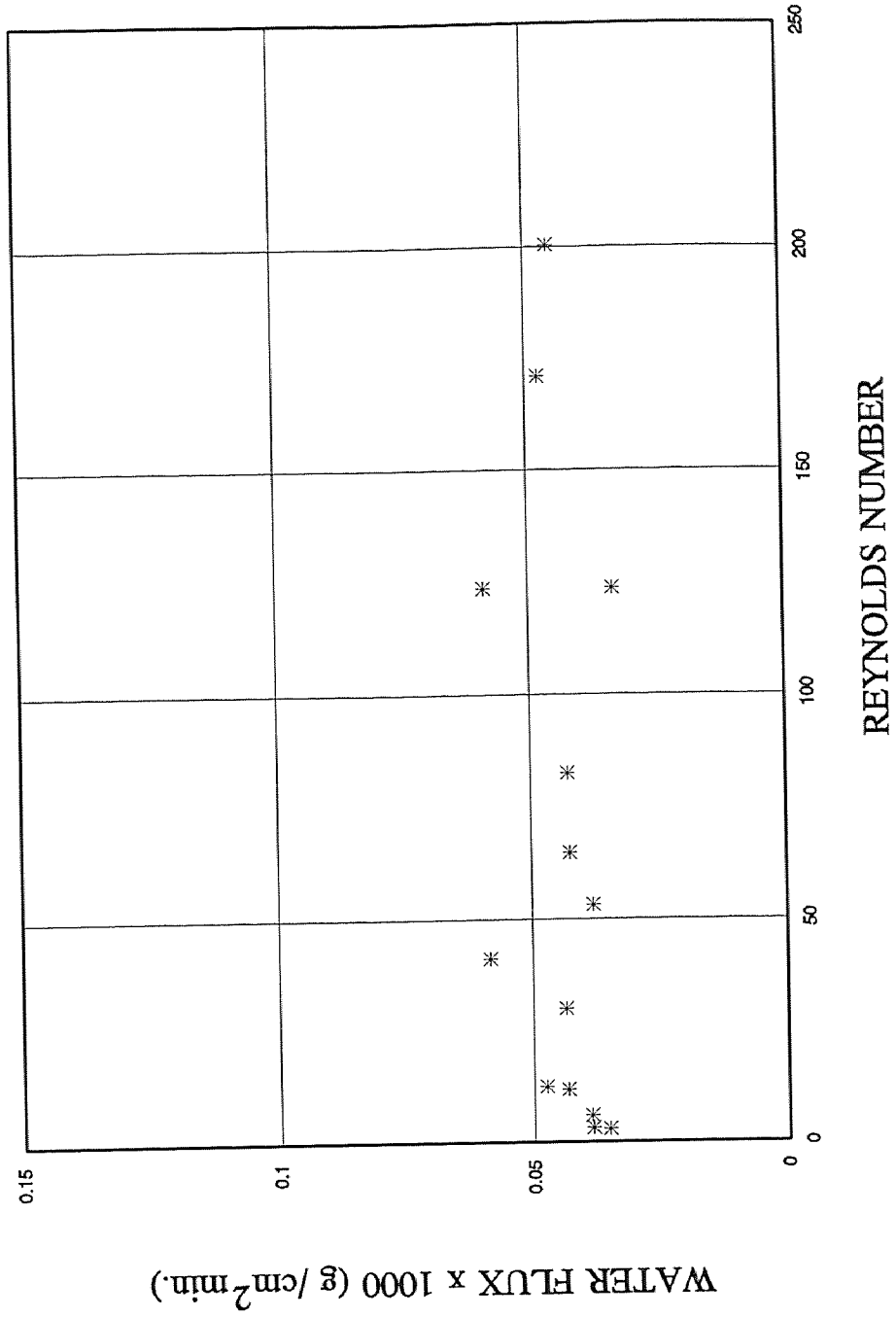
Figure 4.6. Effect of hydrodynamics on water flux in stripmeation

(Temp. = 25C; TCE Conc= 700-900 ppm; Single module feed-bleed mode)
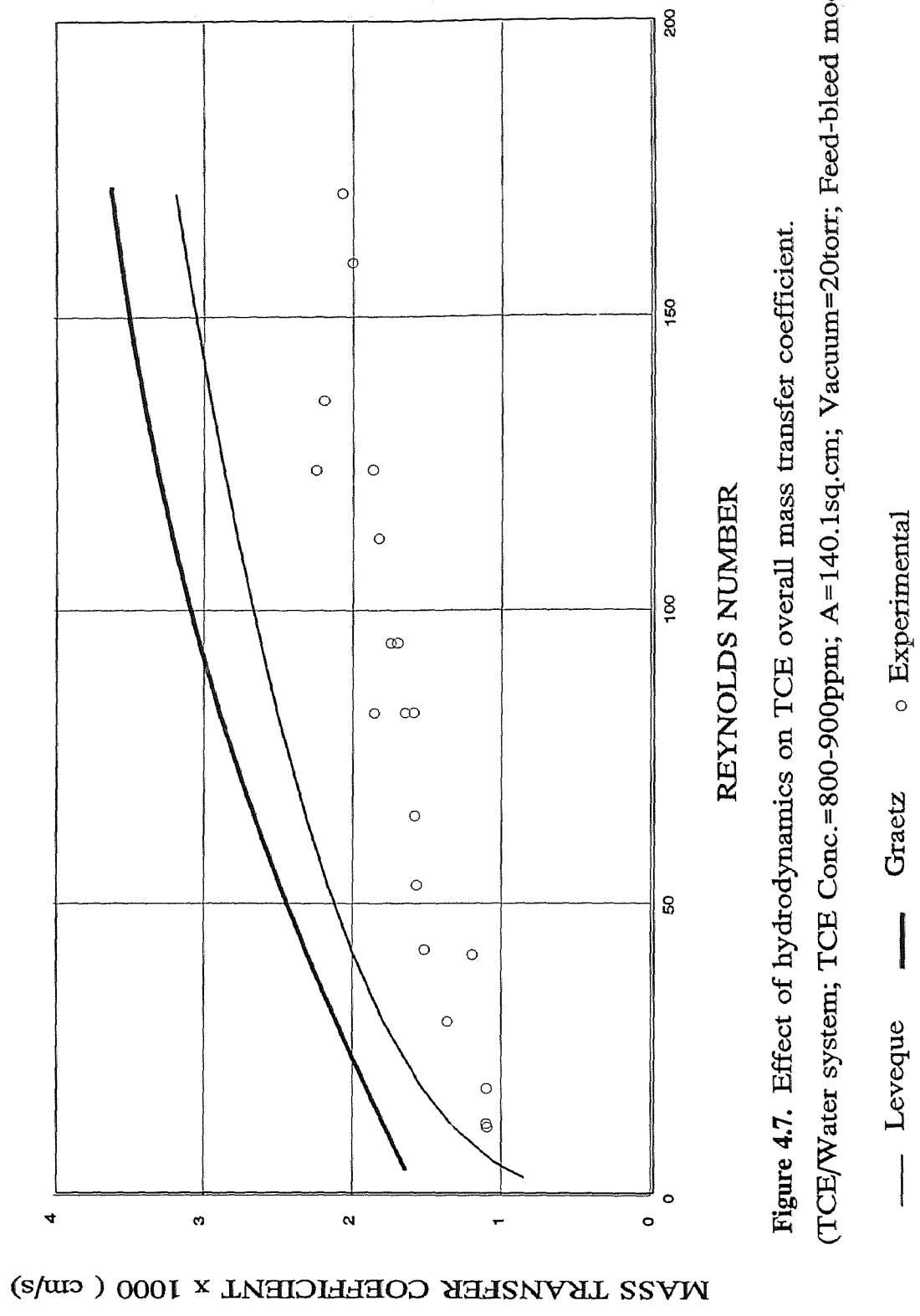
Figure 4.7. Effect of hydrodynamics on TCE overall mass transfer coefficient.

(TCE/Water system; TCE Conc.=800-900ppm; A=140.1sq.cm; Vacuum=20torr; Feed-bleed mode)

4.1.2 Shell Side Experiments

This section compares the performance of the stripmeation process vis-à-vis the conventional pervaporation process. In the following set of experiments, the feed was passed through the shell side of the membrane module. Vacuum was pulled on the tube side. This mode of operation may be described as pervaporation since the feed solution was in direct contact with the membrane coating. Temperature was maintained at 25 °C and the vacuum was kept constant at 20 torr.

4.1.2.1 Effect of Feed Concentration: Aqueous feed was passed through the shell side at a constant flow rate of 2.5 mL/min. The concentration of TCE was varied between 200 ppm and 900 ppm. The pressure drop over the module was negligible . This was expected as the shell side has a more open structure and the resistance to flow is much less compared to the tube side. Figure 4.8 illustrates the experimental data on TCE removal and TCE flux. For the sake of comparison, data from Figure 4.1 are also plotted here. As seen with the tube side results, TCE removal appears to be unaffected by a change in the TCE concentration. It is evident that TCE removal is substantially lower when the feed is passed through the shell side and has an average value of 37% compared to 95% with feed on tube side. TCE flux shows an almost linear increase with increasing feed concentration. Comparing the TCE flux for the two flow configurations, the tube side TCE flux is, as expected, considerably larger than that in the shell side. Figure 4.9 compares the water flux between shell side and tube side feed flow. Water flux is almost constant and has an average value of 0.042 g/cm^2min, which is comparable to the tube side values.
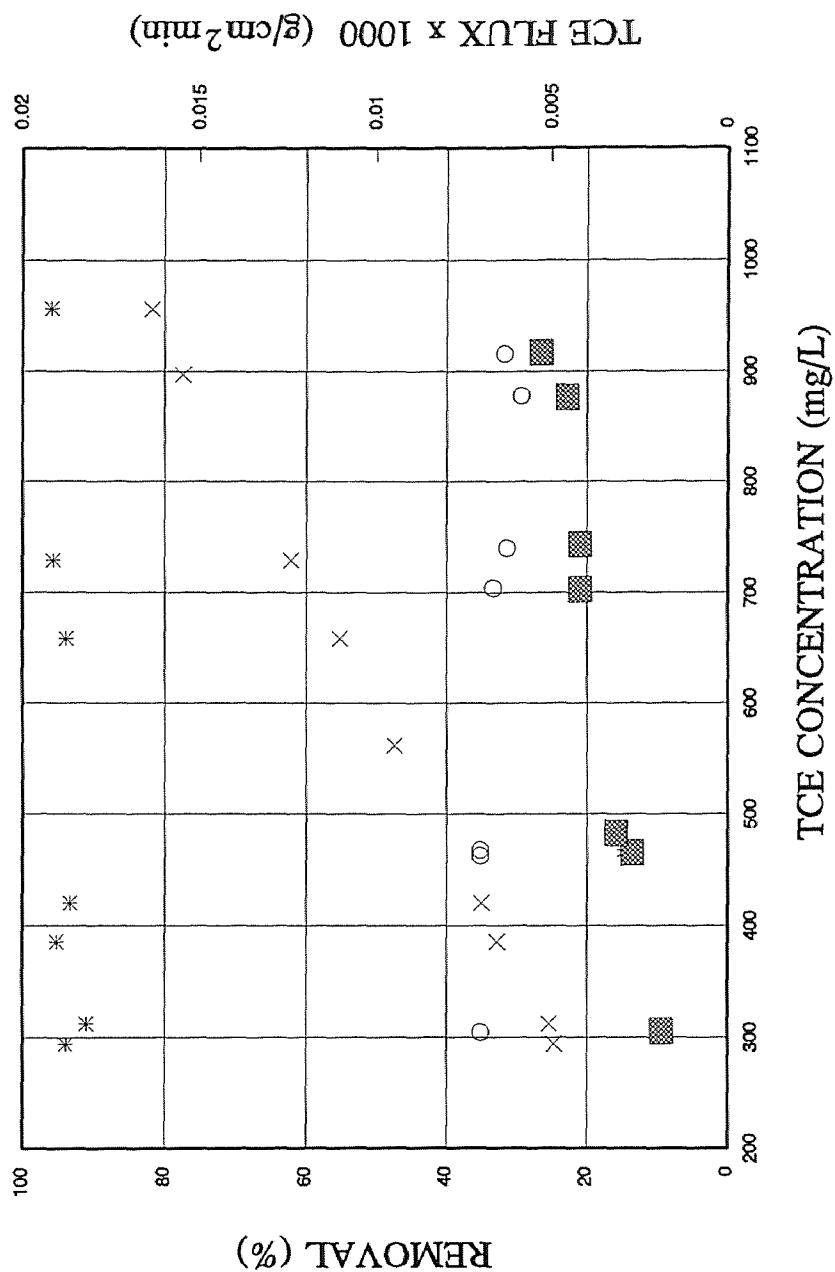
Figure 4.8. TCE removal and TCE flux-comparison of tube-side and shell-side results

(TCE/Water System; Flow Rate = 2.5mL/min; Vac. = 20 torr; TCE= 180-980 ppm)

* Removal/Tube   × TCE flux/Tube   ○ Removal/Shell   ▨ TCE flux/Shell
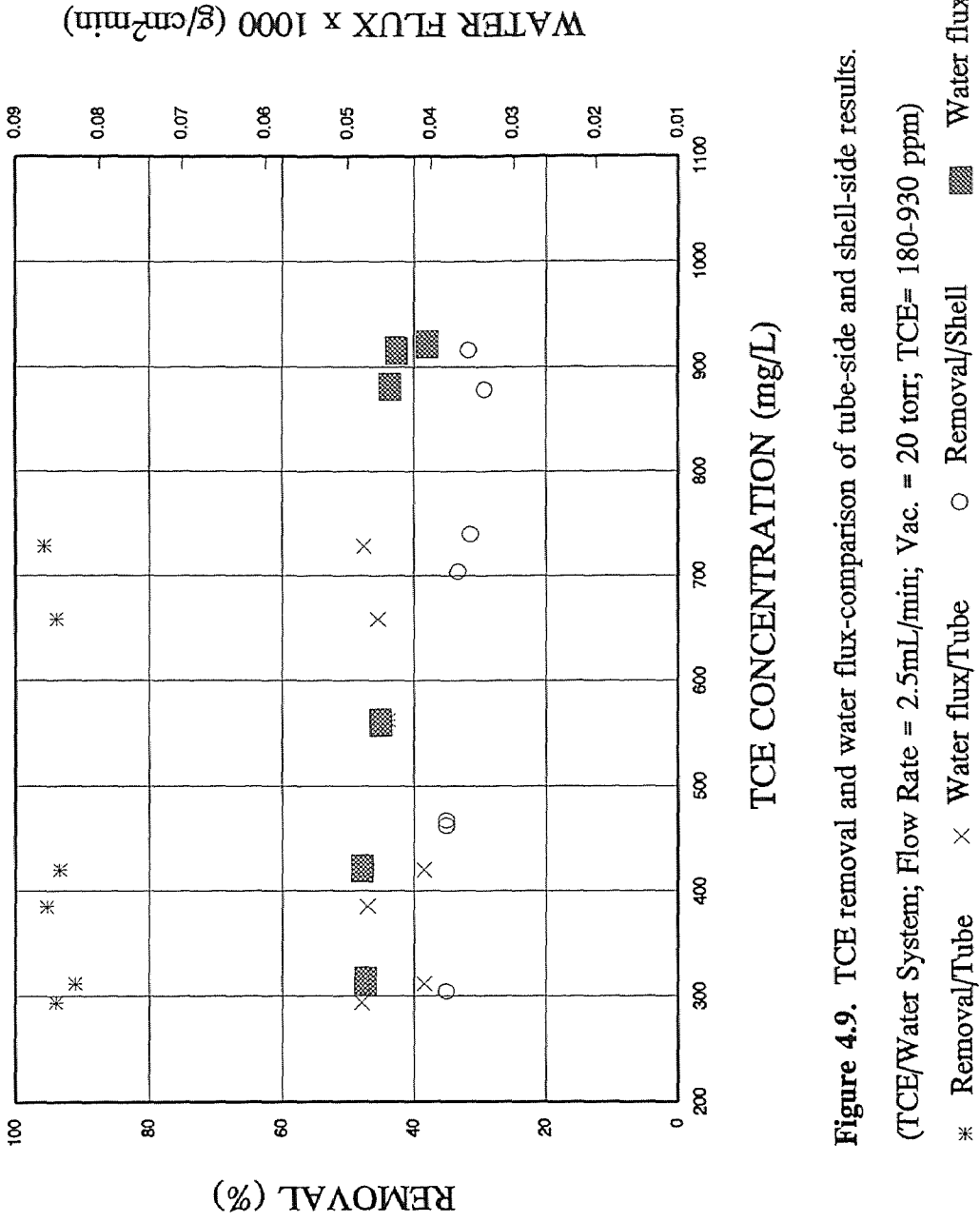
Figure 4.9. TCE removal and water flux-comparison of tube-side and shell-side results.

(TCE/Water System; Flow Rate = 2.5mL/min; Vac. = 20 torr; TCE= 180-930 ppm)

* Removal/Tube   × Water flux/Tube   ○ Removal/Shell   ▨ Water flux/Shell

4.1.2.2 Effect of Feed Flow Rate: The following set of experiments study the effect of hydrodynamics on TCE removal, TCE flux and water flux when the feed is passed on the shell side. Experiments were conducted at feed flow rate varying between 10 mL/min and 40mL/min. The concentration of TCE was kept constant in the range of 800 - 900 ppm. This feed concentration was similar to that for tube side. Figure 4.10 illustrates TCE removal, and TCE flux as a function of the feed flow rate. The removal of TCE drops from 20 % to 6 % as the flow rate changes. TCE flux shows a steady increase with an increase in the feed flow rate. This is expected; as the flow rate increases, much larger amount of TCE enters the membrane module; there is higher concentration of TCE throughout the module leading to higher TCE flux. Results from Figure 4.5 have been plotted for the sake of comparison. TCE removal and TCE flux are much lower when compared to the tube side feed values. Figure 4.11 plots water flux along with the corresponding data from tube side runs (Figure 4.6). Water flux is almost constant and has an average value of 0.04 g/cm^{2}min, which is comparable to the tube-side water flux.

A number of different arguments are useful here. In the conventional pervaporation mode, there is considerable pressure drop in the substrate pores and the tube side when vacuum is applied to the tube side. The corresponding pressure drops in the tube-side feed in "stripmeation" is essentially nonexistent since the shell side is highly open. However, the shell-side velocity is much lower than that on the tube-side due to the much larger open area. Further there are considerable possibilities for bypassing on the shell side. The very low values of the feed flow rate and the highly open
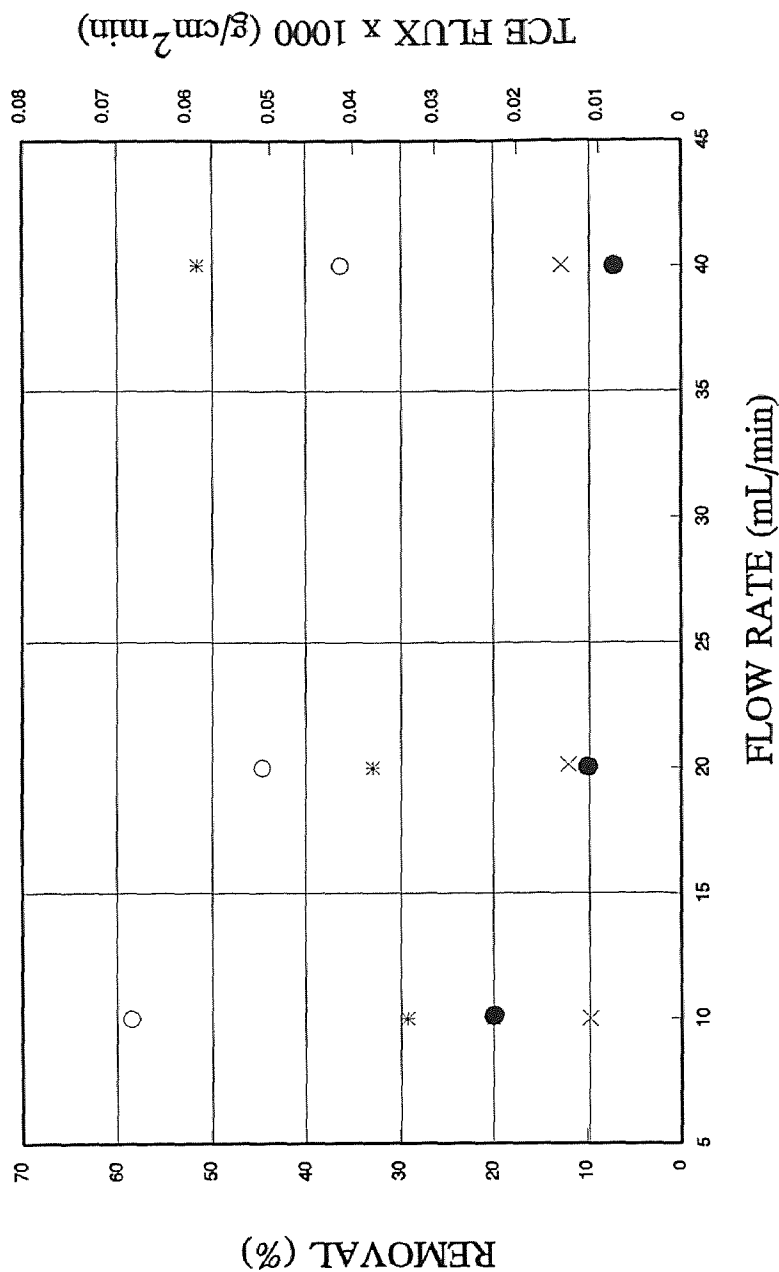
Figure 4.10. Effect of hydrodynamics on TCE removal and TCE flux for feed on shell side

(T=25 C; TCE Conc.= 700-800 ppm; Vacuum = 20 torr; Feed-bleed mode)

● Removal/Shell   × TCE flux/Shell

○ Removal/Tube   * TCE flux/Tube
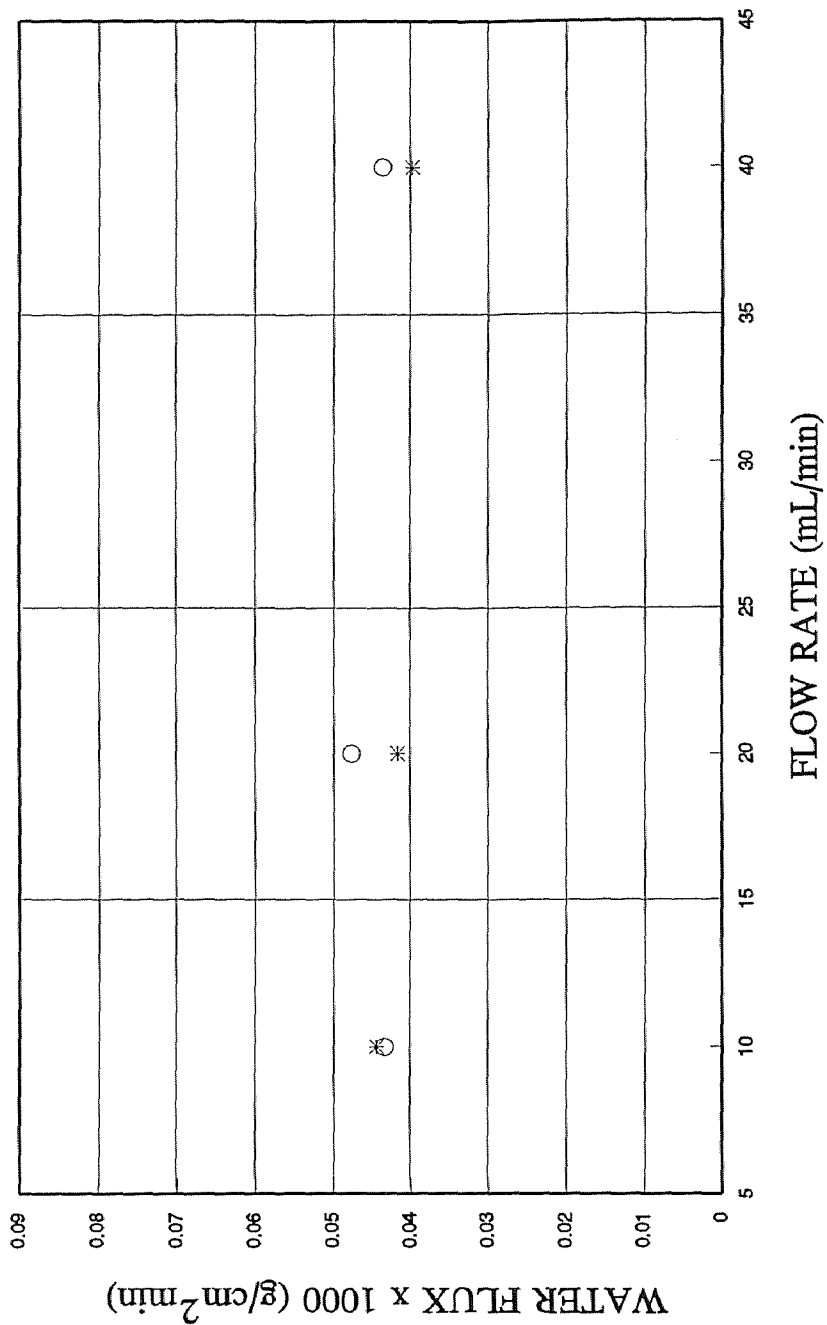
Figure 4.11. Effect of hydrodynamics on water flux for feed on shell side

(T=25 C; TCE Conc.= 700-800 ppm; Vacuum = 20 torr; Feed-bleed mode)

✳   Water flux/Shell   ○   Water flux/Tube

structure of the shell side (high void volume and widely distributed fibers) do, however, reduce the extent and effect of "bypassing" considerably.

4.2 Vapor Permeation Experiments

This section considers the results from experimental runs conducted to estimate the permeance of TCE through the silicone membrane coating. Nitrogen-containing TCE was used as the feed. Feed was passed on the tube side of the hollow fiber module while a vacuum of 20 torr was applied to the shell side. One end of the shell side was plugged so that countercurrent permeate flow was achieved. The emphasis was on having the experimental conditions similar to that in stripmeation experiments so that an accurate estimate of the membrane permeance is obtained. Temperature was maintained at 25°C and the feed gas pressure was close to 1 atm.. Module #1 was used for all experimental runs.

4.2.1 Experimental Results

Experiments were conducted with the feed TCE concentration varying from 220 ppm to 935 ppm. The feed gas entering the tube side of the module was a mixture of gases coming from two separate cylinders: TCE-N_2 and pure N_2 cylinder. The flow rates of the two gases were chosen and set such that the desired TCE concentration in the feed gas was achieved. Table 4.1 provides experimental observations and calculated quantities, namely, feed gas flow rate, TCE feed concentration, TCE flux and TCE permeance (as calculated from Eq.(22)) neglecting permeate side TCE concentrations. These results provide the first guess for starting the calculation. The procedure employed is as follows:

Table 4.1. Results of vapor permeation experiments with TCE in N_2

Module No.	Flow Rate cm^3/sec		TCE Concentration ppmv		ΔC_{lm} gmol/cc (x10^8)	TCE Flux gmol/cm^2.sec (x10^{10})	$k_m m_{vf}$ cm/sec
	Feed in	Feed out	Feed in	Feed out			
1	214.87	207.03	220	141	0.79	0.89	0.011
1	419.06	405.2	467	376	1.87	2.14	0.011
1	306.35	297.76	631	467	2.43	2.68	0.012
1	347.87	339.67	751	567	2.92	3.39	0.011
1	352.90	346.24	867	656	3.37	3.85	0.012
1	272.97	267.02	935	641	3.47	4.14	0.012

first these approximate values of permeance estimated by neglecting the permeate side TCE concentration were fitted to the exponential relation, $(Q_i/\delta_s) = a \times \exp(b\,Px)$, and regressions were made to obtain the values of the parameters a and b. These values were then fed to the simulation model developed by Cha et. al. (1997).The simulation model yielded as output the permeate side partial pressures at two ends of the module for each experimental run. The permeate side partial pressure at the outlet was known from experimental results. This value was compared to the simulated result; if the values were reasonably close, the iteration was considered successful. Otherwise another iteration was done with the permeate side outlet pressure available and new values of parameters a and b were obtained. The following values of parameters a and b gave satisfactory convergence between experimental data and simulated results:

$a = 276 \times 10^{-10}$ gmol s^{-1}cm^{-2}cm Hg^{-1}

$b = 23.37$ atm^{-1}

The permeate side partial pressures so obtained were then used in Eq.(23) to calculate the value of $k_m m_{yf}$ from Eq.(23). These results are provided in Table 4.2. The permeance is reasonably constant and appeared to be unaffected by a change in TCE concentration and has an average value of 0.02 cm/sec. This is expected, as it is known that VOC permeance is essentially constant within the concentration range 200 – 1000 ppm (Cha et. al., 1997).

4.2.2 Resistances -in- Series Model

This section tests the usefulness of the resistances- in-series model described by Eq.(13). The value of the silicone membrane permeance has been estimated to be 0.02 cm/sec.

Table 4.2. Results of vapor permeation experiments and simulations with TCE in N_2

Module No.	Flow Rate cm³/ sec		TCE Concentration ppmv		Simulated TCE concentration Mole fraction		ΔC_{lm} gmol/cc (x10⁸)	TCE Flux gmol/ cm².sec (x10¹⁰)	$k_m m_{vf}$ cm/sec
	Feed in	Feed out	Feed in	Feed out	Closed end	Permeate out			
1	214.87	207.03	220	141	0.0022	0.0029	0.50	0.96	0.019
1	419.06	405.2	467	376	0.0061	0.0070	1.14	2.31	0.0201
1	306.35	297.76	631	467	0.0093	0.0110	1.29	2.89	0.0223
1	347.87	339.67	751	567	0.0075	0.0091	1.99	3.65	0.0183
1	352.90	346.24	867	656	0.0108	0.0127	2.06	4.20	0.0204
1	272.97	267.02	935	641	0.0106	0.0132	2.14	4.46	0.0209

As the value of H_i for TCE at 25°C, is 2.75 mg/L(Turner et al., 1996), a value of 131.5 sec/cm for $H_i/m_{vf}k_m$ is obtained in Eq. (13). Now an estimate is needed for the feed side boundary layer mass transfer coefficient. The Graetz solution (Eq. 14) for fully developed laminar flow in tube has been used to estimate k_f. These values are now substituted in Eq.(13) to find the estimated value of the TCE overall mass transfer coefficient. These results are illustrated in Figure 4.12. The solid line represents the Sh corresponding to the theoretical feed side boundary layer mass transfer coefficient as obtained from the Graetz solution. The dotted line illustrates Sh corresponding to the estimated (from Eq.(3)) value of the overall mass transfer coefficient. The experimental values of overall mass transfer coefficients obtained by conducting experimental runs at a constant feed concentration and varying fiber bore Re (Figure 4.7) are then used to calculate the Sh plotted as unfilled circles in Figure 4.12. It is evident that the difference between the estimated K_o and the experimentally-obtained K_o is minor. This agreement, then, provides a fundamental basis for determining the values of K_o in the stripmeation process for removing VOCs from aqueous solutions through the substrate side of the coated fiber. Figure 4.13 is similar to Figure 4.12 except Leveque solution was used instead of Graetz solution to estimate the tube-side boundary layer mass transfer coefficient. Leveque solution is defined as follows:

$$Sh = 1.62\, Re^{1/3}\, Sc^{1/3}\, (d/l)^{1/3} \tag{24}$$

It is clear that the experimental data do not follow the Leveque solution. This may be due to the fact that Leveque solution is an approximation and is valid only for very thin concentration boundary layer films.
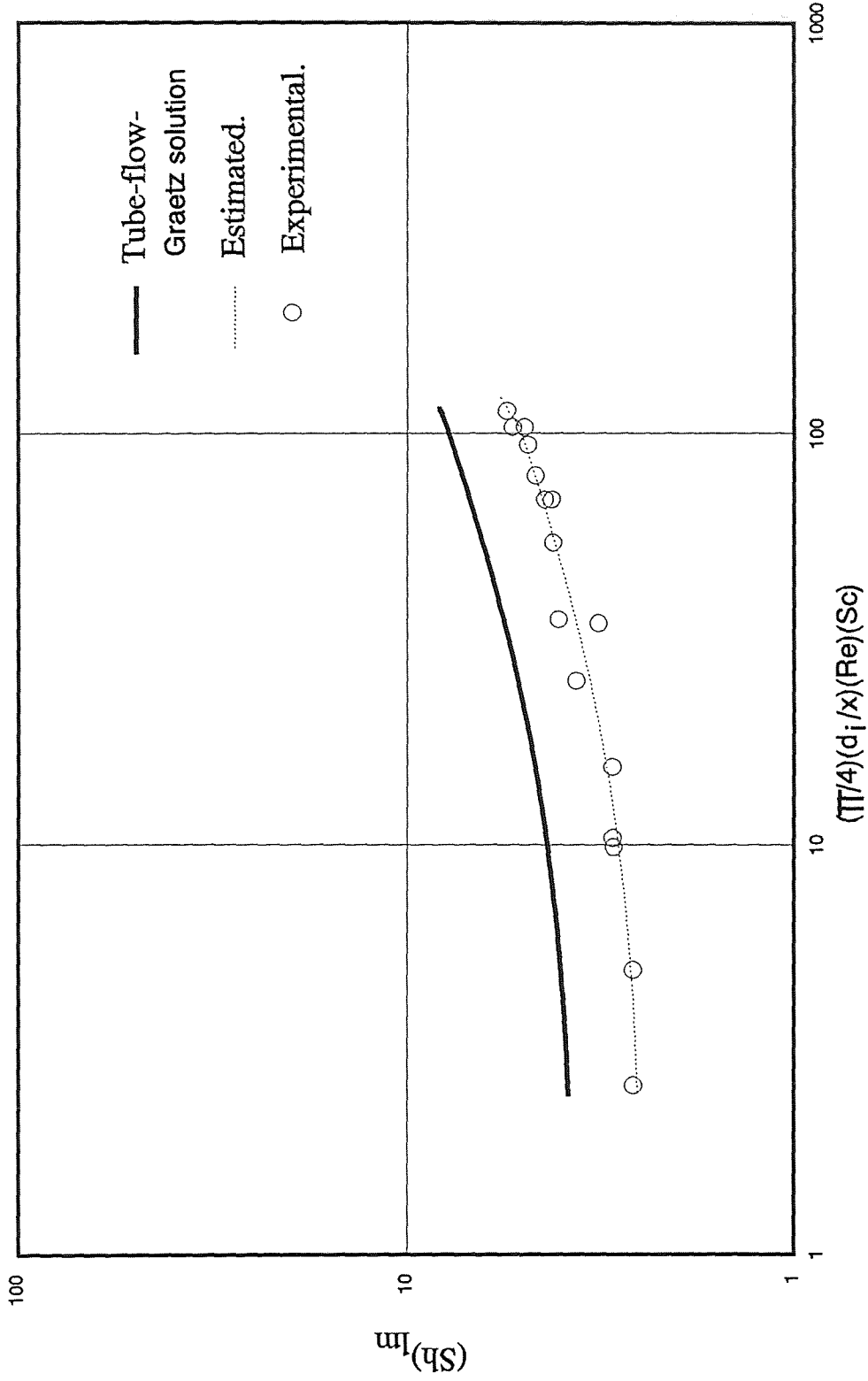
Figure 4.12. Comparison of experimentally obtained TCE mass transfer coefficient with model value estimated using Graetz solution.
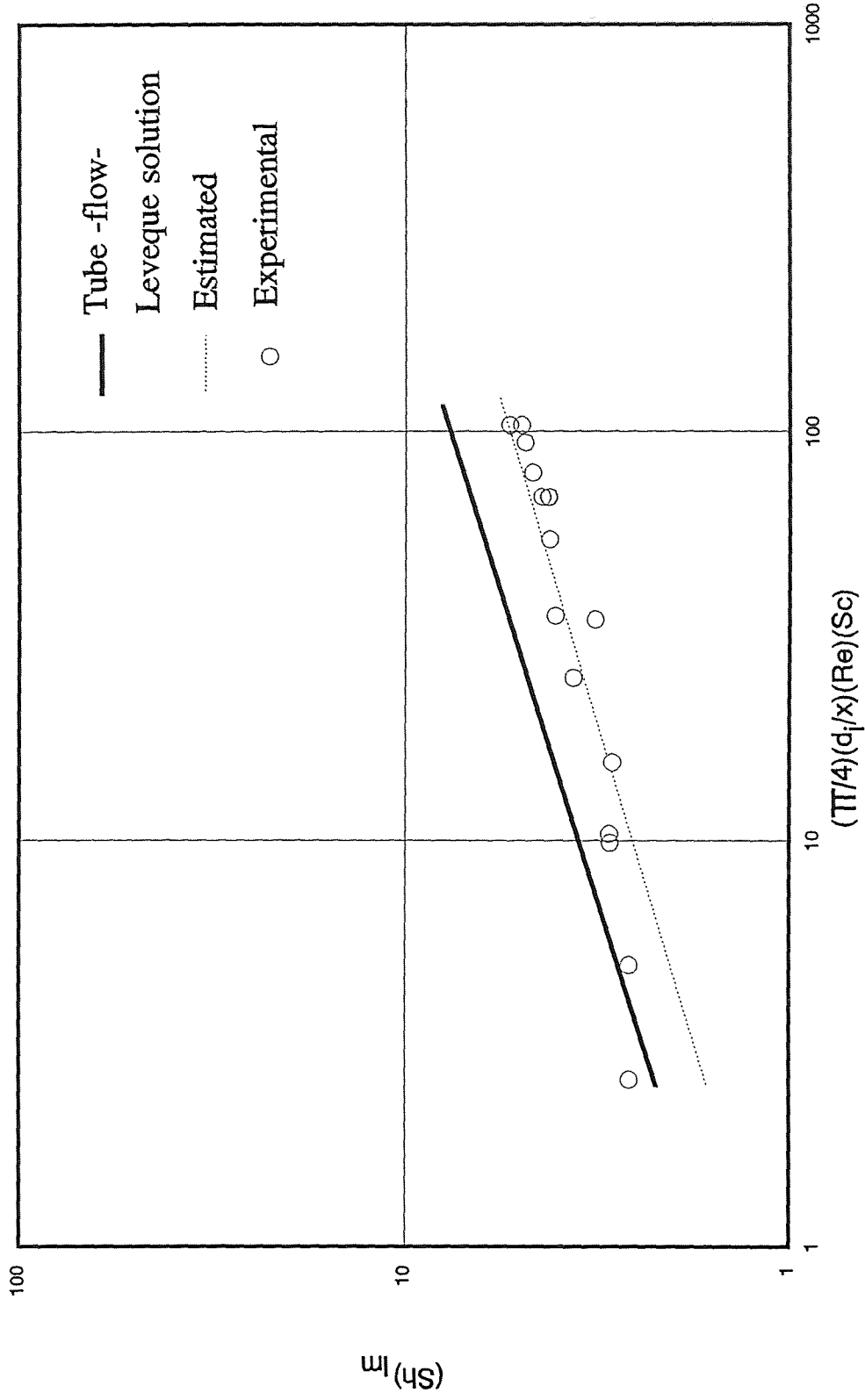
Figure 4.13. Comparison of experimentally obtained TCE mass transfer coefficient with model value estimated using Leveque solution.

The above results illustrate that the transport in the stripmeation process may be described by a resistances-in-series model given by Eq.(13). The membrane resistance and the feed side boundary layer resistance are the controlling resistances for the stripmeation process.

4.3 TCE – Water – SDS System

4.3.1 Tube Side Experiments

This section discusses results obtained from experiments conducted using a surfactant solution, containing a specified concentration of TCE, as feed. SDS was used as the surfactant. Experiments were carried out to investigate the effects of surfactant concentration on TCE removal, TCE flux, and TCE mass transfer coefficient. In the first set of experiments, for a particular concentration of surfactant, the feed concentration was varied. In the second set of experiments, the effect of Reynolds number was studied. Comparison has also been made between tube-side and shell-side performances. Experimental conditions similar to stripmeation experiments were maintained so that the results could be compared. Module #1 was used for all the experiments. Temperature was set at 25°C and a vacuum of 20 torr was applied.

4.3.1.1 Effect of Surfactant Concentration: The experiments were carried out at a constant flow rate of 2.5mL/min. Three surfactant concentrations were studied: 0.3%, 1% and 3%. For each surfactant concentration, experiments were conducted at different TCE concentrations. The results are illustrated in Figures 4.14, 4.15, 4.16 and 4.17. In all
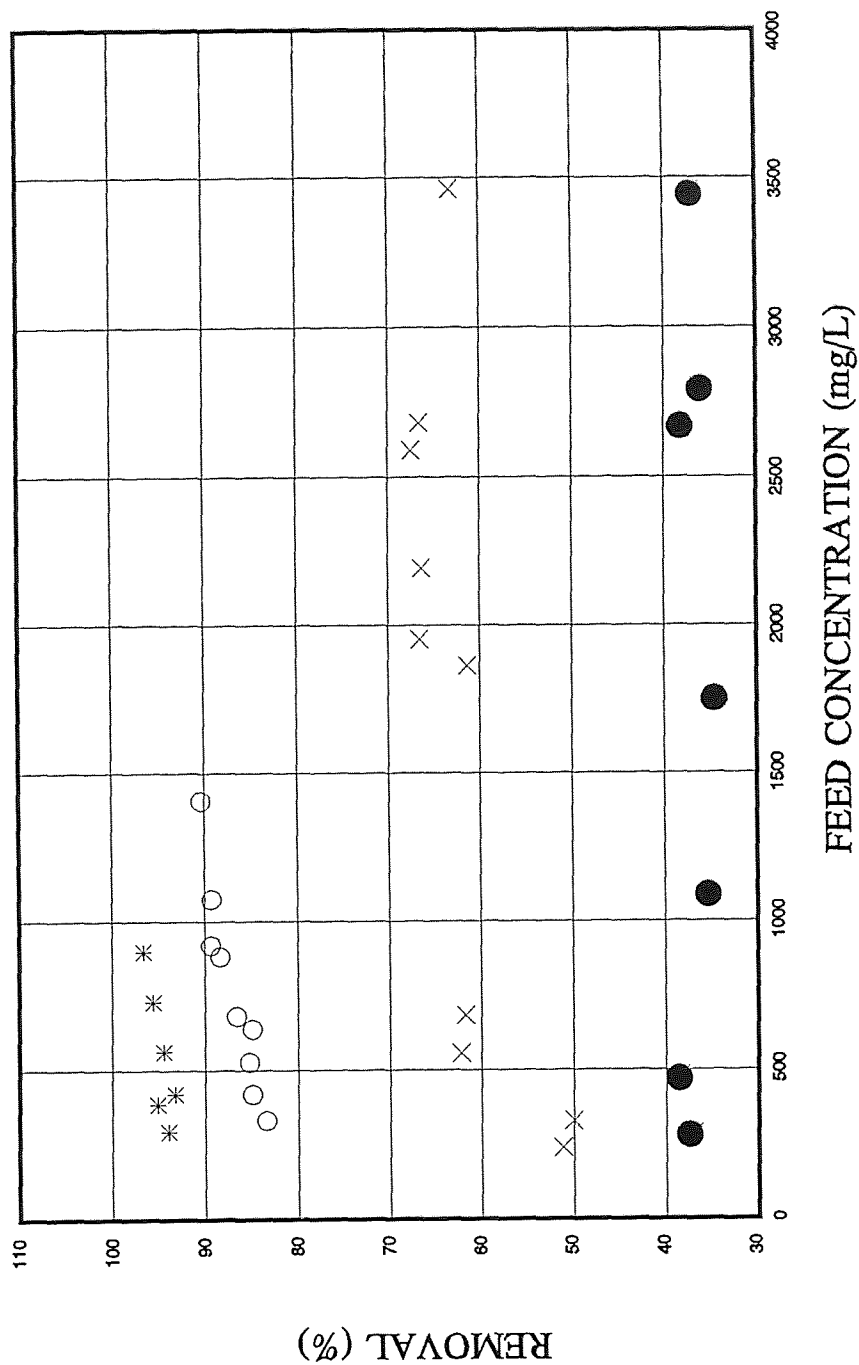
Figure 4.14. Effect of surfactant concentration on TCE removal.

(Temp= 25 C; Vac. = 20 torr; Flow Rate= 2.5 mL/min; TCE = 274-3500 ppm)

✳ No SDS   ○ 0.3%   ✕ 1.0 %   ● 3.0%
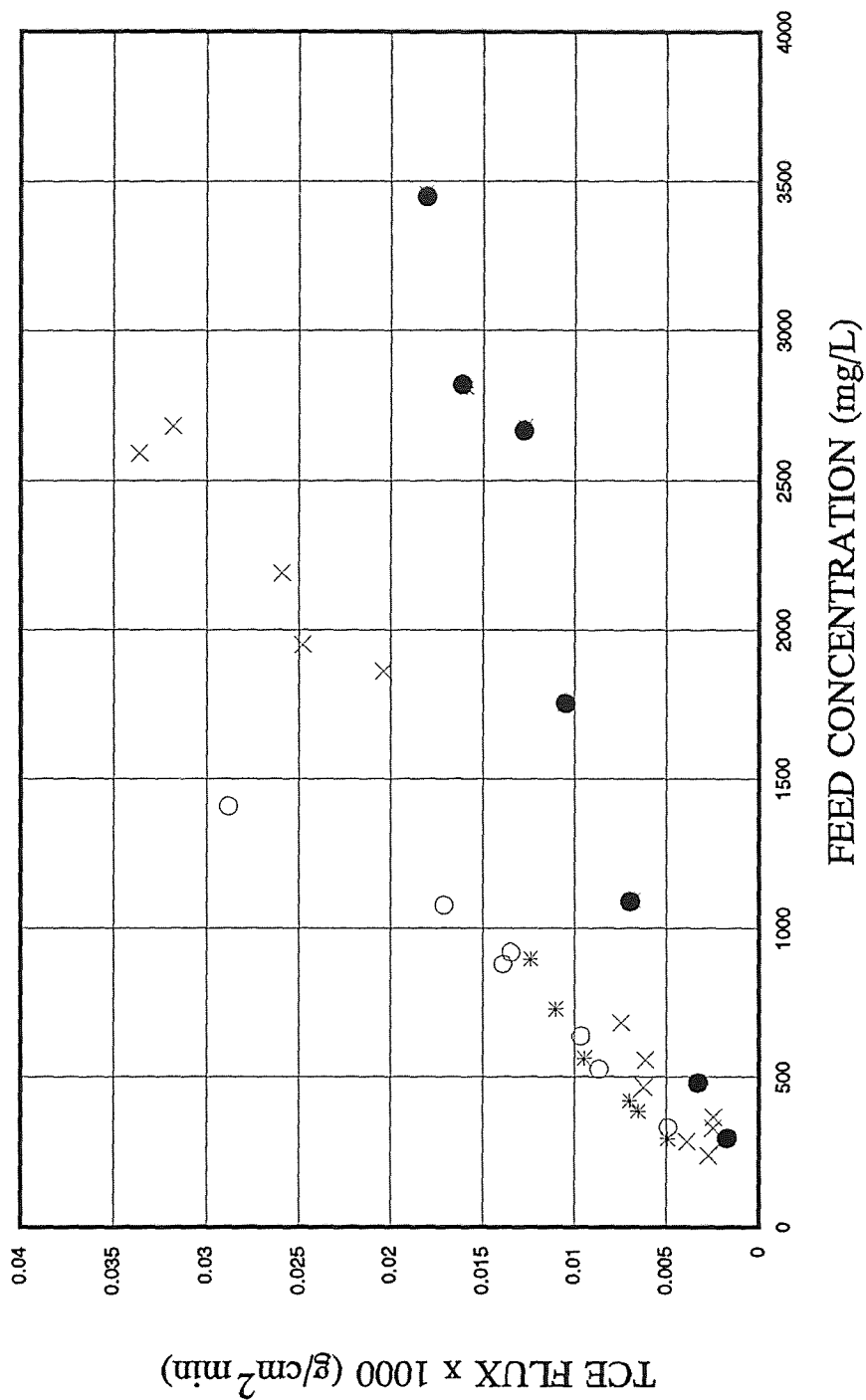
Figure 4.15. Effect of surfactant concentration on TCE flux

(Temp= 25C; Vac. = 20 Torr; Flow Rate= 2.5 mL/min; TCE = 275-3500 ppm)

* No SDS   ○ 0.3%   × 1.0%   ● 3.0%

FEED CONCENTRATION (mg/L)

TCE FLUX x 1000 (g/cm²·min)
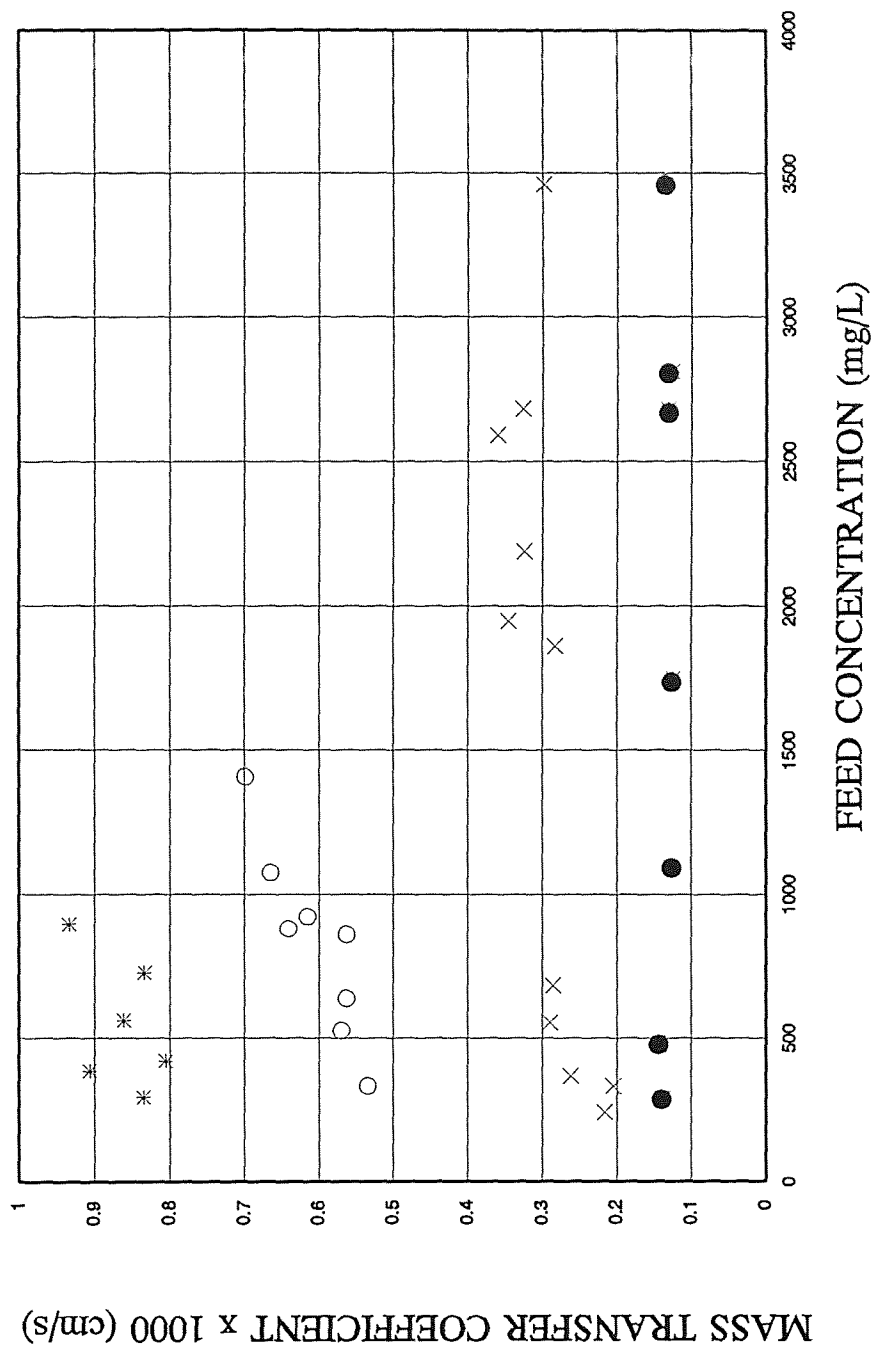
Figure 4.16. Effect of surfactant concentration on TCE mass transfer coefficient.

(Temp= 25C; Vac. = 20 Torr; Flow Rate= 2.5 mL/min; TCE = 275-3500 ppm)

* No SDS   ○ 0.3%   × 1.0%   ● 3.0%

MASS TRANSFER COEFFICIENT x 1000 (cm/s)

FEED CONCENTRATION (mg/L)
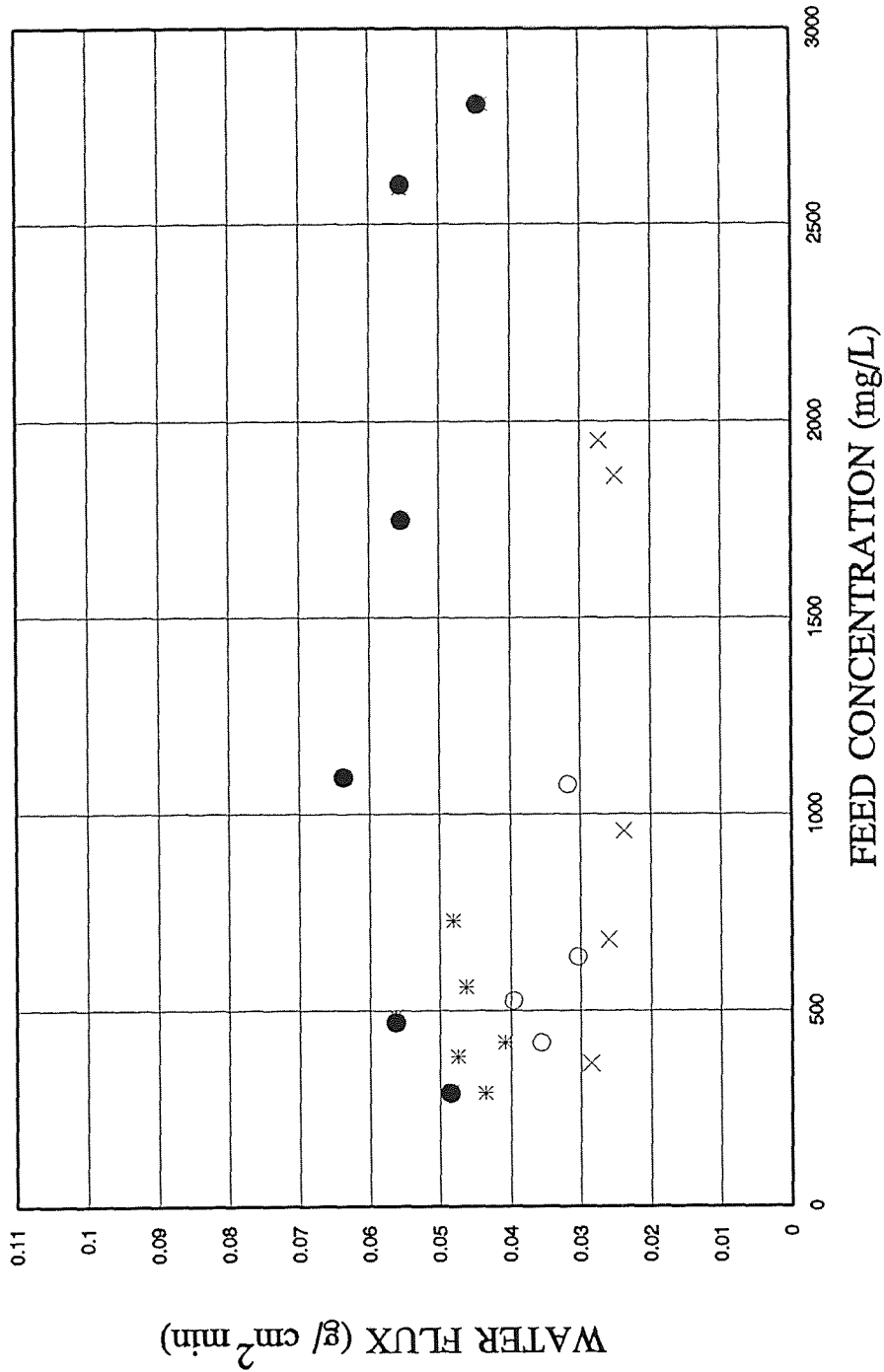
Figure 4.17. Effect of surfactant concentration on water flux

(Temp. = 25 C; Vacuum = 20 Torr; Flow Rate= 2.5 mL/min; TCE = 274-3500 ppm)

* No SDS   ○ 03%   × 1.0%   ● 3.0%

Figures, experimental results for the corresponding stripmeation experiments with no surfactants have also been plotted. Figure 4.14 illustrates the effect of surfactant concentration on TCE removal. It is evident that with increasing surfactant concentration, the TCE removal decreases. Further, for a given surfactant concentration, the TCE removals are somewhat constant with changing feed concentrations. The average TCE removals for surfactant levels of 0.3%, 1.0% and 3.0% are 87%, 61% and 36% respectively. These values are significantly lower than the TCE removal achieved in systems without any surfactants, namely, an average value of 94%. Figure 4.15 plots the flux of TCE as a function of the feed TCE concentration. The flux profile shows a linear increase with feed concentration. It is clear that the TCE flux drops as the surfactant concentration increases. The drop in TCE flux compared to that in a surfactant-free system is 5%, 26% and 42% for SDS concentrations of 0.3%, 1.0% and 3.0% respectively. Figure 4.16 illustrates the behavior of the overall TCE mass transfer coefficient for the different surfactant concentrations. There is a significant drop in the overall mass transfer coefficient with increasing surfactant concentration. In fact, as the surfactant concentration in the feed was increased from 0.3% to 3.0 %, the average value of the overall mass transfer coefficient decreases from 0.6×10^{-3} cm/s to 0.15×10^{-3}, a 75% drop. Figure 4.17 plots the water flux at different surfactant concentrations. As with non-surfactant systems the water flux is reasonably constant with changing feed TCE concentration. As surfactant concentration is increased from 0% (no SDS) to 1.0% the water flux shows a decrease. But at 3.0% SDS concentration water flux is higher compared to 0.3%, 1.0% and non-surfactant feed solutions.

The drop in the TCE flux and the TCE mass transfer coefficient with an increase in the surfactant concentration in the feed may be explained by the fact that SDS molecules form a monomeric layer on the hydrophobic polypropylene substrate. This creates an additional resistance for the transport of TCE. Further, as surfactant concentration increases, the number of surfactant molecules per micelle increases until it reaches a limiting value. Under such conditions the probability of a micelle disintegrating as it collides with the wall of the hollow fiber decreases. Correspondingly the amount of TCE solubilized per surfactant molecule in a micelle decrease; the amount of TCE released via disintegration of one micelle decreases, although the number of such disintegration may increase. Even when a micelle does disintegrate and release free TCE, it may be encapsulated by other micelles. Therefore in a surfactant rich system the availability of free TCE in the system is considerably reduced resulting in lower TCE flux and lower TCE overall mass transfer coefficient.

4.3.1.2 Effect of Feed Flow Rate: The following set of experiments study the effect of fiber bore Reynolds number on the performance on the hollow fiber membrane module when a surfactant solution containing TCE is used as feed. Reynolds number was varied between 3 and 140. TCE concentration in the feed was maintained in the range 1100 – 1200 ppm and 3400-3500 ppm for experiments conducted with 0.3% SDS and 1% SDS feed concentration respectively. Figures 4.18, 4.19, 4.20 and 4.21 illustrate the effect of the feed flow rate on TCE removal, TCE flux, TCE mass transfer coefficient and water flux respectively. Corresponding results for stripmeation experiments (TCE-water system) have also been plotted for the sake of comparison. It is evident (Figure 4.18) that
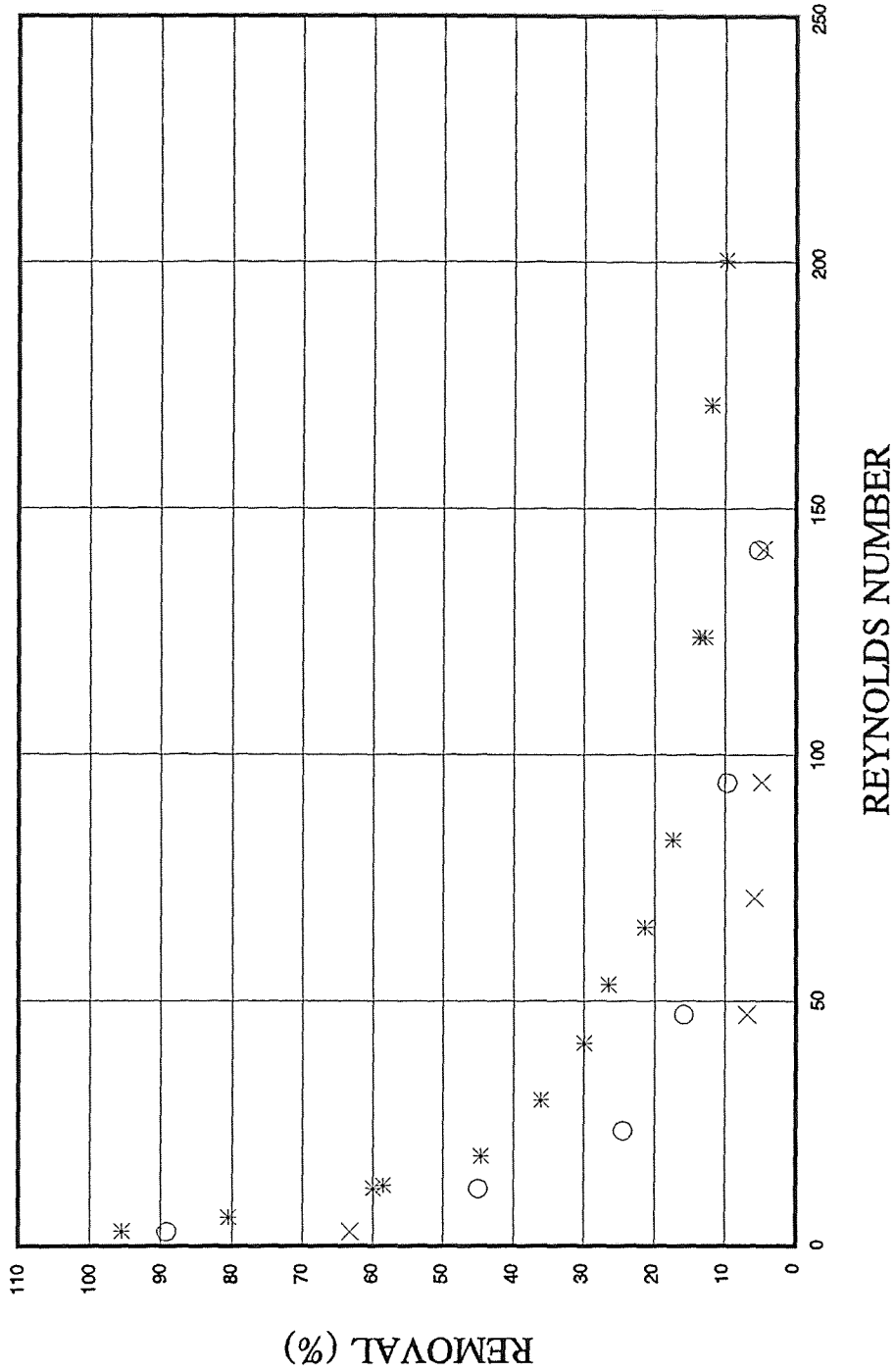
Figure 4.18. Effect of hydrodynamics on TCE removal

(Temp= 25 C; Vacuum = 20 Torr; TCE Conc. = 700-3500 ppm; Feed-bleed mode)

⁎ No SDS   ○ 0.3% SDS   × 1.0% SDS
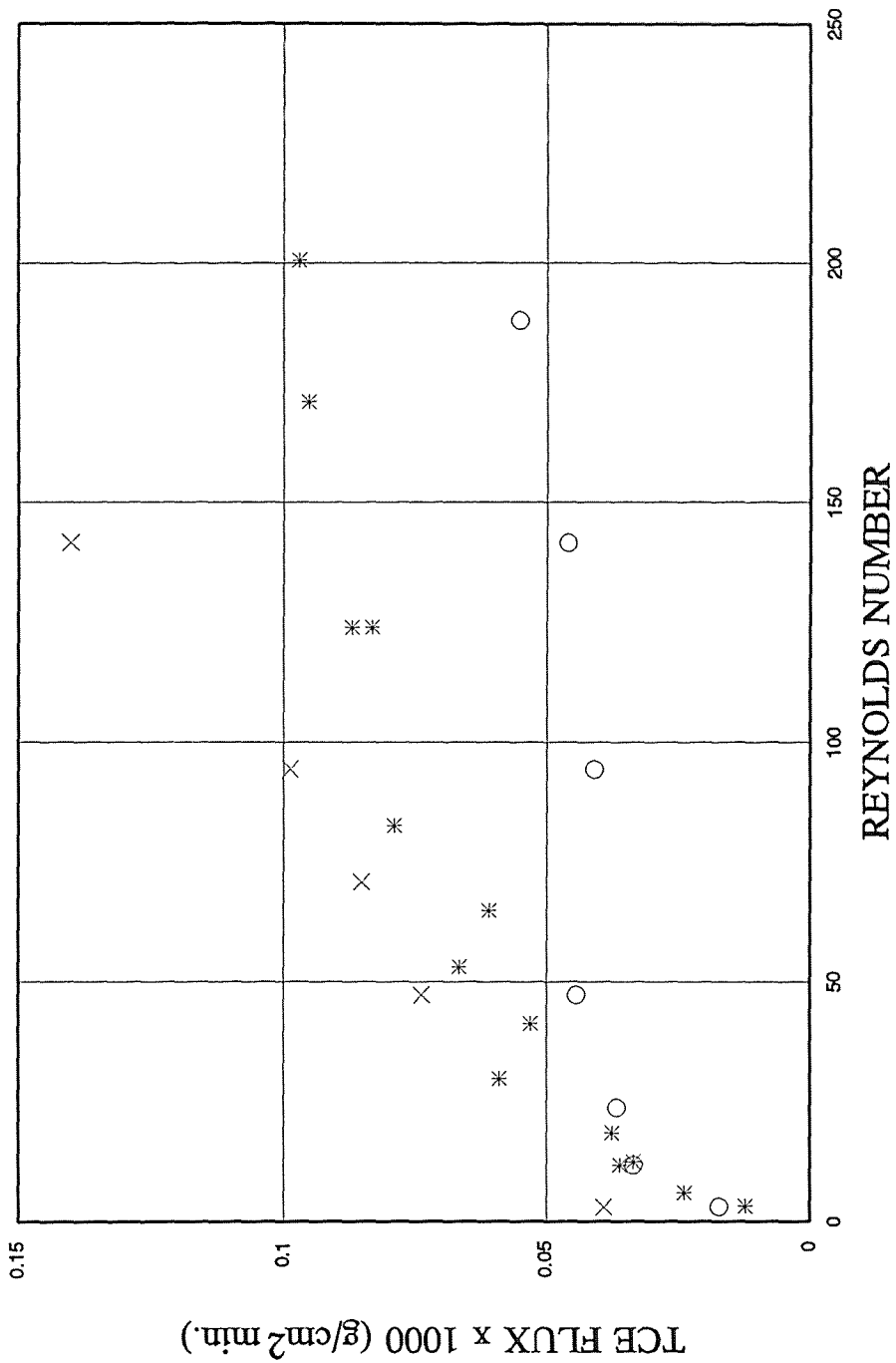
Figure 4.19. Effect of hydrodynamics on TCE flux

(Temp= 25 C; Vacuum 20 Torr; TCE Conc= 700-3500 ppm; Feed-bleed mode)
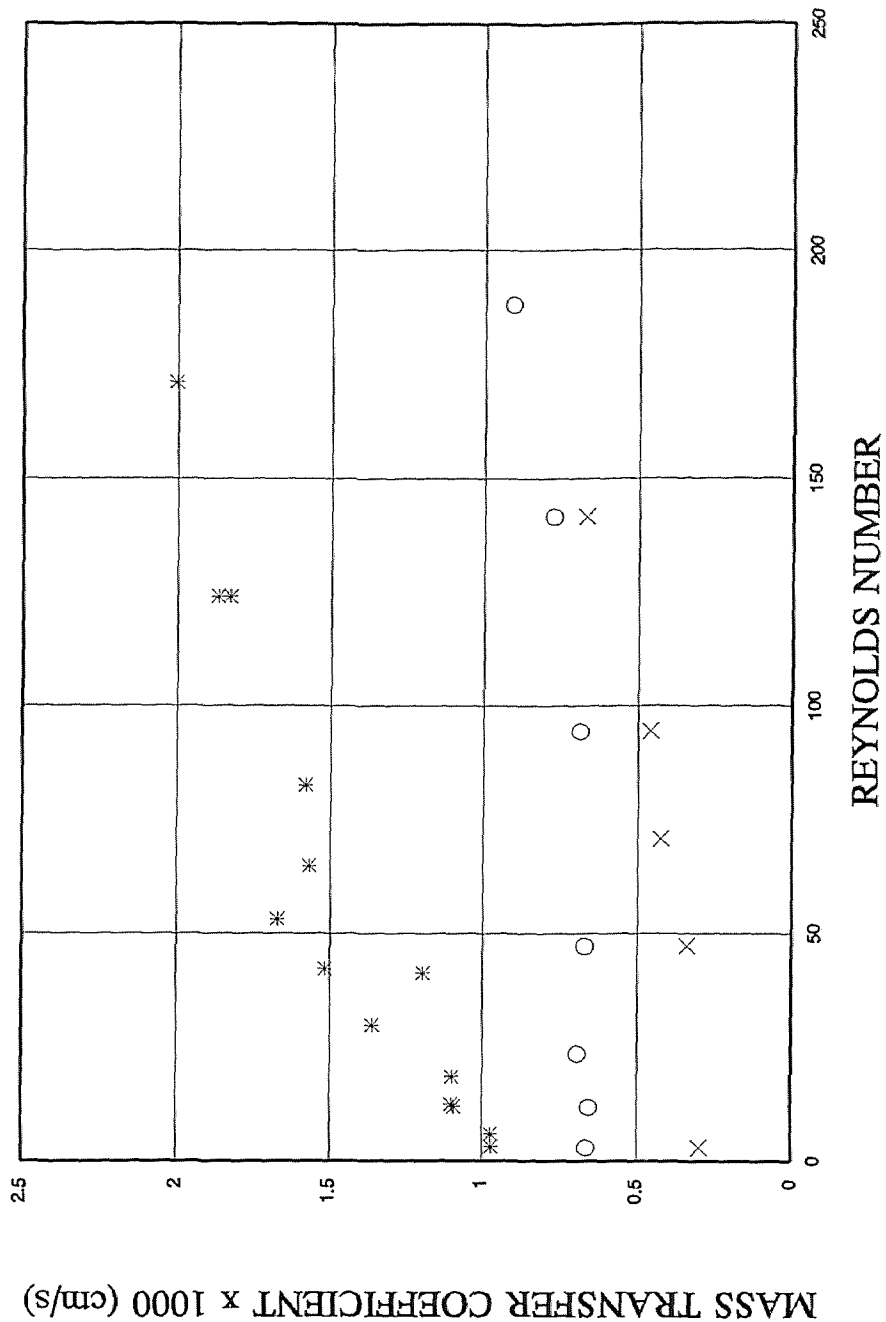
✳ No SDS   ○ 0.3%   ✕ 1.0%

Figure 4.20. Effect of hydrodynamics on TCE mass transfer coefficient

(Temp= 25 C; Vacuum = 20 Torr; TCE Conc= 700-3500 ppm; Feed-bleed mode)
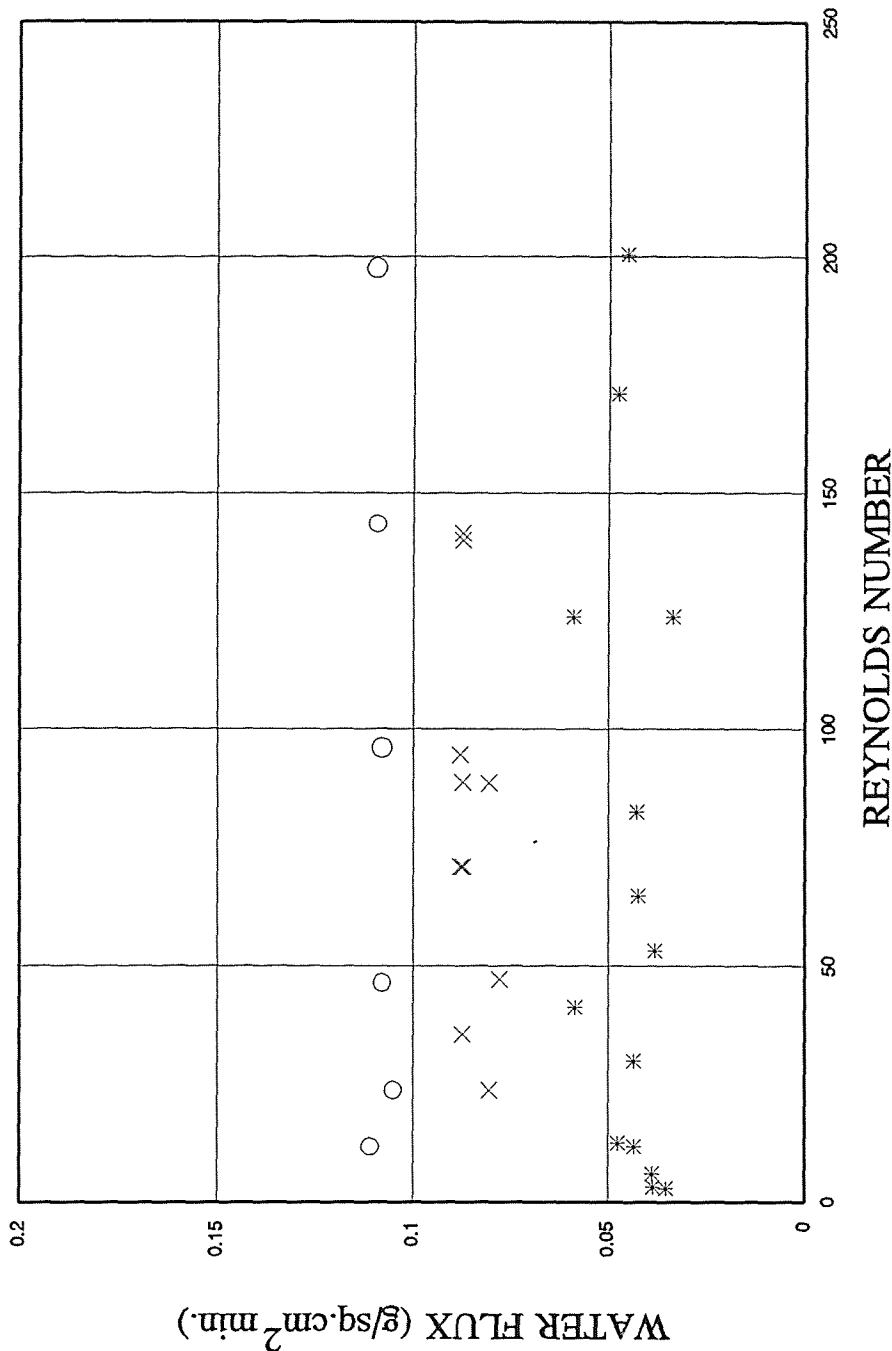
✳ No SDS   ○ 0.3%   ✕ 1.0%

Figure 4.21. Effect of hydrodynamics on water flux

(Temp= 25 C; Vacuum = 20 Torr; TCE Conc= 700-3500 ppm; Feed-bleed mode)

* No SDS   ○ 0.3% SDS   × 1.0%SDS

with increasing Reynolds number, TCE removal drops. For 0.3% SDS, TCE removal drops from 89% (Re=3) to 6% (Re=140). For 1% SDS, the drop is from 62% to 5%. Also, as expected, with increase in SDS concentration, TCE removal is lower. TCE flux (Figure 4.19) shows an interesting behavior. At low Reynolds number, TCE flux shows a linear increase with increase in Reynolds number. At higher Reynolds number, the flux appears to become independent of the feed flow rate and reaches a plateau. It appears from Figure 4.19 that TCE flux at 1% SDS is higher than that at 0.3% SDS. This is due to the fact that experiments at 1% SDS were carried out at feed TCE concentration of 3400 – 3500 ppm, three times the TCE concentration used for 0.3% SDS experiments. The mass transfer coefficient (Figure 4.20) for TCE shows some increase with an increase in Reynolds number. As the Reynolds number was varied from 3 to 140, the overall TCE mass transfer coefficient changes from 7.0×10^{-4} cm/s to 9.0×10^{-4} cm/s for 0.3% SDS and from 3.5×10^{-4} cm/s to 6.5×10^{-4} cm/s for 1.0% SDS solutions. The water flux data (Figure 4.21) does not reflect any specific trend. As the surfactant concentration increases from 0% (No SDS) to 0.3% the water flux increases from 4×10^{-5} g/cm^{2}min to 1.2×10^{-4} g/cm^{2}min (average values). But as surfactant concentration increases from 0.3% to 1.0% the water flux drops to an average value of 8×10^{-5} g/cm^{2}min.

4.3.2 Shell Side Experiments

This section reports results for experiments that were conducted by passing the surfactant feed solution through the shell side of the hollow fiber membrane module. A vacuum of 20 torr was pulled on the tube side. Temperature was maintained at 25°C. Results obtained have been compared with the corresponding tube side data.

4.3.2.1 Effect of Feed Concentration: Feed solution having a SDS concentration of 0.3% was passed at a constant flow rate of 2.5 mL/min. TCE concentration was varied between 370 and 1140 ppm. Figure 4.22 plots the TCE removal and TCE flux as a function of feed concentration. For the sake of comparison, corresponding data for experiments performed with 0.3% SDS feed solution on tube side have also been plotted. As seen with tube side results, TCE removal is unaffected by change in TCE concentration. It is evident that TCE removal is substantially lower when feed is passed through the shell side and has an average value of 30% compared to 86% for feed in tube side. Comparing the TCE flux for the two flow configurations, the TCE flux with tube side flow is considerably larger than that for the shell side flow. The difference in performance for tube-side and shell-side modes of operation may be justified by arguments similar to those discussed for TCE-water system (Section 4.1.2.2). Figure 4.23 plots the water flux for the two flow configurations. As expected the values are comparable.

It is evident that the presence of surfactant in the feed diminishes the performance of the hollow fiber membrane module. TCE removal, TCE flux and TCE overall mass transfer coefficient are lowered when a surfactant-containing feed solution is used. This is due to additional resistances offered to the transport of TCE. Experiments have been performed to estimate these resistances and are discussed in the next section.
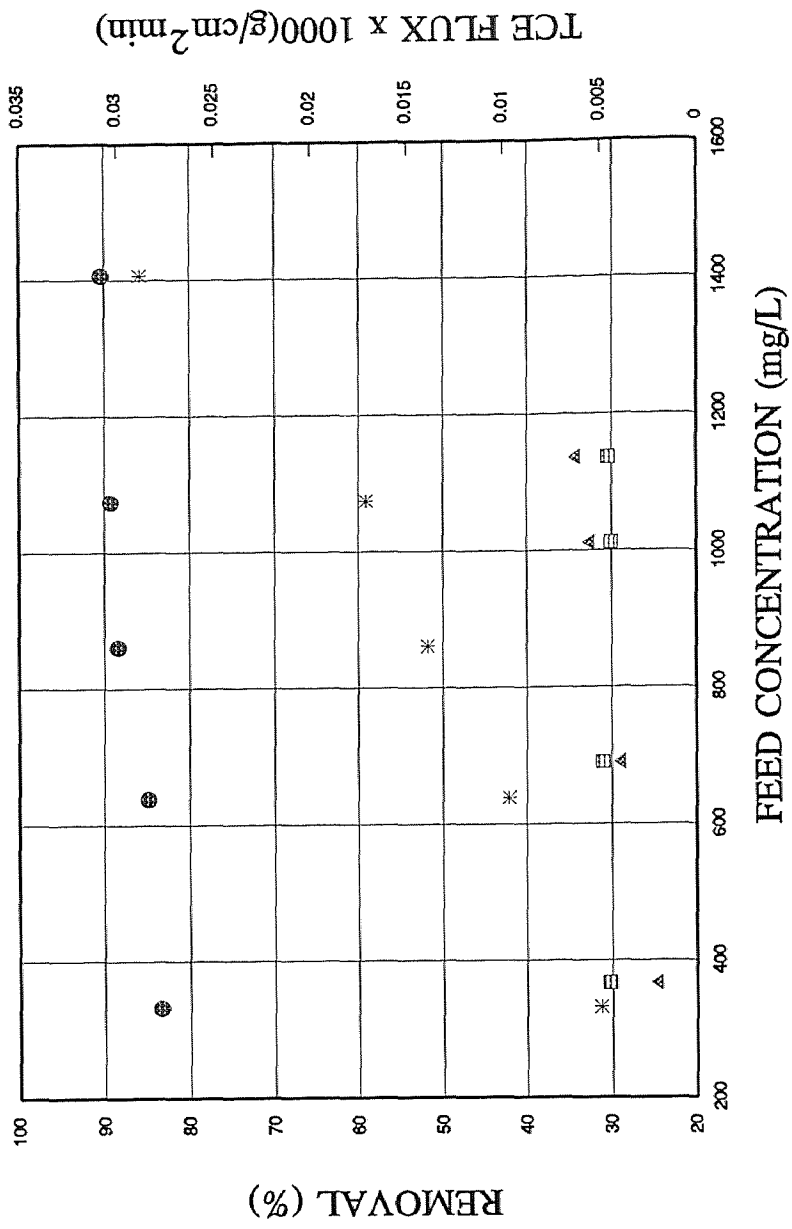
Figure 4.22. TCE removal and TCE flux with feed on shell side

(0.3% SDS; Temp= 25 C; Vacuum = 20 torr; Flow Rate= 2.5 mL/min; TCE = 270-1400 ppm)

⊞   TCE Removal/Shell   ▵   TCE Flux/Shell

⊕   TCE RemovaL/Tube   ✳   TCE Flux/Tube
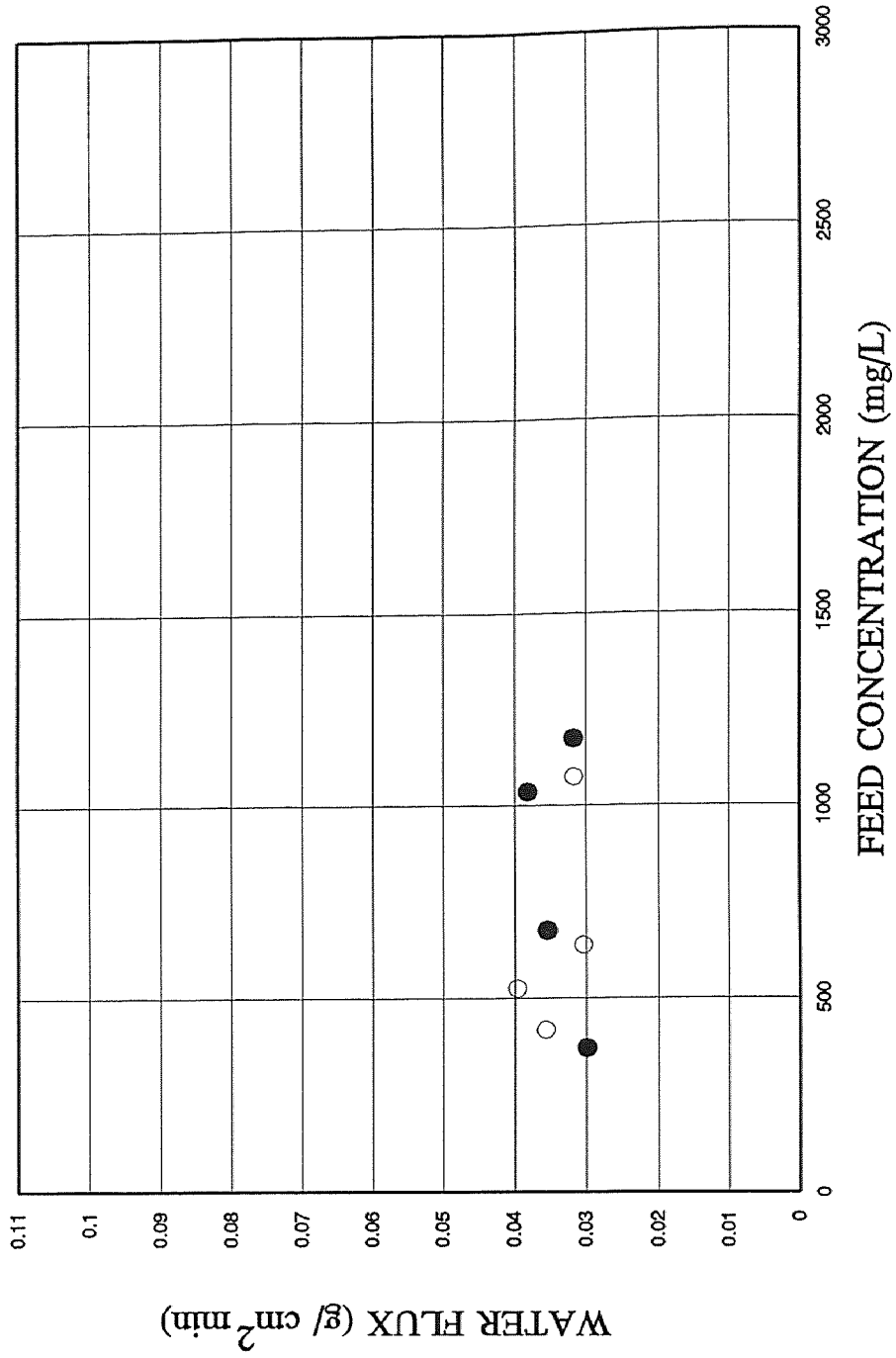
Figure 4.23. Water flux with feed on shell side

(Temp. = 25 C; Vacuum = 20 Torr; Flow Rate= 2.5 mL/min; TCE = 274-3500 ppm)

○ Water Flux/Tube ● Water Flux/Shell

4.4 Wetted Pore Experiments

When a surfactant solution flows through the tube side of the hollow fiber membrane module it wets the pore (if it is above a certain concentration). Therefore the pores of the substrate are filled with the feed solution as compared to being air-filled (as in stripmeation). To estimate the resistance offered by the wetted pore, experiments were conducted with the pores of the polypropylene substrate filled with water. Temperature was kept at 25 °C and a vacuum of 20 torr was maintained. Feed flowed through the tube side of the hollow fiber membrane module.

The results are expected to provide answer to questions such as: At what surfactant concentration is the feed solution wetting the pores? What is the resistance offered to mass transport due to the water filled pore? Are there any additional resistances? The experiments were performed in two phases. In the first phase of experiment, an aqueous solution of TCE was used as feed. In the second phase, a surfactant solution containing TCE was used as feed.

4.4.1 TCE – Water System

4.4.1.1 Effect of Feed Concentration: Experiments were performed at a constant flow rate of 2.5 mL/min. TCE concentration was varied between 180 and 780 ppm. The experimental results have been plotted in Figures 4.24 and 4.25. Results from stripmeation (non-wetted pores) have also been plotted for the sake of comparison. TCE removal (Figure 4.24) seems to be reasonably constant and has an average value of 78%. This is significantly lower than the average TCE removal (93%) for stripmeation experiments. TCE flux (Figure 4.24) shows a similar trend. The TCE overall mass

Figure 4.24. TCE removal and TCE flux in experiments with wetted pore

(Temp. = 25 C; Flow Rate = 2.5mL/min; Vacuum = 20 torr; TCE= 180-960 ppm)

✳ TCE Removal/Non-wetted   ✕ TCE Flux/Non-wetted

○ TCE Removal/Wetted   ● TCE Flux/Wetted

Figure 4.25. TCE mass transfer coefficient in experiments with wetted pore

(Temp. = 25 C; Flow Rate = 2.5mL/min; Vacuum = 20 torr; TCE= 180-960 ppm)

* Non-wetted   ○ Wetted

transfer coefficient (Figure 4.25) for experiments with wetted pores has an average value of 4.8 x 10^{-4} cm/s which is 40% lower compared to the TCE overall mass transfer coefficient for stripmeation experiments. These results are expected as the water-filled pores of the substrate offers an additional resistance to the transport of TCE across the hollow fiber. This resistance is now estimated as follows.

For experiments with wetted pore, the overall mass transfer coefficient, K_{owet}, may be written by modifying Eq (10) as

$$\frac{1}{K_{owet}} = \frac{d_o}{d_i}\frac{1}{k_i^f} + \frac{d_o}{d_{lm}}\frac{H_i}{k_{wp}^f} + \frac{H_i}{m_{vf}k_m} \tag{25}$$

The overall mass transfer coefficient for stripmeation experiments is given by Eq. (13) as

$$\frac{1}{K_o} = \frac{d_o}{d_i}\frac{1}{k_i^f} + \frac{H_i}{m_{vf}k_m} \tag{13}$$

The feed side boundary layer mass transfer coefficient, k_i^f, and the membrane resistance, k_m, may be assumed to be similar for both cases. Also, H_i in Eq. (25) may be assumed to be unity, as pores are water-filled and there is no stripping. Subtracting Eq.(13) from Eq.(25), Eq. (26) is obtained

$$\frac{1}{K_{owet}} = \frac{1}{K_o} + \frac{d_o}{d_{lm}k_{wp}^f} \tag{26}$$

Substituting , K_{owet}= 4.8 x 10^{-4} cm/s, K_o = 8.6 x 10^{-4} cm/s ,d_o= 290 x 10^{-4} cm and d_{lm}= 264 x 10^{-4} cm, k_{wp}^f is obtained as 1.18x 10^{-3} cm/s.

The value of k_{wp}^f, the TCE mass transfer coefficient in the water-filled pore, is comparable to K_o and cannot be ignored. Therefore when conditions are such that the

surfactant feed wets the pores, the resistance offered by the water-filled pores is one of the contributing resistances that lowers the TCE flux across the hollow fiber.

4.4.1.2 Effect of Feed Flow Rate: In the previous section the value of k_{wp}^f has been calculated. Theoretically, the value of k_{wp}^f should be similar for any feed flow rate. Therefore experiments were carried out at different feed flow rates. The pores of the hollow fiber membrane module were kept water-filled. The experiments were conducted at three flow rates: 10 mL/min, 20 mL/min and 40 mL/min. TCE concentration was maintained between 700 and 900 ppm. Figure 4.26 illustrates TCE removal and TCE flux behavior. Figure 4.27 plots the TCE overall mass transfer coefficient for wetted and non-wetted pores. TCE removal (Figure 4.26) changes from 36% to 15% as the flow rate was changed from 10 mL/min to 40 mL/min. TCE flux (Figure 4.26) shows a steady increase with an increase in the feed flow rate. The overall TCE mass transfer coefficient also increases with increasing flow rate. It is evident that TCE removal, TCE flux and TCE overall mass transfer coefficient have lower values compared to stripmeation experiments and this is due to the water-filled pore resistance. Using a procedure similar to that used in section 4.4.1.1, k_{wp}^f was calculated for each flow rate and is listed in Table 4.3. It is clear that k_{wp}^f is reasonably constant with changing flow rate. Therefore, it might be assumed that the approach used for calculation of k_{wp}^f is valid.

A theoretical estimate of the water-filled pore resistance was obtained using the following equation:
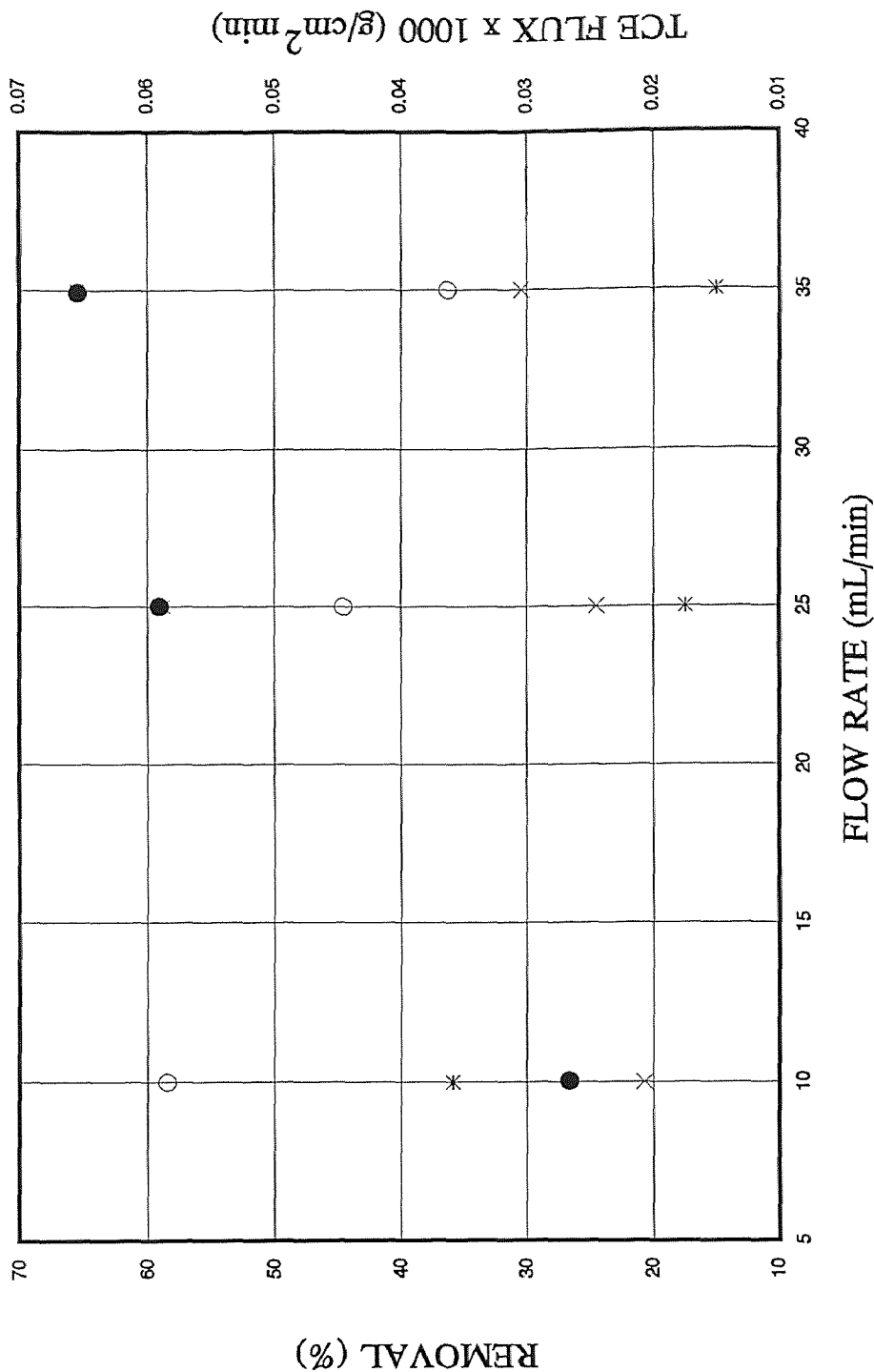
Figure 4.26. Effect of hydrodynamics on TCE removal and TCE flux in experiments with wetted pore

(Temp= 25C; Vacuum = 20 torr; TCE Conc= 700-900 ppm; Feed-bleed mode)

✳ Removal/Wetted × TCE Flux/Wetted

◯ Removal/Non-wetted ● TCE Flux/Nonwetted
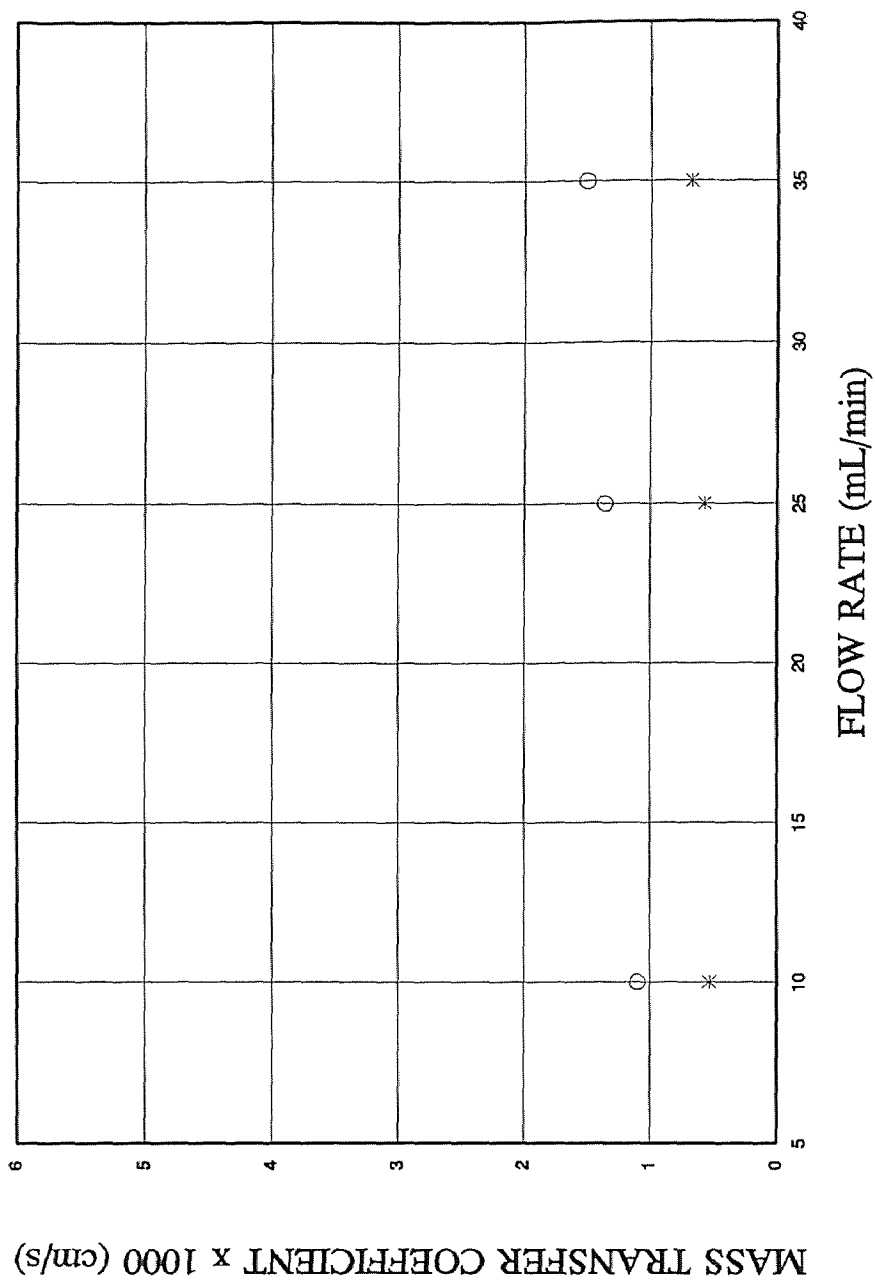
Figure 4.27. Effect of hydrodynamics on TCE mass transfer coefficient in experiments with wetted pore

(Temp= 25C; Vacuum = 20 torr; TCE Conc= 700-900 ppm; Feed-bleed mode)

✳ Wetted   ○ Non-wetted

Table 4.3. Experimental and calculated results to determine water-filled pore resistance.

Flow Rate	Feed Inlet Concentration	Feed Outlet Concentration	Removal	K_{owet}	K_o	k^l_{wp}
(mL/min)	(ppm)	(ppm)	(%)	(cm/s)	(cm/s)	(cm/s)
10	807	517	36.0	5.29×10^{-4}	1.1×10^{-3}	1.02×10^{-3}
25	785	648	17.4	5.72×10^{-4}	1.36×10^{-3}	9.87×10^{-4}
35	812	690	15.0	6.77×10^{-4}	1.51×10^{-3}	1.20×10^{-3}

$$k_{wp}^{f} = \frac{D_{iwp}\varepsilon}{\tau\delta_{s}}$$
(27)

Substituting the values of $D_{iwp} = 9 \times 10^{-6}$ cm^2/s, $\varepsilon = 0.4$, $\tau = 2.5$ and $\delta_{s} = 2.5 \times 10^{-3}$ cm, the

mass transfer coefficient of TCE in a water-filled pore, k_{wp}^{f}, is calculated to be 5.76×10^{-4}

cm/s. It is evident that the theoretically-calculated value of the mass transfer coefficient is

lower than that obtained experimentally i.e., the theoretical estimate of the resistance to

transport of TCE across a water-filled pore is higher compared to the experimentally

observed value. The difference may be due to a monolayer of TCE adsorbed on the wall

of the pores of the substrate. This layer would then facilitate the transport of TCE by

allowing surface diffusion of TCE along the walls of the substrate, from the bulk solution

to the silicone skin.

4.4.2 TCE-Water-SDS System

4.4.2.1 Effect of Surfactant Concentration: This section discusses results from

experiments performed using a surfactant solution containing TCE as feed. The feed

solution was passed through the bore of the hollow fiber membrane module that had

wetted pores. Experiments were performed at a constant flow rate of 2.5 mL/min. Two

surfactant concentrations were used: 0.3% and 1%. For experiments with 0.3% SDS, TCE

concentration in the feed was varied between 300 and 800 ppm. For 1% SDS, TCE

concentration was varied in the range 700-2600 ppm. Figures 4.28, 4.29 and 4.30

illustrate the behavior of TCE removal, TCE flux and TCE mass transfer coefficient

respectively. In all figures, corresponding results from non-wetted pore experiments

have also been plotted. TCE removal for 0.3% SDS has an average value of 78% which is

significantly lower than that for non-wetted pore (86%). For 1% SDS the value for TCE
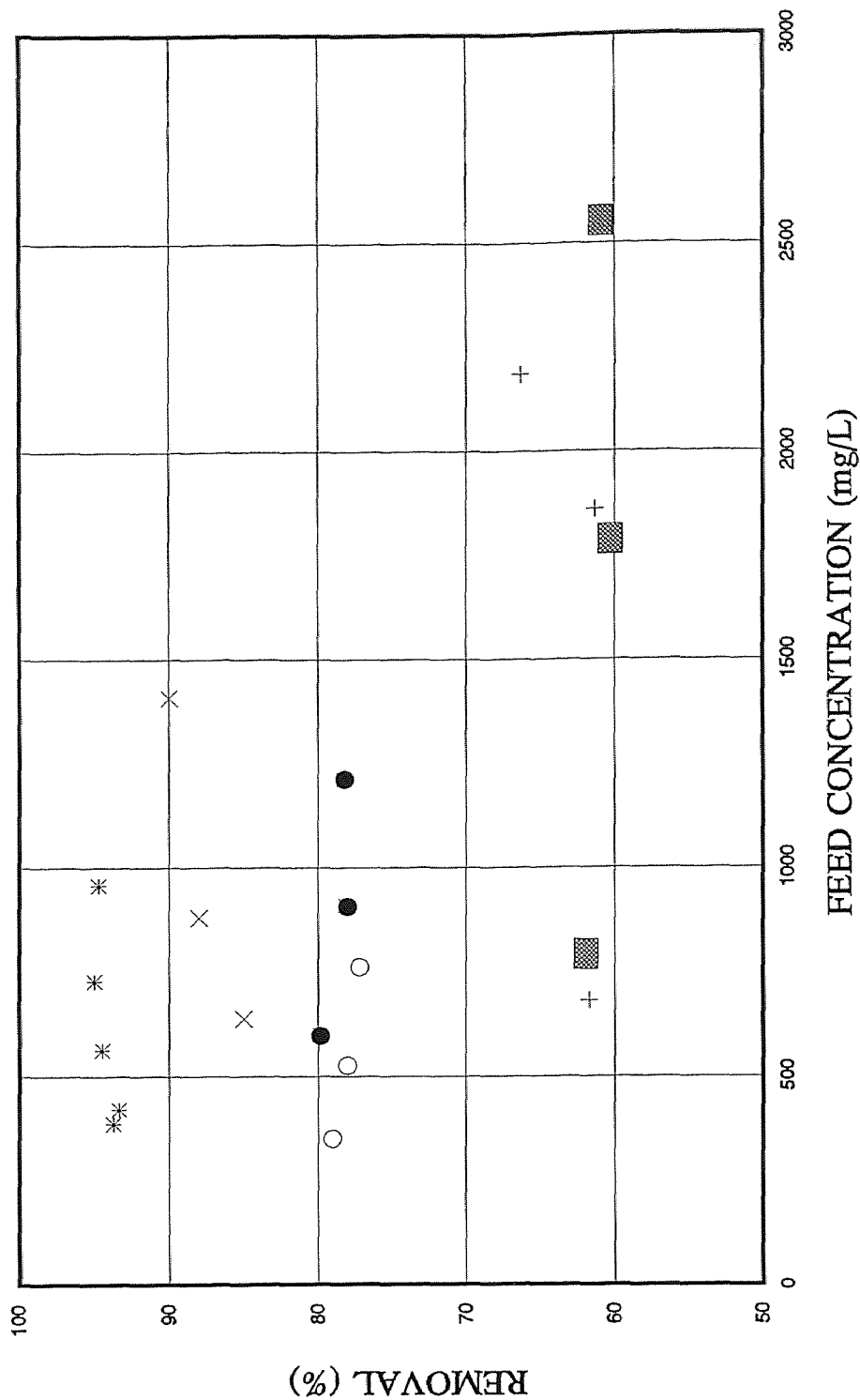
Figure 4.28. Effect of surfactant concentration on TCE removal in experiments with wetted pore

(Temp. = 25 C; Flow Rate = 2.5mL/min; Vacuum = 20 torr; TCE= 180-2600 ppm;)

✳ TCE-water/Non-wetted   ✕ 0.3% SDS/Non-wetted   + 1.0% SDS/Non-wetted

◯ TCE-water/Wetted   ● 0.3% SDS/Wetted   ▦ 1.0% SDS/Wetted
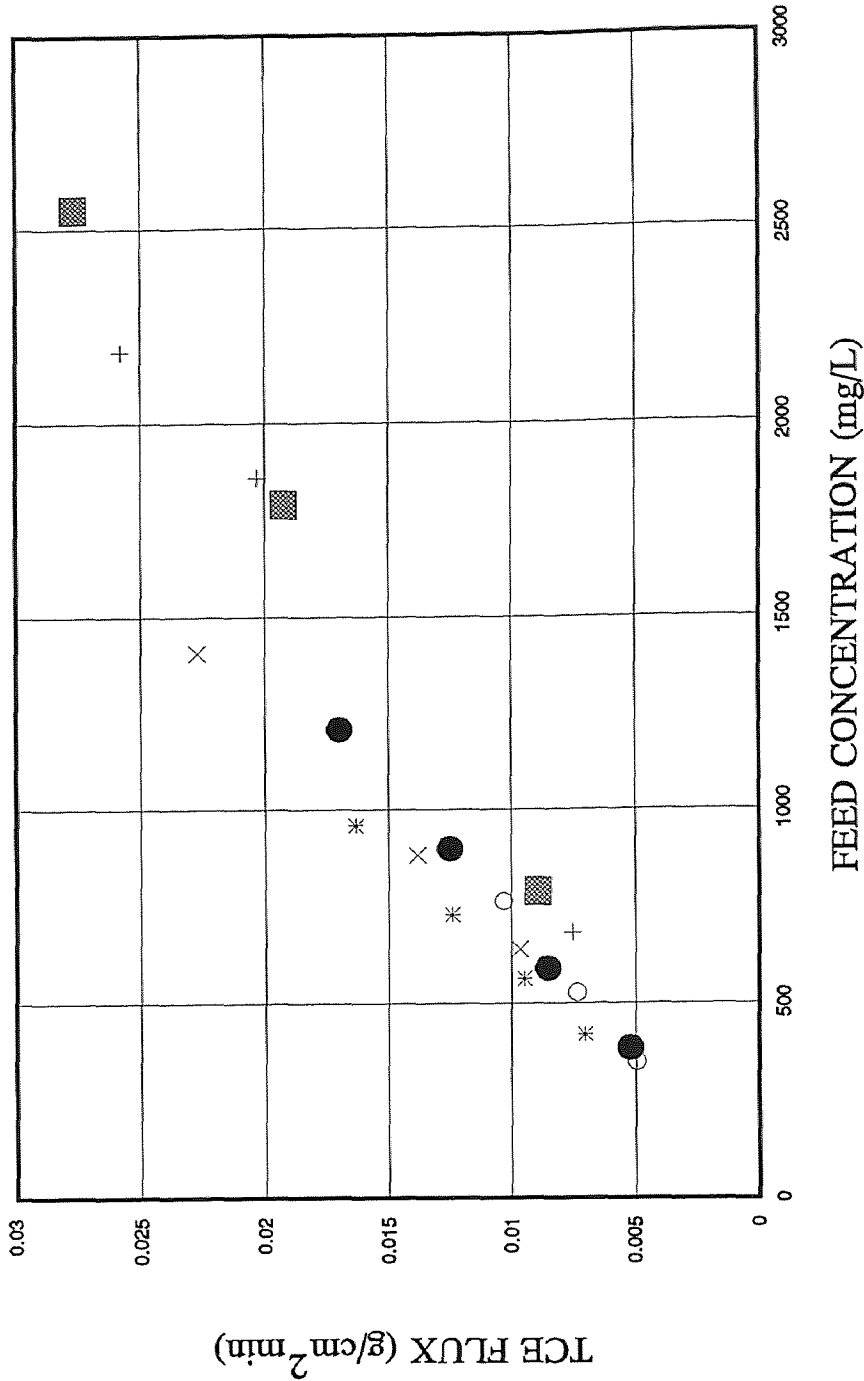
Figure 4.29. Effect of surfactant concentration on TCE flux in experiments with wetted pore

(Temp. = 25 C; Flow Rate = 2.5mL/min; Vacuum = 20 torr; TCE= 180-2600 ppm)

* TCE-water/Non-wetted   × 0.3% SDS/Non-wetted   + 1.0% SDS/Non-wetted

○ TCE-water/Wetted   ● 0.3% SDS/Wetted   ▦ 1.0% SDS/Wetted
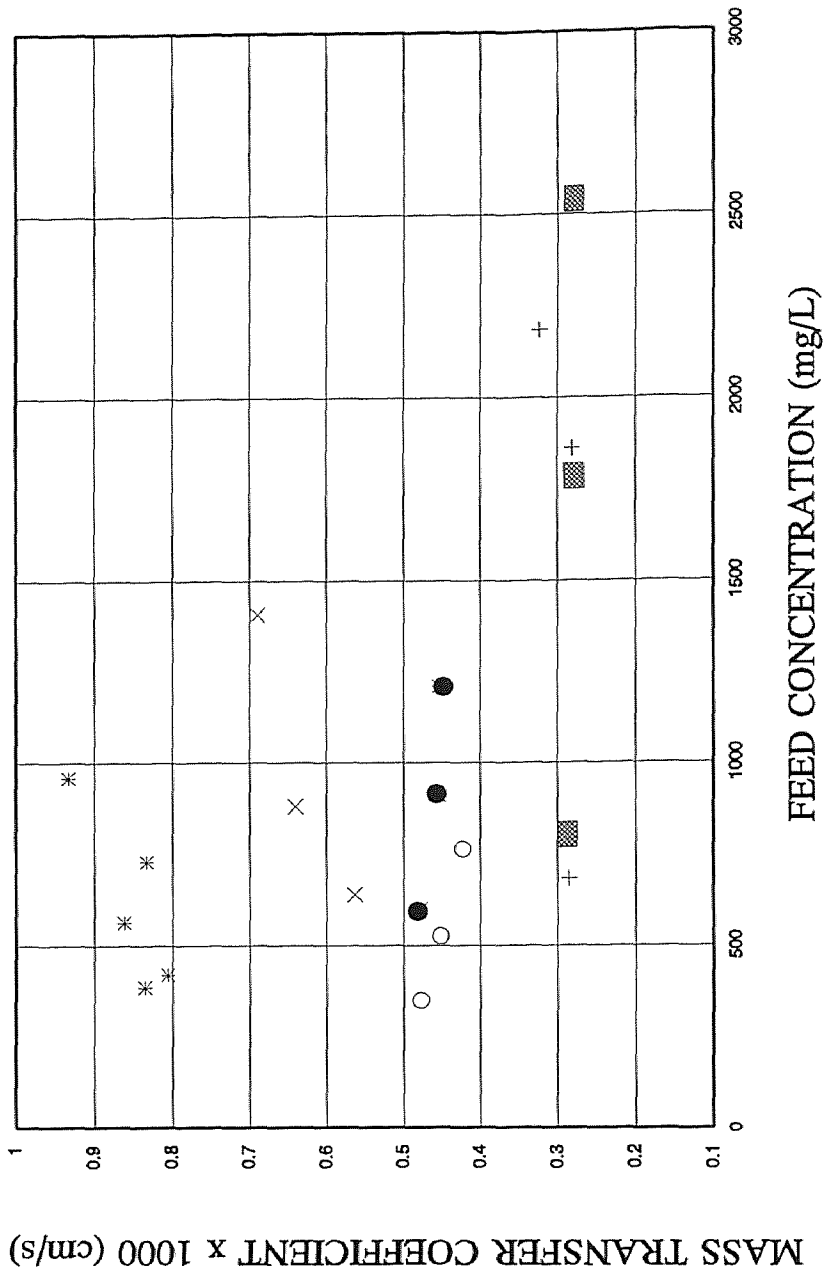
Figure 4.30. Effect of surfactant concentration on TCE mass transfer coefficient in experiments with wetted pore
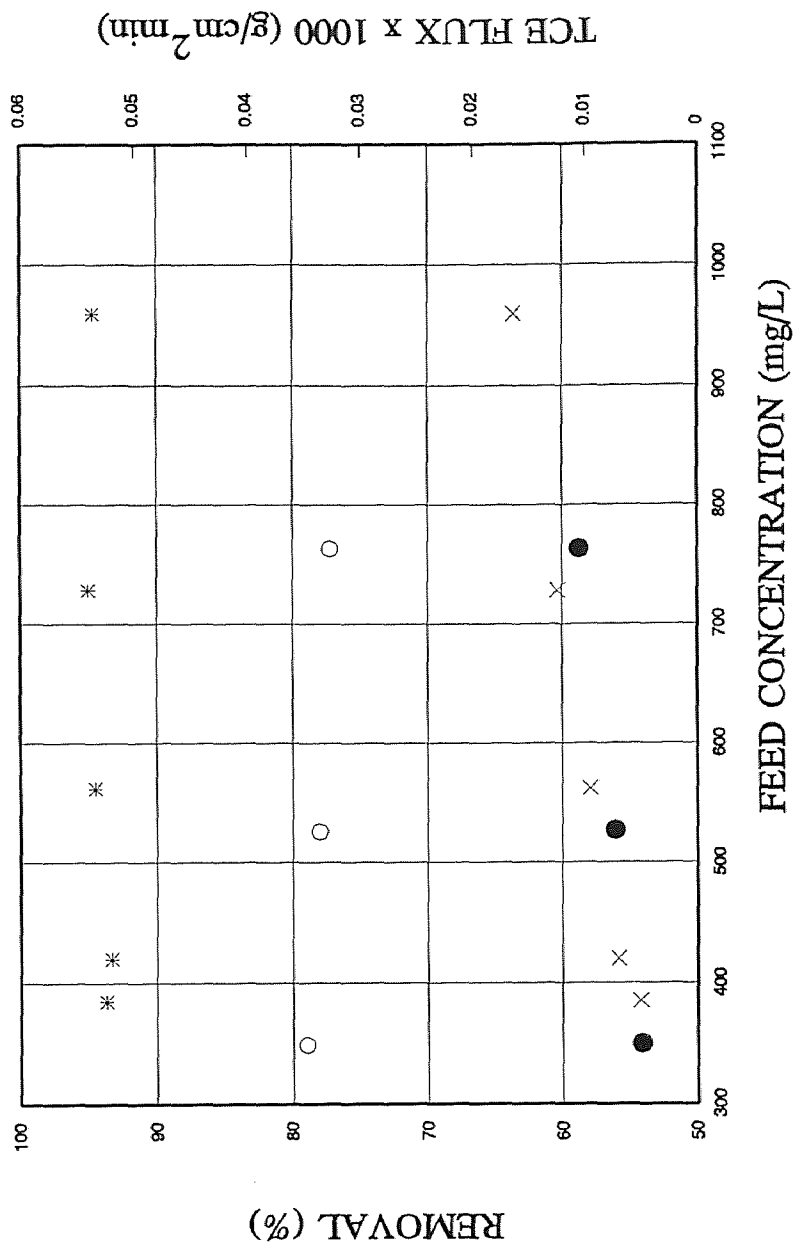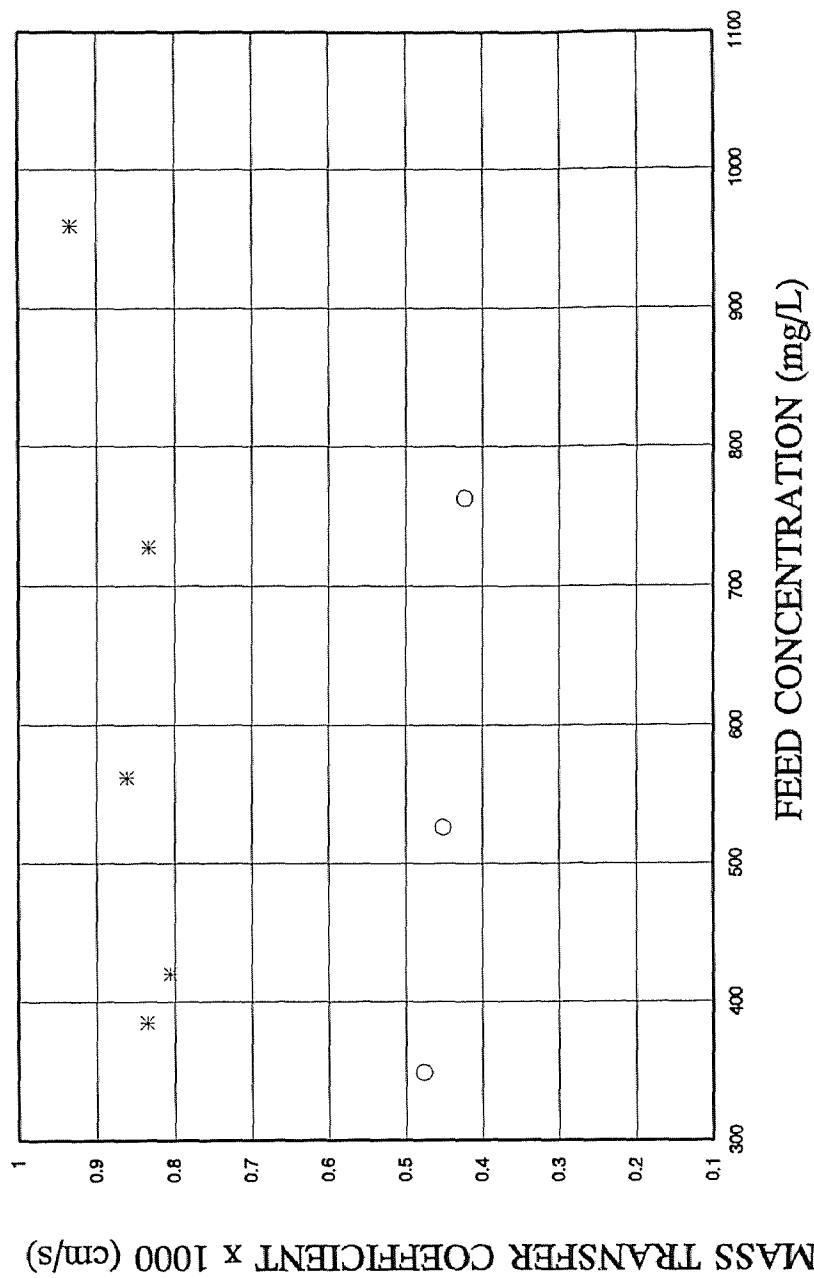
(Temp. = 25 C; Flow Rate = 2.5mL/min; Vacuum = 20 torr; TCE= 180-2600 ppm)

* TCE-water/Non-wetted   × 0.3%SDS/Non-wetted   + 1.0% SDS/Non-wetted

○ TCE-water/Wetted   ● 0.3%SDS/Wetted   ▨ 1.0%SDS/Wetted

removal is similar for wetted and non-wetted cases. From the above results it may be inferred that the pores are not wetted at 0.3% SDS and the lower removal is due to the resistance offered by the water-filled pore. Further, the results indicate that at 1.0% SDS concentration, the pores are wetted. TCE flux (Figure 4.29) for 0.3% SDS (wetted) is, as expected, lower than 0.3% SDS (non-wetted). TCE fluxes for wetted and non-wetted mode of operation at 1.0 % SDS are comparable to each other. Similar behavior is observed for the TCE overall mass transfer coefficient. For 0.3% SDS (wetted) the TCE overall mass transfer coefficient is 4.8×10^{-4} cm /s compared to 6.5×10^{-4} cm/s for non-wetted system. At 1.0% SDS the overall TCE mass transfer coefficient for the two modes of operation are similar.

4.4.2.2 Effect of Feed Flow Rate: Experiments were performed using 0.3%SDS feed solution at different feed flow rates. TCE concentration was varied between 1100-1200 ppm. Experiments were carried out at four flow rates: 2.5 mL/min, 10 mL/min, 25 ml/min and 40 mL/min. The results are shown in Figure 4.31 and 4.32. It is evident that TCE removal and TCE flux (Figure 4.31) are lower for experiments with wetted pore. TCE removal dropped from 79 % to 10 % as flow rate was increased from 2.5 mL/min to 40 mL/min. TCE overall mass transfer coefficient (Figure 4.32) is almost constant with changing feed flow rate. It has an average value of 5.0×10^{-4} cm/s compared to 6.8×10^{-4} cm/s for non-wetted pores. The above results corroborate the fact that at 0.3% SDS the feed solution does not wet the pores.

From section 4.4.2.1 and 4.4.2.2 it may be inferred that the pores are wetted somewhere between 0.3% SDS and 1.0% SDS concentration. As discussed earlier, the
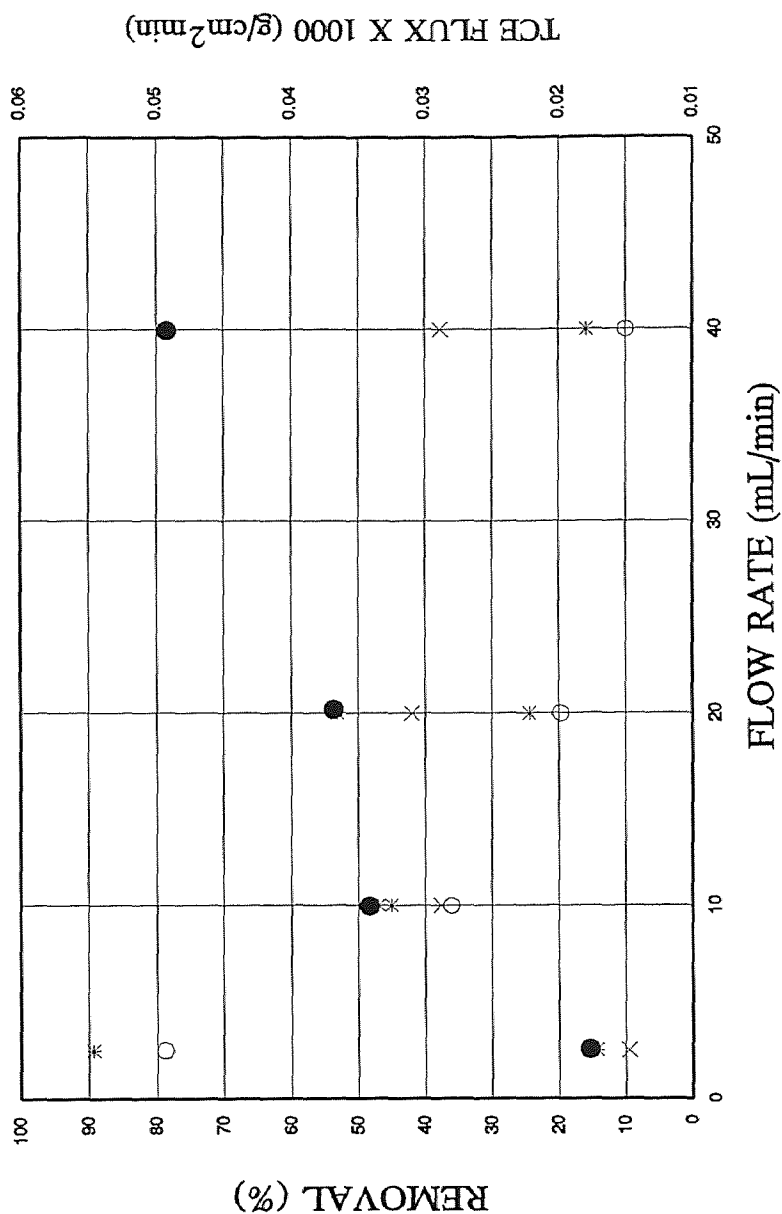
Figure 4.31. Effect of hydrodynamics on TCE removal and TCE flux in experiments with wetted pore using surfactant solution as feed

(0.3% SDS; Temp. = 25 C; Vacuum = 20 torr; TCE Conc.= 1000-1100 ppm; Feed-bleed mode)

* Removal/Non-wetted
○ Removal/Wetted

● TCE Flux/Non-wetted
× TCE Flux/Wetted
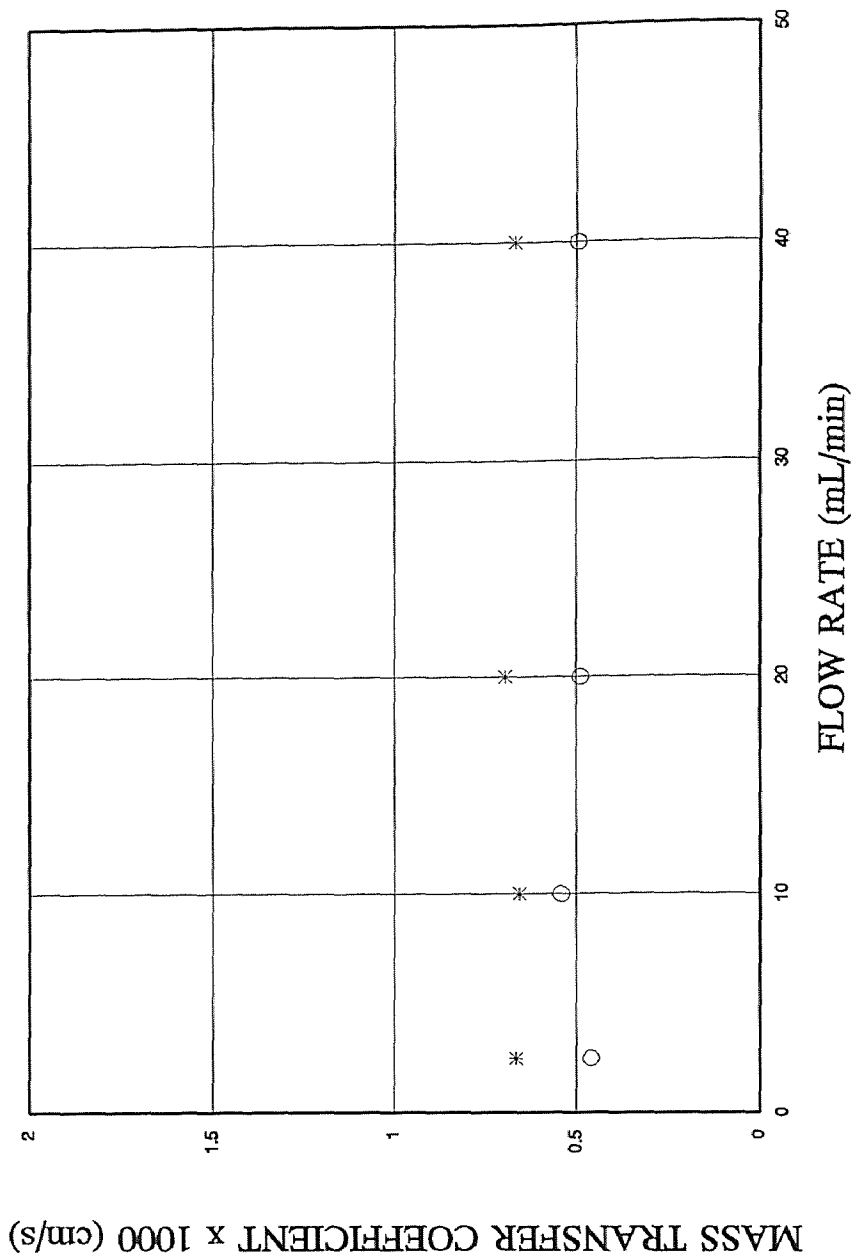
Figure 4.32. Effect of hydrodynamics on TCE mass transfer coefficient in experiments with wetted pore using surfactant solution as feed

(0.3% SDS; Temp= 25 C; Vacuum = 20 torr; TCE Conc= 1000-1100 ppm; Feed-bleed mode)

* Non-wetted   ○ Wetted

controlling resistances for TCE-water system are the feed-side boundary layer resistance and the membrane resistance. For surfactant system there are two additional resistances that impede the transport of TCE. One is the water-filled pore resistance, which is applicable only under conditions when the surfactant solution wets the pore. The other is the resistance offered by surfactant micelles to release free TCE. The TCE molecules are encapsulated in the micellar core and are not available in the bulk. As the surfactant concentration increases the probability of a micelle colliding with the wall and releasing TCE decreases. Therefore the availability of free TCE in the system is limited. Hence as the surfactant concentration increases there is a steady drop in the TCE overall mass transfer coefficient.

CHAPTER 5

CONCLUSIONS

The following conclusions may be drawn from the study on removal of VOCs from surfactant-flushed wastewater using membrane-based modified pervaporation process.

1) The membrane based stripmeation process efficiently removes VOCs from an aqueous solution.

2) The VOC concentration in the feed solution does not affect the extent of removal.

3) Increase in the feed flow rate results in a significant drop in VOC removal. At low flow rates VOC flux shows almost linear increase with increasing Reynolds number. At high feed flow rates, the VOC flux reaches a plateau and is unaffected by Reynolds number.

4) For TCE-water system the resistances-in-series approach may be used to estimate the transport rate of the VOC. It was found that the feed side boundary layer resistance and the membrane resistance were the controlling resistances.

5) For system containing surfactant solution as feed, increase in surfactant concentration resulted in lower VOC removal and lower VOC flux.

6) The presence of surfactants resulted in an additional resistance in the system. The resistance was a strong function of the surfactant concentration in the feed.

7) It was observed that the surfactant feed wets the pores of the substrate beyond a specific surfactant concentration. The water-filled pores (for wetted pores) offer significant resistance to transport of VOC.

8) The drop in VOC flux may be due to unavailability of free VOC in the bulk aqueous phase. At high surfactant concentrations most of the VOC is encapsulated in the micellar core and not present in the aqueous phase.

9) Additional resistance may be due to an adsorbed monomeric layer of surfactant on the porous polypropylene substrate.

10) For both systems, surfactant and non-surfactant, it was observed that tube-side feed configuration was more efficient compared to shell-side feed.

APPENDIX A

PERVAPORATION

A.1 Introduction

The term pervaporation was mentioned by Kober (1917) in a publication reporting separation of water from aqueous solutions of albumin and toluene through cellulose nitrate films. The potential of pervaporation and its basic principles were established by Binning and co-workers (1958, 1961, 1962). In the early 1980s, Gesellschaft fur Trenntechunik (GFT) Co. developed a composite membrane that had porous substrate coated with a thin layer of poly(vinyl alcohol). This paved the way for use of pervaporation as an economical and effective commercial process for dehydrating ethanol.

Pervaporation separation is governed by the chemical nature of the macromolecules that comprise the membrane, the physical structure of the membrane, the permeant-permeant and permeant-membrane interactions, the physical structure of the membrane, and the physico-chemical properties of the mixture. Pervaporation can be operated at low feed pressures and even below ambient temperatures. Also, there is no need to add additional chemicals for the separation which makes it an attractive separation process in biotechnology, especially for the concentration of heat-, stress-, chemical-sensitive biochemicals (Farber, 1935). As in reverse osmosis, the liquid in contact with the membrane dissolves in it and causes membrane swelling, which in turn alters membrane properties like permeability and selectivity. But this is true only at high solute concentrations. Downstream vapor pressure must be maintained as low as possible

so that the driving force for permeation is maximum and the process is economically feasible. Unlike reverse osmosis, pervaporation transport is not limited by osmotic pressure. The feed pressure is not critical as driving force for mass transfer through the membrane is achieved by lowering the chemical potential of the permeate stream. Tanimura et al. (1990) compare reverse osmosis with pervaporation and show that for a given membrane and a given liquid mixture both the permeation flux and the separation factor in pervaporaion are higher. Compared to distillation, where separation is based on relative volatility, in pervaporation, the basis of separation is the physical-chemical interaction between the membrane material and the permeating molecules. Therefore, pervaporation is commonly considered to be a profitable complement to distillation for the separation of aezotropic and close-boiling mixtures which requires at present energy-intensive processes.

The pervaporation process involves a phase change of permeating species from the liquid to the vapor-state, therefore needing energy for the vaporization. Hence, from an energy consumption point of view, pervaporation is a promising process especially for those systems where the concentration of the preferentially permeating species in the feed is low. The heat of vaporization required for permeation can be supplied either in the feed liquid or by sweeping fluid on the permeate side or directly to the membrane. Wnuk et al. (1992) and Boddeker et al. (1993) have reported experimental data on pervaporation processes using heated membranes. There is yet to be conclusive evidence as to which mode is the most efficient.

A.2. Mass Transport in Pervaporation Process

There are principally two approaches to describe mass transport in pervaporation: (i) solution-diffusion model and (ii) the pore flow model. Both these models will be discussed in some detail in this section.

The solution-diffusion model proposes the following mechanism to describe the pervaporation process: (i) sorption of the permeant from the feed liquid to the membrane, (ii) diffusion of the permeant in the membrane, and (iii) desorption of the permeant to the vapor phase on the downstream side of the membrane. A schematic representation of the solution diffusion model is illustrated in Figure A.1. Solubility and diffusivity are the two parameters that are important in the model. Both of these parameters are concentration dependent and in literature one finds various empirical expressions describing the concentration dependence of the two parameters. Depending on the system and process conditions a suitable relationship may be chosen. The solution-diffusion model has found wide acceptance amongst membrane researchers (Kataoka et al., 1991 a,b; Wijmans and Baker, 1995).

Systems that have a single component transporting through a non-porous homogeneous membrane have been relatively well described by the solution-diffusion model(Fels and Huang, 1971; Greenlaw et al.; 1977, Brun et al.; 1985, a, b). Exponential or linear expressions have been used to describe the concentration dependence of diffusivity. For binary or multi-component mixtures, the mass transport is complicated by the permeant-permeant interaction and permeant-membrane interaction There is yet to be a comprehensive theory describing the mass transport for such systems. Fels and Huang (1971) pursued the approach of free-volume theory for diffusion of organic substances in
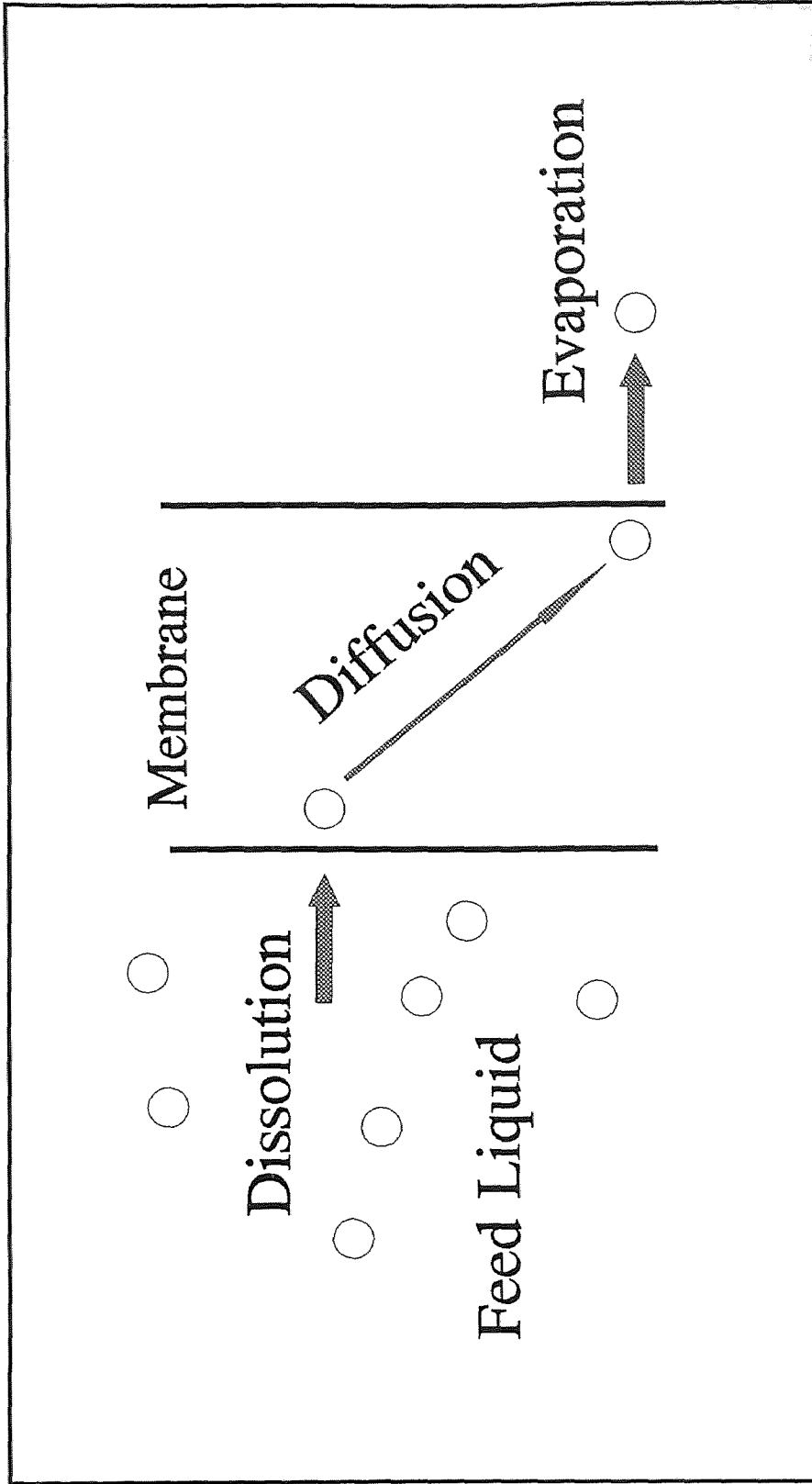
Figure A.1. Schematic representation of the Solution-Diffusion model in pervaporation

polymers to describe transport of binary mixtures through pervaporation membranes. However, discrepancy between theory and experiments were found due to ambiguity in estimating the free-volume parameter. Also, the model was criticized for not including any permeant - permeant interaction parameter. Fels and Huang model was later modified by introducing the interaction parameters (Huang and Rhim, 1992; Rhim and Huang, 1989, 1992), and a further improvement was made by Yeom and Huang (1992) to account for the effect of the flux coupling. Using the experimentally obtainable parameters, the modified model enables prediction and interpretation of pervaporation performance for a given separation system. However, the model cannot be used to estimate the effect of permeate pressure because it assumes zero concentration of the permeating species on the membrane side. Doong et al., (1995) has proposed a more comprehensive model using the free volume approach for multi component pervaporation processes.

Lee (1975) used concentration independent diffusion coeffecients and constant solubilities for both permeating species in his proposed model to describe mass transport in binary systems. This was an oversimplification and can hardly be applicable to liquid mixtures. Greenlaw et al., (1977) presented a simple model that was based on the assumption that the contribution of the permeants to their diffusivities is linearly additive. He used the model to describe pervaporation of hexane/heptane mixtures, that behave ideally. However, his model is inapplicable to non-ideal cases like alcohol-water mixtures.

Brun et al., (1985 b) have proposed a 'six-coefficient exponential model' to describe transport of binary mixtures. The model parameters need to be determined by

fitting experimental data to flux equation. However, as model parameters involved were many, it was difficult to asertain the physical significance of any particular parameter. To reduce the ambiguity, the model suggested estimation of parameters by conducting sorption experiments in addition to pervaporation experiments so that the parameters related to membrane interface equilibrium could be determined independently. But this is true only for systems where Henry's law is obeyed as a constant solubility was assumed in the model derivation.

Mulder and Smolders (1984, 1985 a, b, 1986) developed a more complex model that incorporated sorption and diffusion aspects. The flux was described by two coupled non-linear differential equations that included permeant-permeant and permeant-membrane interaction parameters. However, the functional relationships between operational variables and the membrane performance are difficult to find because the model supposes the knowledge of diffusivity as a function of permeate concentration. This limits the practical use of the model. Blume et al., (1990) considered pervaporation as a combination of liquid evaporation and vapor permeation, which facilitated the mathematical treatment. This approach does not differentiate between systems in which the liquid feed is in contact the with the membrane and the feed vapor is in contact with the membrane. However, this description does not seem accurate as membranes swelling by a liquid is more significant than by a vapor of the same species, and thus, it is expected that the membrane will exhibit different diffusivity to a penetrant in a liquid and vapor states.

Matsuara and coworkers have proposed a transport model based on pore flow mechanism (Okada and Matsuura, 1991, 1992; Okada et al., 1991). The pore flow model

assumes a bundle of straight cylindrical pores on the membrane surface and describes mass transport by the following three steps: (i) liquid transport from the pore inlet to a liquid-vapor phase boundary, (ii) evaporation at the phase boundary, and (iii) vapor transport from the boundary to the pore outlet. Figure A.2 gives a schematic representation of the pore flow model. The distinguishing feature of the model is that it assumes a liquid-vapor phase boundary inside the membrane, and pervaporation is considered to be a combination of liquid transport and vapor transport in series. Compared to the solution diffusion model the pore flow model gives a more clearer picture of the location of the phase change of the permeant in the membrane. The physical structure of the membrane is better explained by the pore flow model. However, models describing solute transport are few and quantitative expressions are yet to be fully developed. Pore flow models also encounters problems because they use macroscopic quantities such as friction and viscosity (Okada and Matsuura, 1991) and fluid continuity does not always hold for small pores. The solution-diffusion model considers the pores as passageways allowing communication between the upstream and the downstream membrane face by Knudsen flow or viscous flow mechanism. It is clear that the pore concept in the pore-flow model is not similar to that in the solution-diffusion model. However, both models predict correctly that membranes, with pores large enough for Knudsen or viscous flow to occur, have no or little selectivity.

A.3 Polymeric Membrane Materials for Pervaporation

Polymeric materials are widely used for pervaporation membranes. They maybe classified as glassy polymer membranes, rubbery polymeric membranes and ionic
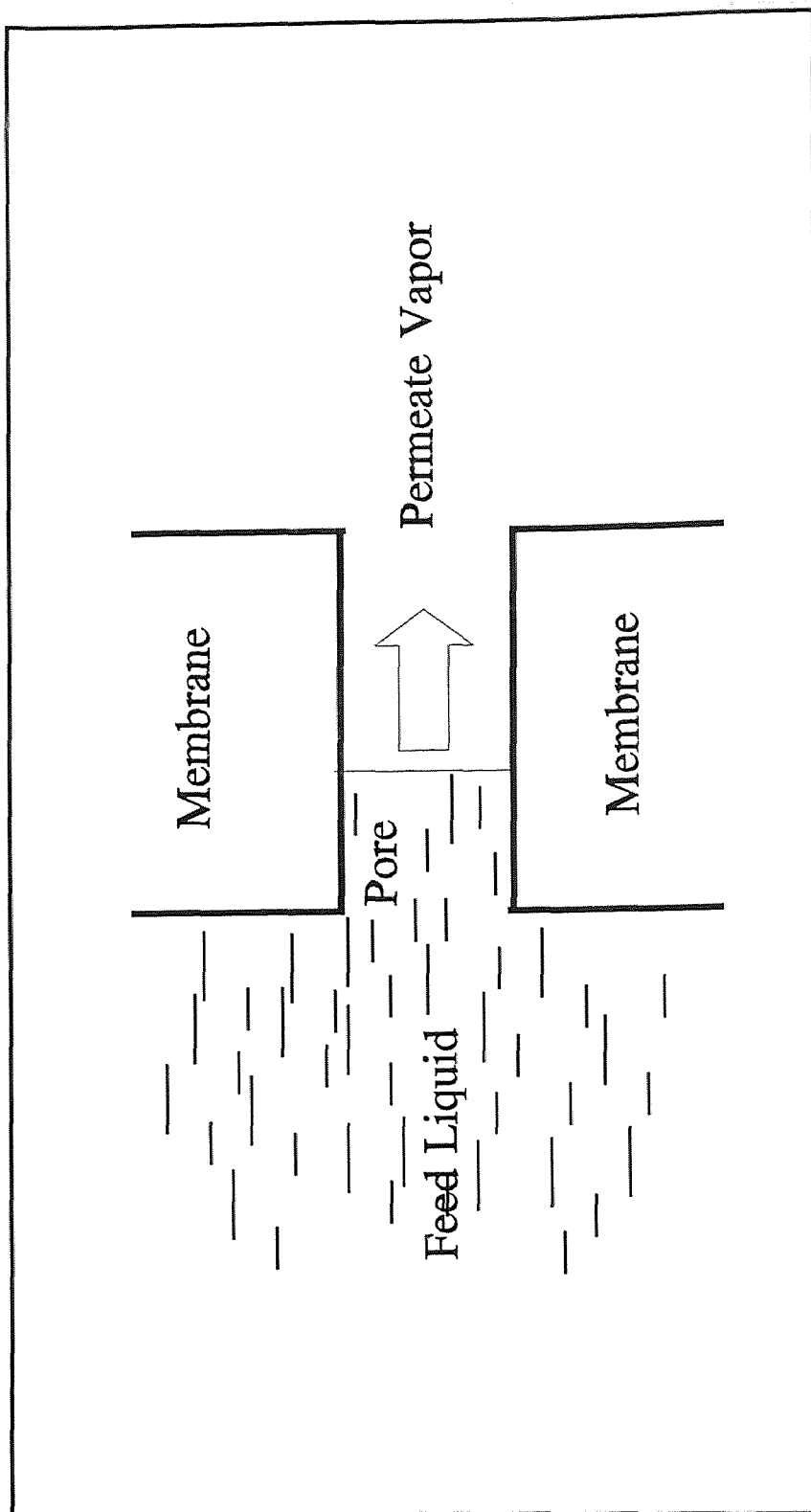
Figure A.2. Schematic representation of the Pore-flow model in pervaporation

polymer membranes. Usually, glassy polymers are suitable for making water selective membranes used for solvent dehydration. Rubbery polymers are favorable to the selective removal of organic compounds from water. Ionic polymer membranes that have an affinity for water, are also finding use as dehydration membranes.

Poly (vinyl alcohol) (PVA), poly (acrylic acid)(PAA), chitosan and aromatic polyimide materials are amongst the most commonly used for making dehydration membranes. A membrane with low hydrophilicity generally exhibits a low water flux and dehydration but some membranes with high hydrophilicity like PVA and PAA need cross-linking for improved stability and selectivity. Feng (1995) conducted an extensive survey on pervaporation membranes which has been documented by Neel (1991). It shows that silicone-based polymers (primarily polydimethylsiloxane(PDMS)) are mainly used for selective permeation of organic compounds from aqueous solutions, and PTMSP and other silicone-containing polyacetylene derivatives are under development as potential membrane materials (Nagase et al., 1990, 1991, a, b; Kang et al., 1994). Usually, silicone membranes exhibit limited selectivity for some mixtures such as lower alcohols-water and acetic acid-water (Netke et al., 1995). To improve selectivity Bartels-Caspers et al., (1992) and Vankelcon et al., (1995) have attempted to fill the membrane with organophilic adsorbent.

According to solution-diffusion model, membrane permeability is determined by diffusivity and solubility. While smaller permeating molecules usually exhibit larger diffusivity, the solubility is often influenced by the chemical affinity of the permeating species to the membrane material. Consider separation of an aqueous organic mixture where water molecules are smaller than their organic counterparts. A hydrophilic

membrane favors both solubility and diffusivity for selective permeation of water, while an organophilic membrane must have a large solubility to the organic compound in order to permeate the organic compound preferentially. Polymers with high selectivity are often preferred for further study because the disadvantage associated with low permeability can be partly compensated by introducing asymmetry to the membrane structure, thereby reducing the effective thickness of the membrane. Among the many approaches used for membrane material selection, a few are: solubility parameter approach (Mulder et al., 1985; Welzlaff et al., 1985; Mulder and Smolders, 1985a, 1986, 1991), contact angle approach (Farnand and Noh, 1989), polarity parameter approach (Shimidzu and Yoshikawa, 1991) and surface thermodynamics approach (Oss et al., 1983; Lee et al., 1989).

A.4 Hollow Fiber Module Configuration in Pervaporation

Flat membranes housed in plate-and-frame modules and spiral-wound modules have traditionally been more popular for pervaporation processes. But hollow fiber modules are becoming more common as their design is getting better . Hollow fiber membrane permeaters are constructed similar to the shell and tube heat exchanger. The feed solution can be introduced to either the shell side or the bore side depending on the system requirements. Hollow fiber membranes have the following advantages: high membrane packing density (compared to flat membranes), self-supporting (flat membranes need mechanical support) and the hollow fibers themselves form the vacuum vessel if the shell-fed mode of operation is used. However, when the feed is passed on the shell side and permeate is withdrawn from the fiber bore, the permeate pressure build-up inside the

hollow fiber substantially reduces the driving force for the process (Huang and Feng, 1993). This may be reduced by using larger fiber diameters but the high membrane area packing density will be sacrificed. Conventionally in pervaporation the shell side mode of operation is more widely used because the mass transfer coefficient can be considerably higher than that in the tube side (Gooding et al., 1995; Feng and Huang, 1997)Shell-side feed in the hollow fiber of interest encounters a separate problem in SEAR processes. The NAPLs are often contaminated by heavy oils. Shell-side operation will lead to permeation of these heavy oils through the non-porous rubbery skin into the microporous substrate. The permeated oils will create a severe permeate side pressure drop problem in pervaporation by partially or totally blocking substrate pores as well as the fiber bores.

Tube-side feed mode of operation will, however, have no such problem. The permeated oils can be removed through thousands of inter-fiber gaps just as the permeate vapor can be removed. However, there is considerable possibility that these heavy oils may form an immobilized liquid membrane in the substrate pores on the feed side. This may increase the selectivity of the VOC over water substantially. Such a phenomenon was deliberately created by Yang et al. (1995) who had employed a contained nonvolatile organic liquid membrane in contact with a silicone capillary for pervaporation removal of toluene and TCE from water. The organic liquid membrane reduced the water flux by 3 to 5 times.

Tube side fed mode may be successfully used only if the composite membrane can withstand the applied pressure difference. Hydrophobic microporous hollow fiber substrate plasma polymerized with silicone are examples of composite membrane which can support the pressure difference (Papadoupolous and Sirkar, 1994). Both the modes of

operation, shell side feed and tube side feed have their advantages and their application depend on the system that needs to be separated.

A.5   Pervaporation in Industry

Pervaporation is one of the most active areas in membrane research and is finding acceptance as a commercially viable process. The applications of pervaporation can be classified into three broad categories: dehydration of organic solvents, removal of organic compounds from aqueous solutions and separation of anhydrous organic mixtures. Currently pervaporation has been commercialized for two applications: one is the dehydration of alcohols and the other is the removal of organic compounds from contaminated waters. The separation of organic-organic mixtures needs more development due to lack of membrane stability under relatively harsh conditions, but it represents the largest opportunity for energy and cost savings. Separation of methanol/methyl tert-butyl ether (MTBE)/ C_4 aezotropes is now being actively investigated due to commercial interest of producing octane enhancers for gasolene (Chen et al., 1989; Farnand and Noh, 1989; Shah et al., 1989; Doghieri et al., 1994; Nakagawa and Matsuo, 1994; Park et al., 1995; Chen and Martin, 1995). Membrane pervaporation is also being investigated as a chemical sensor in instrumental analysis (Mattos and de Castro, 1994; Papaefstathiou et al., 1995; Papaefstathiou and de Castro, 1995). Once a suitable membrane is available, pervaporation can also find a niche in some reversible reactions such as esterification and condensation to remove one or more products species selectively, thereby shifting the equilibrium towards the product side (David et al., 1991, a, b, 1992; Okamoto et al., 1991,1993; Bagnel et al., 1994).

Dehydration of aqueous electrolyte solutions (Schaetzel et al., 1993) and aroma recovery and beer dealcoholization in the food industry (Lee and Kayani, 1991; Karlsson and Tragardh, 1993, 1994; Lamar et al.,1994) are other potential applications of pervaporation.

Pervaporation membrane devices are characterized by their modular construction. They maybe used in small and large processes because there is no significant economy of scale. Also, it is easy to integrate with other techniques so that the hybrid technique is more effective than a separation effected by either technique alone. In a comprehensive assessment of fluid separation techniques, pervaporation is ranked third amongst 31 techniques evaluated (Bravo et al., 1986).

APPENDIX B

COMPUTER PROGRAMS

B.1 AICHE.FOR

```
C
C This is a program tried to model the process of a hollow fiber
C module which has VOC flow in the tube and vacuum in the shell side
C using IMSL BVPFD/DBVFD.
C

C
C Specifications for Parameters
C
      INTEGER   LDYFIN,LDYINI,MXGRID,NEQNS,NINIT
      PARAMETER (MXGRID=100, NEQNS=5, NINIT=10,
LDYFIN=NEQNS,
      &   LDYINI=NEQNS)
      INTEGER I, J, NCUPBC, NFINAL, NLEFT, NOUT
      REAL    CONST, ERREST(NEQNS), FCNBC, FCNEQN, FCNJAC,
FLOAT
      &      PISTEP, TOL, XFINAL(MXGRID), XINIT(NINIT), XLEFT,
      &      XRIGHT, YFINAL(LDYFIN,MXGRID), YINIT(LDYINI,NINIT)
      LOGICAL LINEAR, PRINT
      INTRINSIC FLOAT
      EXTERNAL  BVPFD, CONST, FCNBC, FCNEQN, FCNJAC, SSET,
UMACH
      COMMON XINLET,Q0VOC,BVOC,Q0N2,BN2,PFEED,PVAC,
      &      BETA,VFEED,FBOUND
C
C
```

```
*********************************************************************
C
C This portion is to collect the experimental data. The converted
C data is derived from INFORM.FOR
C
      OPEN (1,FILE='INFORM.DAT',STATUS='OLD')
      READ (1,*) XINLET, PFEED
      READ (1,*) FBOUND
      READ (1,*) PVAC
      READ (1,*) BETA, VFEED
```

```
      READ (1,*) Q0VOC, BVOC
      READ (1,*) Q0N2, BN2
      CLOSE (1, STATUS='KEEP')
C   PRINT *, Q0VOC, BVOC, Q0N2, BN2
C
C QVOC= AVOC*exp(BVOC*PRVOC)
C QN2= AN2*exp(BN2*PRVOC) at constant temperature,
C where QVOC and QN2 are the permeability of VOC and N2
C
C ^^^^^^^^^^^^^^^^^^^^^^^^^^^^^^^^^^^^^^^^^^^^^^^^^^^^^^^^^^^^^^^^
C
C Set Parameters
C
      NLEFT=2
      NCUPBC=0
      TOL=0.0001
      XLEFT=0.0
      XRIGHT=1.0
      PISTEP=0.0
      PRINT= .FALSE.
      LINEAR= .FALSE.
C
C Define XINIT
C
      DO 10 I=1, NINIT
      XINIT(I)=XLEFT+(I-1)*(XRIGHT-XLEFT)/(FLOAT(NINIT-1))
C   PRINT *, XINIT(I)
  10    CONTINUE
C
C Get YINIT from YINIT.DAT which is calculated from YINIT.FOR by
C cocurrent assumptions
C
      OPEN (2,FILE='YINIT.DAT',STATUS='OLD')
      DO 20 I=1, NINIT
      READ (2,*) YINIT(1,I),YINIT(2,I),YINIT(3,I),
      &      YINIT(4,I),YINIT(5,I)
C   PRINT *, YINIT(1,I),YINIT(2,I),YINIT(3,I),YINIT(4,I),YINIT(5,I)
  20 CONTINUE
      CLOSE (2, STATUS='KEEP')
C
C Solve Problem
C
      CALL BVPFD(FCNEQN, FCNJAC, FCNBC, FCNEQN, FCNBC, NEQNS,
NLEFT,
      &      NCUPBC, NLEFT, XRIGHT, PISTEP, TOL, NINIT, XINIT,
      &      YINIT, LDYINI, LINEAR, PRINT, MXGRID, NFINAL,
```

```
     &        XFINAL, YFINAL, LDYFIN, ERREST)
C
C Print Results
C
     OPEN (3,FILE='AICHE-V.DAT',STATUS='NEW')
     CALL UMACH(2,NOUT)
     WRITE (NOUT, 9997)
     WRITE (NOUT, 9998) (I,XFINAL(I),(YFINAL(J,I), J=1,NEQNS),I=1,
     &    NFINAL)
     WRITE (NOUT, 9999) (ERREST(J), J=1,NEQNS)
     WRITE (3, *) ((YFINAL(J,I), J=1,NEQNS),I=1,
     &    NFINAL)
     WRITE (3,*) 'ERROR ESTIMATES'
     WRITE (3,*) (ERREST(J), J=1,NEQNS)
     CLOSE (3, STATUS='KEEP')
9997     FORMAT (4X,'I',7X,'X',14X, 'Y1', 13X, 'Y2', 13X, 'Y3',
     &        13X,'Y4',13X,'Y5')
9998     FORMAT (I5,1P6E15.6)
9999     FORMAT (' ERROR ESTIMATES', 4X, 1P5E15.6)
     END
C
C Subroutines
C
C


&&&&&&&&&&&&&&&&&&&&&&&&&&&&&&&&&&&&&&&&&&&&&&&&&&&&
     &&&&&&&&&&&&&&&&&&&&&&&&&&&&&&&
C
     SUBROUTINE FCNEQN (NEQNS, X, Y, P, DYDX)
C
C Y(1), Y(2), Y(3), Y(4), and Y(5) are L*, V*, x, y, and gamma1* in the
C derivation, respectively.  DYDX(1), DYDX(2), DYDX(3), AND DYDX(4)
C are dL*/ds, dV*/ds, dx/ds, dy/ds, dgamma1*/ds, respectively
C
     INTEGER NEQNS
     REAL X, Y(NEQNS), P, DYDX(NEQNS), ALA, ALB
     COMMON XINLET,Q0VOC,BVOC,Q0N2,BN2,PFEED,PVAC,
     &        BETA,VFEED,FBOUND
C
C Define differential equations
C
C   PRINT *, Q0VOC, BVOC, Y(5), Y(3)
     ALA=FUNA(NEQNS,X,Y)
     ALB=FUNB(NEQNS,X,Y)
C   PRINT *,Y(1),Y(2),Y(3),Y(4)
```

```fortran
      Y1P1=ALA*(Y(5)*Y(3)-PVAC*Y(4))
      Y1P2=ALB*(Y(5)*(1.0-Y(3))-PVAC*(1.0-Y(4)))
      DYDX(1)=Y1P1+Y1P2
      Y2P1=Y1P1
      Y2P2=Y1P2
      DYDX(2)=Y2P1+Y2P2
      Y3P1=ALA*(1.0-Y(3))*(Y(5)*Y(3)-PVAC*Y(4))
      Y3P2=ALB*Y(3)*(Y(5)*(1.0-Y(3))-PVAC*(1.0-Y(4)))
      DYDX(3)=(Y3P1-Y3P2)/Y(1)
      IF (X.EQ.0.0) THEN
        Y4AN1=ALA*(1.0-Y(4))*(Y(5)*DYDX(3)+Y(3)*DYDX(5))
        Y4AN2=ALB*Y(4)*(-Y(5)*DYDX(3)+(1.0-Y(3))*DYDX(5))
        Y4AN3=BVOC*(Y(3)*DYDX(5)+DYDX(3)*Y(5))*ALA*
     &        (1.0-Y(4))*(Y(5)*Y(3)-PVAC*Y(4))
        Y4AN4=BN2*(Y(3)*DYDX(5)+DYDX(3)*Y(5))*ALB*
     &        Y(4)*(Y(5)*(1.0-Y(3))-PVAC*(1.0-Y(4)))
       Y4AN=Y4AN1-Y4AN2+Y4AN3-Y4AN4
        Y4DN1=2.0*Y(3)*Y(5)*(ALA-ALB)
        Y4DN2=ALA*PVAC
        Y4DN3=3.0*(ALA-ALB)*PVAC*Y(4)
        Y4DN4=2.0*ALB*(Y(5)-PVAC)
       Y4DN=Y4DN1+Y4DN2-Y4DN3+Y4DN4
      DYDX(4)=Y4AN/Y4DN
      ELSE
        Y4P1=ALA*(1.0-Y(4))*(Y(5)*Y(3)-PVAC*Y(4))
        Y4P2=ALB*Y(4)*(Y(5)*(1.0-Y(3))-PVAC*(1.0-Y(4)))
      DYDX(4)=(Y4P1-Y4P2)/Y(2)
      ENDIF
      DYDX(5)=BETA*VFEED*Y(1)/Y(5)
      RETURN
      END
C
```

&&&&&&&&&&&&&&&&&&&&&&&&&&&&&&&&&&&&&&&&&&&&&&&&&&&&
&&&&&&&&&&&&&&&&&&&&&&&&&

```fortran
C
C Subroutine to evaluate Jacobian
C
      SUBROUTINE FCNJAC (NEQNS, X, Y, P,DYPDY)
      INTEGER NEQNS
      REAL X,Y(NEQNS),P,DYPDY(NEQNS,NEQNS),YPRIME(6)
      COMMON XINLET,Q0VOC,BVOC,Q0N2,BN2,PFEED,PVAC,
     &        BETA,VFEED,FBOUND
C
      ALA=FUNA(NEQNS,X,Y)
      ALB=FUNB(NEQNS,X,Y)
```

```
      DELTA=1.0E-5
C
C    Evaluate deratives
C
      DO 10 I=1,NEQNS
      K=I
      YPRIME(I)=FUNC(NEQNS,X,Y,I)
   10 CONTINUE
C
C    Estimate partial derative numerically
C
      DO 30 J=1,NEQNS
      Y(J)=Y(J)+DELTA
      DO 20 I=1,NEQNS
      K=I
      DYPDY(I,J)=(FUNC(NEQNS,X,Y,K)-YPRIME(I))/DELTA
   20 CONTINUE
      Y(J)=Y(J)-DELTA
   30 CONTINUE
      RETURN
      END
C
C Function to calculate the Jacobian values
C
      FUNCTION FUNC(NEQNS,X,Y,I)
      REAL Y(NEQNS)
      COMMON XINLET,Q0VOC,BVOC,Q0N2,BN2,PFEED,PVAC,
     &      BETA,VFEED,FBOUND
      ALA=FUNA(NEQNS,X,Y)
      ALB=FUNB(NEQNS,X,Y)
      GO TO (1,2,3,4,5),I
    1 Y1P1=ALA*(Y(5)*Y(3)-PVAC*Y(4))
      Y1P2=ALB*(Y(5)*(1.0-Y(3))-PVAC*(1.0-Y(4)))
      FUNC=Y1P1+Y1P2
      RETURN
    2 Y2P1=ALA*(Y(5)*Y(3)-PVAC*Y(4))
      Y2P2=ALB*(Y(5)*(1.0-Y(3))-PVAC*(1.0-Y(4)))
      FUNC=Y2P1+Y2P2
      RETURN
    3 Y3P1=ALA*(1.0-Y(3))*(Y(5)*Y(3)-PVAC*Y(4))
      Y3P2=ALB*Y(3)*(Y(5)*(1.0-Y(3))-PVAC*(1.0-Y(4)))
      FUNC=(Y3P1-Y3P2)/Y(1)
      RETURN
    4 IF (X.EQ.0.0) THEN
      Y3P1=ALA*(1.0-Y(3))*(Y(5)*Y(3)-PVAC*Y(4))
      Y3P2=ALB*Y(3)*(Y(5)*(1.0-Y(3))-PVAC*(1.0-Y(4)))
```

```fortran
      DYDX3=(Y3P1-Y3P2)/Y(1)
      DYDX5=BETA*VFEED*Y(1)/Y(5)
        Y4AN1=ALA*(1.0-Y(4))*(Y(5)*DYDX3+Y(3)*DYDX5)
        Y4AN2=ALB*Y(4)*(-Y(5)*DYDX3+(1.0-Y(3))*DYDX5)
        Y4AN3=BVOC*(Y(3)*DYDX5+DYDX3*Y(5))*ALA*
     &        (1.0-Y(4))*(Y(5)*Y(3)-PVAC*Y(4))
        Y4AN4=BN2*(Y(3)*DYDX5+DYDX3*Y(5))*ALB*
     &        Y(4)*(Y(5)*(1.0-Y(3))-PVAC*(1.0-Y(4)))
       Y4AN=Y4AN1-Y4AN2+Y4AN3-Y4AN4
       Y4DN1=2.0*Y(3)*Y(5)*(ALA-ALB)
       Y4DN2=ALA*PVAC
       Y4DN3=3.0*(ALA-ALB)*PVAC*Y(4)
       Y4DN4=2.0*ALB*(Y(5)-PVAC)
       Y4DN=Y4DN1+Y4DN2-Y4DN3+Y4DN4
      FUNC=Y4AN/Y4DN
      ELSE
        Y4P1=ALA*(1.0-Y(4))*(Y(5)*Y(3)-PVAC*Y(4))
        Y4P2=ALB*Y(4)*(Y(5)*(1.0-Y(3))-PVAC*(1.0-Y(4)))
      FUNC=(Y4P1-Y4P2)/Y(2)
      ENDIF
      RETURN
    5 FUNC=BETA*VFEED*Y(1)/Y(5)
      RETURN
      END
C
C


C Subroutine to set boundary conditions
C
      SUBROUTINE FCNBC (NEQNS, YLEFT, YRIGHT, P, F)
      INTEGER NEQNS
      REAL YLEFT(NEQNS), YRIGHT(NEQNS), P, F(NEQNS)
      COMMON XINLET,Q0VOC,BVOC,Q0N2,BN2,PFEED,PVAC,
     &       BETA,VFEED,FBOUND
C
C Define boundary conditions
C
      ALA=FUNA(NEQNS,X,YLEFT)
      ALB=FUNB(NEQNS,X,YLEFT)
C    PRINT *,ALA,ALB,Q0VOC,Q0N2
      F(1)=YLEFT(2)-0.0
      Y4B1=ALB*YLEFT(5)+(ALA-ALB)*(YLEFT(5)*YLEFT(3)+PVAC)
      Y4B2=4.0*ALA*YLEFT(5)*PVAC*YLEFT(3)*(ALA-ALB)
```

```
      Y4B3=2.0*PVAC*(ALA-ALB)
      ZZZ=(Y4B1-SQRT(Y4B1**2-Y4B2))/Y4B3
C   PRINT *,ZZZ,ALA,ALB
      F(2)=YLEFT(4)-ZZZ
C
C BCL and XINLET are boundary conditions of L* and x at S=1, respectively
C
      F(3)=YRIGHT(1)-FBOUND
      F(4)=YRIGHT(3)-XINLET
      F(5)=YRIGHT(5)-PFEED
      RETURN
      END
C
C Function to calculate the ALA value
C
      FUNCTION FUNA(NEQNS,X,Y)
      REAL Y(NEQNS)
      COMMON XINLET,Q0VOC,BVOC,Q0N2,BN2,PFEED,PVAC,
     &      BETA,VFEED,FBOUND
      FUNA=Q0VOC*EXP(BVOC*Y(5)*Y(3))
      RETURN
      END
C
C Function to calculate the ALB values
C
      FUNCTION FUNB(NEQNS,X,Y)
      REAL Y(NEQNS)
      COMMON XINLET,Q0VOC,BVOC,Q0N2,BN2,PFEED,PVAC,
     &       BETA,VFEED,FBOUND
      FUNB=Q0N2*EXP(BN2*Y(5)*Y(3))
      RETURN
      END
```

B.2 YINIT.FOR

```
C This is a program to guess the initial value of YINIT in the AICHE-*.for.
C This program uses IMSL IVPRK/DIVPRK subroutine.
C
C Specifications for parameters
C NGRID is the number of grid
C
      INTEGER MXPARM, NEQ, NGRID
      PARAMETER (MXPARM=50, NEQ=5, NGRID=10)
```

```
C
      INTEGER IDO,ISTEP,NOUT
      REAL FCN, FLOAT, PARAM(MXPARM), T, TEND, TOL, Y(NEQ)
      INTRINSIC FLOAT
      EXTERNAL FCN, IVPRK, SSET, UMACH
      COMMON
XINLET,Q0VOC,BVOC,Q0N2,BN2,PFEED,PVAC,BETA,VFEED
C
C This portion is to collect the experimental data for calculations
C
      OPEN (1,FILE='INFORM.DAT',STATUS='OLD')
      READ (1,*) XINLET, PFEED
      READ (1,*) FBOUND
      READ (1,*) PVAC
      READ (1,*) BETA, VFEED
      READ (1,*) Q0VOC, BVOC
      READ (1,*) Q0N2, BN2
      CLOSE (1, STATUS='KEEP')
C
      CALL UMACH(2,NOUT)
C
C Set initial conditions
C
      T=0.0
      Y(1)=FBOUND
      Y(2)=1.0E-08
      Y(3)=XINLET
      Y(5)=PFEED
      ALA=FUNA(NEQ,X,Y)
      ALB=FUNB(NEQ,X,Y)
C    PRINT *, ALA,ALB
      Y4B1=ALB*Y(5)+(ALA-ALB)*(Y(5)*Y(3)+PVAC)
      Y4B2=4.0*ALA*Y(5)*PVAC*Y(3)*(ALA-ALB)
      Y4B3=2.0*PVAC*(ALA-ALB)
      Y(4)=(Y4B1-SQRT(Y4B1**2-Y4B2))/Y4B3

C
C Set error tolerance
C
      TOL=0.001
C
C Set PARAM to default
C
      CALL SSET (MXPARM, 0.0, PARAM,1)
C
C Select absolute error control
```

```
C
      PARAM(10)=1.0
C
C Print header
C
      WRITE (NOUT, 9999)
 9999   FORMAT(4X, 'ISTEP',5X, 'TIME')
      IDO=1
      XLEFT=0.0
      XRIGHT=1.0
      OPEN (2, FILE='YTEMP.DAT',STATUS='NEW')
      DO 10 ISTEP=1,NGRID
        TEND=XLEFT+(ISTEP-1)*(XRIGHT-XLEFT)/FLOAT(NGRID-1)
C      TEND=FLOAT(ISTEP)/FLOAT(NGRID)
C      TEND=FLOAT(ISTEP)
        CALL IVPRK(IDO, NEQ, FCN, T, TEND, TOL, PARAM, Y)
        WRITE (NOUT,'(I6,6F8.5)') ISTEP, T, Y
      WRITE (2,*) T, Y
  10 CONTINUE
      CLOSE (2, STATUS='KEEP')
C
C Final call to release workspace
C
      IDO=3
      CALL IVPRK(IDO, NEQ, FCN, T, TEND, TOL, PARAM, Y)
      CALL REVERSE(NEQ,NGRID)
      END
C
C Subroutine FCN
C
      SUBROUTINE FCN(NEQ,T,Y,YPRIME)
      INTEGER NEQ
      REAL T,Y(NEQ),YPRIME(NEQ),ALA,ALB,BETA,VREF
      COMMON
XINLET,Q0VOC,BVOC,Q0N2,BN2,PFEED,PVAC,BETA,VFEED
C
C Define differential equations
C
C   PRINT *, T,Y(3), Y(5),ALA
      ALA=FUNA(NEQ,X,Y)
      ALB=FUNB(NEQ,X,Y)
      Y1P1=ALA*(Y(5)*Y(3)-PVAC*Y(4))
      Y1P2=ALB*(Y(5)*(1.0-Y(3))-PVAC*(1.0-Y(4)))
      YPRIME(1)=(Y1P1+Y1P2)*(-1.0)
      Y2P1=Y1P1
      Y2P2=Y1P2
```

```
      YPRIME(2)=Y2P1+Y2P2
      Y3P1=ALA*(1.0-Y(3))*(Y(5)*Y(3)-PVAC*Y(4))
      Y3P2=ALB*Y(3)*(Y(5)*(1.0-Y(3))-PVAC*(1.0-Y(4)))
      YPRIME(3)=(Y3P1-Y3P2)*(-1.0)/Y(1)
      IF (T.EQ.0.0) THEN
        Y4AN1=ALA*(1.0-Y(4))*(Y(5)*YPRIME(3)+Y(3)*YPRIME(5))
        Y4AN2=ALB*Y(4)*(-Y(5)*YPRIME(3)+(1-Y(3))*YPRIME(5))
        Y4AN3=BVOC*(Y(3)*YPRIME(5)+YPRIME(3)*Y(5))*ALA*
     &        (1.0-Y(4))*(Y(5)*Y(3)-PVAC*Y(4))
        Y4AN4=BN2*(Y(3)*YPRIME(5)+YPRIME(3)*Y(5))*ALB*
     &        Y(4)*(Y(5)*(1.0-Y(3))-PVAC*(1.0-Y(4)))
       Y4AN=Y4AN1-Y4AN2+Y4AN3-Y4AN4
        Y4DN1=2.0*Y(3)*Y(5)*(ALA-ALB)
        Y4DN2=ALA*PVAC
        Y4DN3=3.0*(ALA-ALB)*PVAC*Y(4)
        Y4DN4=2.0*ALB*(Y(5)-PVAC)
       Y4DN=Y4DN1+Y4DN2-Y4DN3+Y4DN4
      YPRIME(4)=Y4AN/Y4DN
      ELSE
        Y4P1=ALA*(1.0-Y(4))*(Y(5)*Y(3)-PVAC*Y(4))
        Y4P2=ALB*Y(4)*(Y(5)*(1.0-Y(3))-PVAC*(1.0-Y(4)))
        YPRIME(4)=(Y4P1-Y4P2)/Y(2)
      ENDIF
      YPRIME(5)=BETA*VFEED*Y(1)*(-1.0)/Y(5)
      RETURN
      END
C
C Subroutine to reverse the order of Y value from IVPRK.  Since the
C calculation results derived from cocurrent configuration, it is
C necessary to reverse the value of L* and x, which were represented
C by Y(1) and Y(3) in the previous program
C
      SUBROUTINE REVERSE(NEQ,NGRID)
      INTEGER NEQ,NGRID
      REAL TT(20), YNEW(10,20)
      OPEN (3, FILE='YTEMP.DAT', STATUS='OLD')
      DO 100 I=1,NGRID
      READ (3,*) T, Y1, Y2, Y3, Y4, Y5
      TT(I)=T
      YNEW(1,NGRID+1-I)=Y1
      YNEW(2,I)=Y2
      YNEW(3,NGRID+1-I)=Y3
      YNEW(4,NGRID+1-I)=Y4
      YNEW(5,NGRID+1-I)=Y5
100   CONTINUE
      CLOSE (3, STATUS='KEEP')
```

```
      OPEN (4, FILE='YINIT.DAT', STATUS='NEW')
      DO 200 J=1,NGRID
C   WRITE (4,*) TT(J),YNEW(1,J),YNEW(2,J),YNEW(3,J),YNEW(4,J)
      WRITE (4,*) YNEW(1,J),YNEW(2,J),YNEW(3,J),YNEW(4,J),YNEW(5,J)
 200  CONTINUE
      CLOSE (4, STATUS='KEEP')
      RETURN
      END
C
C Function to calculate the ALA value
C
      FUNCTION FUNA(NEQ,X,Y)
      REAL Y(NEQ)
      COMMON
XINLET,Q0VOC,BVOC,Q0N2,BN2,PFEED,PVAC,BETA,VFEED
      FUNA=Q0VOC*EXP(BVOC*Y(5)*Y(3))
      RETURN
      END
C
C Function to calculate the ALB values
C
      FUNCTION FUNB(NEQ,X,Y)
      REAL Y(NEQ)
      COMMON
XINLET,Q0VOC,BVOC,Q0N2,BN2,PFEED,PVAC,BETA,VFEED
      FUNB=Q0N2*EXP(BN2*Y(5)*Y(3))
      RETURN
      END
```

B.3 INFORM.FOR

```
C This program is to collect the experimental data, convert
C the unit, and change those parameter into dimensionless form.
C The function of this program is to manage the data for IMSL program
C
      CHARACTER MOD*25,VOC*25
      READ *, MOD, VOC
      READ *, FIBLEN
C
C FIBLEN= length of fiber, cm
C
      READ *,TEMP
      TABS=TEMP+273.15
```

```
      READ *, AVOC
      READ *, BVOC
C     BVOC=BVOC/14.696
      READ *, AN2
      READ *, BN2
C     BN2=BN2/14.696
C
C TEMP= experimental temperature, oC
C QVOC= AVOC*exp(BVOC*PRVOC)
C QN2= AN2*exp(BN2*PRVOC) at constant temperature,
C where QVOC and QN2 are the permeability of VOC and N2
C
      READ *,DIN
      READ *,DOUT
C
C DIN, DOUT= inside and outside diameters of fiber, respectively, cm
C
      READ *,PREIN
      READ *,PREVAC
      READ *,VIN
      ATM=76.0
      PREF=76.0/ATM
      PFEED=PREIN/ATM/PREF
      PVAC=PREVAC/ATM/PREF
      VREF=VIN
      VFEED=VIN/VREF
C
C PREIN= pressure in the inlet of the feed, cm-Hg
C VIN= viscosity in the inlet of the feed, poise (g/cm/s)
C
      THICK=(DOUT-DIN)/2.0
C
C THICK= thickness of the fiber, cm
C
      READ *, FINLET
      READ *, FREFA
      FBOUND=FINLET/FREFA
      READ *, NFIBER
      RCONST=82.057
      FREF=1.0*FREFA/60.0/RCONST/(25.0+273.15)/NFIBER
C
C FINLET= feed inlet measured at R.T. and 1 atm, CC/min
C NFIBER= no. of fibers
C FREFA= reference flow rate, cc/min
C FREF= flow rate per fiber, mol/sec
C
```

```
      READ *, XINLET
C
C XINLET= mole fraction of VOC in the inlet of the pore
C
      PI=3.14159
      QREF1=FREF/PI/DOUT/PREF/FIBLEN
      QREF=QREF1/76.0
      PRINT *, 'ref permeability, (mol)/(s*cm2*cmHg) = ', QREF
C
C Dimensionless conversion to make XRIGHT=1 or S=1 in the derivation
C QREF= reference permeability coeff., (mol)/(s*cm2*cmHg)
C BETA= constant for dimesionless change, g/(cm*atm*sec**2)
C 1 atm = 1.0133E6 g/(cm*sec**2)
C
      BETA=128.0*RCONST*TABS*FREF**2*VREF/
   &      (PI**2*DIN**4*DOUT*(QREF1)*PREF**3)
      BETA=BETA/1.0133E6
      PRINT *, 'BETA, dimensionless, g/(cm*atm*s**2)= ',BETA
C
C Calculation of dimensionless constant
C
      Q0VOC=AVOC/QREF
      Q0N2=AN2/QREF
C
C Print and save the calculated data
C
      OPEN (5, FILE='INFORM.DAT',STATUS='NEW')
      WRITE (5,*) XINLET, PFEED, ' inlet X of VOC and pressure, atm'
      WRITE (5,*) FBOUND, ' boundary condition at feed inlet'
      WRITE (5,*) PVAC, '  pressure of the vacuum side, atm'
      WRITE (5,*) BETA, VFEED, ' dimensionless beta and feed viscosity'
      WRITE (5,*) Q0VOC, BVOC, ' exp data of
QVOC=Q0VOC*EXP(BVOC*PVOC)'
      WRITE (5,*) Q0N2, BN2, ' exp data of QN2=Q0N@*EXP(BN2*PVOC)'
      CLOSE (5,STATUS='KEEP')
      END
```

B.4 CAL.FOR

```
C
OPEN (1,FILE='AICHE-V.DAT',STATUS='OLD')
OPEN (2,FILE='INFORM.DAT',STATUS='OLD')
READ (1,*) FOUT,V,XOUT,Y,POUT
```

```
READ (2,*) XIN, PREF
REMOVE=(XIN-XOUT)/XIN*100.0
POUT=POUT*76.0
CLOSE (1,STATUS='KEEP')
CLOSE (2,STATUS='KEEP')
PRINT *,'   '
PRINT *,'outlet flow rate, CC/min = ', FOUT
PRINT *,'outlet VOC mole fraction = ', XOUT
PRINT *,'outlet pressure, cmHg = ', POUT
PRINT *,'percent removal =  ',REMOVE
STOP
END
```

REFERENCES

Abriola, L.M., K.D. Pennel, G.A. Pope, J.J. Dekker and D.J. Luning-Prak.1995. "Impact of Surfactant Flushing on the Solubilization and Migration of DNAPL." *ACS Symposium Series.* **594**, 10.

Bagnell, L., K. Cavell, A.M. Hodges, A.W.H. Mau and A.J. Seen. 1995. "Use of Catalytically Active Pervaporation Membranes in Esterification Reactions to Simultaneously Increase Product Yield, Membrane Permselectivity and Flux." *J. Mem. Sci.* **85**, 291.

Ball, R. and S. Wolf. 1990. "Design Considerations for Soil Cleaning by Soil Vapor Extraction ." *Environmental Progress.* **34**, 187.

Bhave R.R. and K.K. Sirkar. 1986. " Gas Permeation and Separation by a Aqueous Membrane Immobilized across the Whole Thickness or in a Thin Section of Hydrophobic Microporous Celgard Films." *J. Mem. Sci.* **27**, 41.

Binning, R.C and F.E. James. 1958. "Permeation: A New Commercial Separation Tool." *Pet. Eng.* **30**, 113.

Binning, R.C., R.J. Lee, J.F. Jennings and E.C. Martin. 1961. "Separation of Liquid Mixtures by Permeation." *Ind. Eng. Chem.* **53**, 45.

Binning, R.C., J.F. Jennings and E.C. Martin. 1962. "Removal of Water from Organic Chemical." *U.S. Patent 3,035,060.*

Blume, I., J.G. Wijmans and R.W. Baker. 1990. "The Separation of Dissolved Organics from Wastewater by Pervaporation." *J. Mem. Sci.* **49**, 253.

Boddeker, K.W., G. Bengston, H. Pingel and S. Dozei. 1993. "Pervaporation of High Boiler using Heated Membranes." *Desalination.* **90**, 249.

Bravo, J.L., J.R. Fair, J.L. Humphrey, C.L. Martin and A.F. Seibert. 1986. *Fluid Mixture Separation Technologies for Cost Reduction and Process Improvement.* Noyes Data, Park Ridge, N.J.

Brun, J.P., C. Larchet, G. Bulvestre and B. Auclari. 1985a. "Sorption and Pervaporation of Dilute Aqueous Solution of Organic Compounds through Polymeric Membranes." *J. Mem. Sci.* **25**, 55.

Cha, J.S., V. Malik, D. Bhaumik, R. Li and K.K. Sirkar. 1997. "Removal of VOCs from Waste Gas Streams by Permeation in a Hollow Fiber Permeator." *J. Mem. Sci.* **128**, 195.

REFERENCES
(Continued)

Chandra, S. "Removal of Volatile Organic Compounds from Contaminated Groundwater by Pervaporation." *M.S. Thesis, Dept of Chemical Engineering,* New Jersey Institute of Technology, Newark, NJ. August: 1996.

Chen, W.J and C.R. Martin. 1995. "Highly Methanol Selective Membranes for Pervaporation Separation of Methyl t- Butyl Ether/Methanol Mixtures.*" J. Mem. Sci.* **104**, 105.

Chen, M.S.K., G.S. Markiewicz and K.G. Venugopal. 1989. "Development of Membranes for Pervaporation TRIM Process for Methanol Recovery from $CH_3OH/MTBE/C4$ Mixtures." *AIChE Symposium Series.* **85**, 82.

Clarke, A.N., K.H. Oma and M.M. Megchee. 1993. "Soil Cleaning by Surfactant Washing. II. Design and Evaluation of the Component of the Pilot Scale Surfactant Recycle System." *Sep. Sci. Technol.* **28**, 2103.

David, D.O., R. Gref, Q.T. Nguyen and J. Neel. 1991a. "Pervaporation-Esterification Coupling. I. Basic Kinetic Model." *Chem. Eng. Res. Dev.* **69**, 341.

David, D.O., R. Gref, Q.T. Nguyen and J. Neel. 1991b. "Pervaporation-Esterification Coupling. II. Modeling of the Influence of the Operating Parameters." *Chem. Eng. Res. Dev.* **69**: 355.

David, D.O., Q.T. Nguyen and J. Neel. 1991b. "Pervaporaion Membrane Endowed with Catalytic Properties, Based on Polymer Blends." *J. Mem. Sci.* **73**, 129.

Doghieri, F., A. Nardella, G.C. Sarti and C. Valenti. 1994. "Pervaporation of Methanol-MTBE Mixture through Modified Polyphenylene Oxide Membranes." *J. Mem. Sci.* **94**: 283.

Ellis, W.E., J.R. Payne and G.D. McNabb. 1985. "Treatment of Contaminated Soils with Aqueous Surfactants". *US EPA Report.* **EPA/600/2-85/129**, 86.

Farber, L.. 1935. "Application of Pervaporation." *Science.* **82**, 158.

Farnand, B.A and S.H. Noh. 1989. "Pervaporation as an Attractive Process for the Separation of Methanol from C4 Hydrocarbons in the Production of MTBE and TAME." *AIChE Symposium Series.* **85**(No.272), 89.

Fountain, J.C., C. Waddel-Sheets, A. Lagowski, C. Taylor, D. Frazier, and M. Byrne. 1995. "Enhanced Removal of DNAPLs using Surfactants." *ACS Symposium Series.* **594**, 177.

REFERENCES
(Continued)

Fels, M and R.Y.M. Huang. 1971. "Theoretical Interpretation of the Effect of Mixture Composition on Separation of Liquids in Polymers." *J. Macromol. Sci. Phys.* **B5**, 89.

Feng, X. *"Studies on Pervaporation Membranes and Pervaporation Process."* *Ph.D.Thesis,* University of Waterloo, Waterloo, Ontario, Canada. 1995.

Gannon, O.K., P. Bibring and K. Raney. 1989. "Soil Clean-Up by In-Situ Surfactant-Flushing. III. Laboratory Results." *Sep. Sci. Technol.* **24**, 1073

Gooding, C.H., P.J. Hickey and M.L. Crowder.1991. *"Mass Transfer Characteristics of a New Pervaporation Module for Water Purification."* Proceedings of the 5th International Conference on Pervaporation Processes in Chemical Industry, R. Bakish (Ed), Bakish Materials Corp., Englewood, NJ. 237.

Greenlaw, F.W., R.A. Shelden and E.V. Thompson. 1977. "Dependence of Permeation Rates on Upstream and Downstream Pressure. II. Two Component Permeant." *J. Mem. Sci.* **2**, 333.

Havinga R. and Cotruvo J.A. 1989. "Drinking Water Standards and Risk Assesment." *J. Water, Environ. Mgmt.* **3**, 6.

Huang, R.Y.M and J.W. Rhim. 1992. "Prediction of Pervaporation Separation Characteristics for Methanol-Pentane-Nylon-6-Polyacrylic Acid Blended Membrane System." *J. Mem. Sci.***71**, 211.

Kang, Y.S., E.M. Shin, B. Jung and J-J Kim. 1994. "Composite Membranes of Poly(1-Trimethylsilyl-1propyne) and PDMS and their Pervaporation Properties for Ethanol Water Mixtures." *J. Appl. Polym. Sci.* **53**, 317.

Karlsson, H.O.E and G. Tragardh. 1993. "Aroma Compound Recovery with Pervaporation. Feed Flow Effects." *J. Mem. Sci.* **81**, 163.

Lamer, T., M.S. Rohart, A. Voilley and H. Baussart. 1994. "Influence of Sorption and Diffusion of Aroma Compounds in Silicone Rubber on their Extraction by Pervaporation." *J. Mem. Sci.* **90**, 251.

Lee, C.H.. 1975. "Theory of Reverse Osmosis and Some other Membrane Permeation Operations." *J. Appl. Polym. Sci.* **19**, 83.

Lee, Y.M., D. Bourgeois and G. Belfort. 1989. "Sorption, Diffusion and Pervaporation of Organics in Polymeric Membranes." *J. Mem. Sci.* **44**, 161.

REFERENCES
(Continued)

Lee, E.K and V.J. Kalyani. 1991. "Process of Treating Alcohol Beverage by Vapor-Arbitrated Pervaporation." *U.S. Patent 5,014,447.*

Lipski, C and P.Cote. 1990. "The Use of Pervaporation for the Removal of Organic Contaminants from Water." *Environ. Progr.* **9**, 254.

Markelov, M. and J.P. Guzowski Jr. 1993. "Matrix Independent Headspace Gas Chromatographic Analysis. The Full Evaporation Technique". *Analytica Chim. Acta.* **15**, 234.

Mattos, I.L and M.D.L. de Castro. 1994. "Study of Mass Transfer Efficiency in Pervaporartion Process." *Anal. Chim. Acta.* **298**, 159.

Mulder, M.H.V and C.A. Smolders. 1984. "On the Mechanism of Separation of Ethanol/Water Mixture by Pervaporation. I. Calculations of Concentration Profiles." *J. Mem. Sci.* **17**, 289.

Mulder, M.H.V and C.A. Smolders. 1985a. "Preferential Sorption versus Preferential Permeability in Pervaporation." *J. Mem. Sci.* **22**, 155.

Mulder, M.H.V and C.A. Smolders. 1985a. "On the Mechanism of Separation of Ethanol/Water Mixture by Pervaporation. II. Experimental Concentration Profiles." *J. Mem. Sci.* **23**, 41.

Mulder, M.H.V and C.A. Smolders. 1986. "Pervaporation Solubilty Aspect of the Solution-Diffusion Model." *Sep. Puri. Method.* **15**, 1.

Nagase, Y., K. Ishihara and K. Matsui. 1990. "Chemical Modification of Poly(substituted acetylene). II. Pervaporation of Ethanol/Water Mixture through Poly(1-trimethylsilyl-1-propyne)/PDMS Graft Copolymer Membrane." *J. Polym. Sci. Phys. Ed.* **28**, 377.

Nagase, Y., K. Sugimoto, Y. Takimura and K. Matsui. 1990. "Chemical Modification of Poly(substituted acetylene). VI. Introduction of Fluoroalkyl Group into Poly(1-Trimethylsilyl-1-Propyne) and Improved Ethanol Permselectivity at Pervaporation." *J. Appl. Polym. Sci.* **43**, 1227.

Nagase, Y., Y. Takimura and K. Matsui. 1990. "Chemical Modification of Poly (substituted acetylene). V. Alkylsilylation of Poly(1-Trimethylsilyl-1-Propyne) and Improved Liquid Separating Property at Pervaporation." *J. Appl. Polym. Sci.* **42**, 185.

REFERENCES
(Continued)

Nash, J.H. 1987. "Field Studies of In-Situ Soil Washing". *US EPA Report*. EPA/600-2-85/110, 88.

Nakagawa, K. and K. Matsuo. 1994. " Process for Producing Ether Compounds," *United States Patent 5,292,963.*

Neel, J.. 1991. " Introduction to Pervaporation." *Pervaporation Membrane Separation Processes*. R.Y.M. Huang (Ed). Elsevier, Amsterdam.

Okada, T.T. and T. Matsuura. 1991. " A New Transport Model for Pervaporation. " *J. Mem. Sci.* **59**, 133.

Okada, T.T. and T. Matsuura. 1992. "Prediction of Transport-Equation for Pervaporation on the Basis of Pore-Flow Mechanism. *J. Mem. Sci.* **70**, 163.

Okamoto, K., T. Semoto, K. Tanka and H. Kita. 1991. "Application of Pervaporation to Phenol-Acetone Condensation Reaction." *Chem. Lett.* **1**, 167.

Oma, K.H, A.N. Clarke and M.M. Megchee. 1993. "Soil Cleaning by Surfactant Washing. III. Design and Evaluation of the Integrated Pilot Scale Surfactant Recycle System." *Sep. Sci. Technol.* **28**, 2319.

Okamoto, M. Yamamoto, Y. Otoshi, K., T. Semoto, M. Yano, K. Tanka and H. Kita. 1991. "Pervaporation-Aided Esterification of Oelic Acid." *J. Chem. Eng. Jpn.* **26**, 475.

Papaefstahiou, I. and M.D.L. de Castro. 1995. "Approaches for Improving the Precision and Sensitivity of Binary Liquid Mixtures in Poly(vinyl chloride) Membranes by Pervaporation." *J. Polym. Sci., Polym. Phys.* **33**, 291.

Papaefstahiou, I. M.T. Tena and M.D.L. de Castro. 1995. "On-Line Pervaporation Separation Process for Potentiometric Determination of Fluoride in Dirty Samples." *Anal. Chim. Acta.* **308**, 246.

Park, H.C., N.E. Ramaker. M.H.V. Mulder and C.A. Smolders. 1995. "Separation of MTBE-Methanol Mixtures by Pervaporation." *Sep. Sci. Techol.* **30**, 419.

Pennel, K.D., L.M. Abriola and W.J. Weber Jr. 1993. "Surfactant-Enhanced Solubilization of Dodecane in Soil Columns." *Environ. Sci. Technol.* **27**, 232.

Prasad, R. and K.K. Sirkar. 1988. "Dispersion Free Solvent Extraction with Microporous Hollow Fiber Modules." *AIChE J.* **34**, 177.

REFERENCES
(Continued)

Rangarajan, R., M.A. Mazid, T. Matsuura and S. Sourirajan. 1984. "Permeation of Pure Gases under Pressure through Asymmetric Porous Membranes: Membrane Characterisation and Prediction of Performance." *Ind. Eng. Chem. Process Des. Dev.*, **23**, 79.

Rhim, J.W. and R.Y.M. Huang. 1989. "On the Prediction of Separation Factor and Permeability on the Separation of Binary Mixtures by Pervaporation." *J. Mem. Sci.* **46**, 355.

Rhim, J.W. and R.Y.M. Huang. 1992. "Prediction of Pervaporation Separation Characteristics for Ethanol-Water-Nylon 4-Membrane System." *J. Mem. Sci.* **70**, 105.

Saraf, A.N.. "Removal and Recovery of VOCs and Oils from Surfactant-Flushed Recovered Water by Membrane Permeation." *M.S. Thesis, Dept of Chemical Engineering*, New Jersey Institute of Technology, Newark, NJ. August: 1997.

Schaetzel P., E. Favre, Q.T. Nguyen and J. Neel. 1993. " Mass Transfer Analysis of Pervaporation through an Ion-Exchange Membrane." *Desalination.* **35**, 125.

Shah, V.M., C.R. Bartels, M. Pasternak And J. Reale. 1989. " Opportunities for Membrane in the Production of Octane Enhancers." *AIChE Symposium Series.* **85(No. 272)**, 93.

Shen, T.T. and G.H. Sewell. 1988. "Control of VOC Emissions from Waste Management Facilities". *J. Environ. Eng.* **114**, 1392.

Shiau, B., J.D. Rouse, D.A. Sabatini and J.H. Harwell. 1995. " Surfactant Selection for Optimizing Surfactant-Enhanced Subsurface Remediation." *ACS Symposium Series.* **594**, 65.

Shimidzu, T. and M. Yoshikawa. 1991. "Synthesis of Novel Copolymer Membrane for Pervaporation." *Pervaporation Membrane Separation Processes.* R.Y.M. Huang (Ed). Elsevier, Amsterdam.

Skelland, A.H.P. 1974. *Diffusional Mass Transfer*, Wiley, New York.

Tanimura, S., S. Nakao and S. Kimura. 1990. " Ethanol Selective Membranes for Reverse Osmosis of Ethanol/Water Mixture." *AIChE J.* **36**, 1118.

Turner, L.H., Y.C. Chiew, R.C. Ahlert and D.S. Kosson. 1996. " Measuring Vapor-Liquid Equilibrium for Aqueous-Organic Systems: Review and a New Technique." *AIChE J.* **42**, 6.

REFERENCES
(Continued)

Underwood, J.L., K.A. Debelak and D.J. Wilson. 1993. "Soil Clean-Up by In-Situ Surfactant-flushing. VI. Reclamation of Surfactant for Recycle." **28**, 1647.

Uragami, T. and M. Saito. 1989. "Analysis of Pervaporation and Separation Characteristics and New Techniques for Separation of Aqueous Solution through Alginic Acid Membrane." *Sep. Sci. Technol.* **24**, 541.

Uragami, T. and M. Saito. 1990. "Analysis of Permeation and Separation Characteristics and New Techniques for Separation of Aqueous Alcoholic Solutions through Alginic Acid Membranes". *Sep. Sci. Technol.* **31**, 668.

Uragami, T. and H. Shinomaya. 1992. " Permeation and Separation Characteristics of Ethanol-Water Mixtures through Chitosan Derivative Membranes by Pervaporation and Evapomeation." *Polymer.* **31**, 668.

Uragami, T. and T. Morikawa. 1992. " Permeation and Separation Characteristics of Ethanol-Water Mixtures through Polydimethylsiloxane Membranes by Pervaporation and Evapomeation." *J. Appl. Polym. Sci.* **44**, 2009.

van Oss, C.J., J. Visser, D.R. Absolom, S.N.Omneyi and A.W. Neumann. 1983. " The Concept of Negative Hamaker Coefficents. II. Thermodynamics, Experimental Evidence and Application." *Adv. Colloid Interface Sci.* **18**, 133.

Vankelcom, I.F., D. Depre, S. De Beukelaer and J.B. Uytterhoeven. 1995. "Influence of Zeolite in PDMS Membrane. Pervaporation of Water/Alcohol Mixtures." *J. Phys. Chem.* **99**, 13193.

Wenzlaff, A., K.W. Boddeker and K. Hattenbach. 1985. "Pervaporation of Ethanol-Water Mixtures through Ion-Exchange Membrane." *J. Mem. Sci.* **22**, 333.

Wijmans, J.G. and R.W. Baker. 1995. "The Solution-Diffusion Model: A Review." *J. Mem. Sci.* **107**, 1.

Wnuk R. and H. Chmiel. 1992. "Direct Heating of Composite Membrane in Pervaporation and Gas Separation Processes." *J. Mem. Sci.* **68**, 293.

Yang, D., S. Majumdar, S. Kovenklioglu and K.K. Sirkar. 1995. "Hollow Fiber Contained Liquid Membrane Pervaporation System for the Removal of Toxic Volatile Organics from Wastewater." *J. Mem. Sci.* **103**, 195.

Yeom, C.K. and R.Y.M. Huang. 1992. "Modeling of Pervaporation Separation of Ethanol-Water Mixtures through Crosslinked Poly(vinyl alcohol) Membrane." *J. Mem. Sci.* **67**, 39.